Acta Geologica Polonica, Vol. 75 (2025), No. 4, e56
DOI: 10.24425/agp.2025.155950

Origin of flints in the Upper Cretaceous and Danian Chalk of England, Denmark and the North Sea: Evidence from their geological setting, mineralogy, geochemistry, paramagnetic properties and ultrastructure

CHRISTOPHER V. JEANS[1], DAVID WRAY[2], GIULIO I. LAMPRONTI[1], HASSAN A. SHEIKH[1] and ALEXANDER EVTUSHENKO[3]

[1] *Department of Earth Sciences, University of Cambridge, Downing Place, Cambridge, CB2 3EQ, UK; e-mail: cj302@cam.ac.uk*
[2] *School of Science, University of Greenwich, Pembroke, Chatham Maritime, Kent, ME4 4TB, UK*
[3] *Department of Chemical Engineering and Nanotechnology, University of Cambridge, Philippa Fawcet Drive, Cambridge CB3 0AS, UK*

ABSTRACT:

Jeans, C.V., Wray, D., Lampronti, G.I., Sheikh, H.A. and Evtushenko, A. 2025. Origin of flints in the Upper Cretaceous and Danian Chalk of England, Denmark and the North Sea: Evidence from their geological setting, mineralogy, geochemistry, paramagnetic properties and ultrastructure. *Acta Geologica Polonica*, **75** (4), e56.

Two types of flints are recognized in the Upper Cretaceous Chalk of England, the North Sea and Denmark. Alpha-quartz/moganite flints are associated with the high quartz smectite-mica clay assemblage that probably derived its silica from mainly oceanic sources related possibly to the development of the Atlantic Ocean, and opal-CT flints that are associated with the low-quartz smectite-mica clay assemblage that derived its silica ultimately from the deep weathering of continental rocks on the Mid-European Island. Eight different groups of alpha-quartz/moganite flints are described based on mineralogy, colour, core/cortex definition, size, relationship to bedding, and location. The presence of authigenic paramagnetic and non-paramagnetic minerals demonstrate that certain of these groups of flints developed in the oxic and suboxic diagenetic zones although the majority formed in the anoxic zone. Their major, minor and trace element chemistry is discussed in relation to the timing of their development. A predictive schematic model is put forward linking flint development with diagenesis, burrow-type and the plumbing system of the Chalk. The origin of flint veins and sheets is discussed within the context of the known relationship between pore size and the degree of super saturation needed for cement precipitation.

Key words: Cretaceous; Chalk; Upper Greensand; Flints/cherts; Mineralogy; Geochemistry; Paramagnetic properties; NW Europe.

INTRODUCTION

Dark flint of diagenetic origin either as bands of nodules – often of grotesque complex form – or as isolated individuals, or as veins or sheets break the monotony of the spectacular sea cliffs of White Chalk that characterize the Upper Cretaceous marine strata of western and northern Europe (Text-fig. 1). The study of flints is not a modern phenomenon. They have played an important role in the development of the early hominid species in western Europe during the last 2.5 million years. Flints' remarkable

toughness and ability to maintain a sharp edge and fashioned tools allowed hominid society to develop both within itself and in relation to the animal and vegetable worlds. It was soon realized that not all flints were equally suitable for tool making and that their natural properties could also be modified by heat treatment (e.g. Gurova *et al*. 2020). Centres of flint mining and tool manufacture developed where flints of good quality were accessible and abundant. Grimes Graves in Norfolk, East England was such a Neolithic centre. Here flints bands are abundant in the Turonian Chalk, the most famous is the Floorstone, a thick band (~100 mm) of nearly continuous black flint, a block of which has been used as a standard in our investigations (see later). The main manufacturing activity at this site was between 2600 and 2300 BC (Paleolithic or Stone Age) but continued into the Bronze and Iron ages because of flint's low cost compared to metals. The final event, other than for its continued use in areas of Chalk outcrop as a building stone (see later), was the replacement in ~1860 of the flint striker for the muskets of the dominant armies of the world by rifles fired by percussion caps. Flint strikers are still sought by historical reenactment societies. The public's interest in flints – whether as nodules *in situ* within the Chalk, as rolled pebbles on the beach, as stone-age tools, or other uses – has been brought together in Walter Shepherd's book *Flint Its Origin, Properties and Uses* (Shepherd 1972).

New scientific knowledge about flints started making progress in the second half of the 20th Century. Until then their chemical composition (SiO_2) was known, mineralogically they were considered to consist of alpha-quartz combined with a poorly crystalline SiO_2 phase. In Denmark there was particular interest in the stability of flint in concretes (Gry and Sondergaard 1958), and a landmark paper described the chemistry and structure of the Dark flint from Stevns, Denmark (Micheelsen 1966). An alkali-soluble phase was revealed by the etching of an "α-quartz" Turonian black flint (sample SuR20 of Jeans 1978, p.117) and this has turned out (see later) to be moganite, a new silica mineral that was described by Flörke *et al.* (1976, 1984) from vesicles in a lava on the Canaries Island. Moganite was first identified in a Chalk flint by Heaney and Post (1992) and has

Text-fig. 1. Etretat cliffs. A – Cliffs (87.5 m) at Etretat on the Haute Normandy coast showing the abundance of flint layers defining the stratigraphy of the Upper Turonian and Lower Coniacian Chalk. The chalk arch – Porte d'Aval – on the left shows the Auguille à Etretat chalk stack (51 m) in the background. B – Details of the cliffs at Etretat showing (1) the lower part of the chalk sequence where the irregular bedding is picked out by flint bands and hard grounds, and (2) the upper part that displays a regularly bedded chalk and flint sequence. (photos: R.N. Mortimore).

since been shown to occur in considerable amounts (up to 20% and more) in the flints of Campanian age in Poland, France and Belgium (Jurkowska and Świerczewska-Gładysz 2020a; Table 2). Our own analyses (see later) of flints from the Upper Cretaceous Chalk throughout England and Denmark and Albian cherts from southern England demonstrate that moganite is widespread and no less abundant.

DEVELOPMENT OF SILICA NODULES

Two general models for the development of silica nodules in the marine setting have been put forward and have been applied to the development of Chalk flints. Hearth and Moberly (1971), based on research on oceanic sediments recovered by the JOIDES drilling programme, suggested that opal-CT and alpha-quartz silicifications are part of a maturation series in which the former changes to the latter with time. In contrast Lancelot's (1973) hypothesis was based on the recognition of a lithological control on the occurrence of the silicification types and that alpha-quartz and opal-CT silicifications were not originally part of a maturation series, but were precipitated from pore waters of different chemistry, and subsequently only after burial diagenesis is the opal-CT converted to the alpha-quartz assemblage.

In a review of the diagenetic origin of the Chalk flints Hancock (1975, p. 523) suggested there was no actual evidence from the flints themselves to draw any conclusions. Three years later it was demonstrated that, in the Aptian–Turonian marine strata of southern England including part of the Chalk, Lancelot's basic hypothesis applied but there was no evidence of any control by lithology or by the abundance of large foreign cations in the porewaters of the host sediment (Jeans 1978). This however did not hinder the general acceptance and application of the Hearth and Moberly (1971) model. By 2006 the general understanding of Chalk flints was that they were originally precipitated as opal-CT but during burial diagenesis they gradually transformed to alpha-quartz (Clayton 1986, p. 53; Wray and Gale 2006, pp. 149–151).

More than ten years later Mortimore (2019, pp. 41–42) suggested there could be two general routes to flint formation. One involves biogenic silica deposited with the Chalk sediment being converted over time to alpha-quartz through a process that involves bacterial decay of organic matter (Clayton 1986) and temperature change with depth of burial (Madsen and Stemmerik 2010). This process of flint formation requires the replacement of chalk carbonate by silica, either by dissolution-precipitation or by solid state cation exchange. The main pathways for the chemical changes are the *Thalassinoides* burrow networks, where better permeability is preserved, in contrast to the more cemented and consolidated surrounding chalk. A second route of flint formation is that of Lindgreen and Jakobsen (2012) who suggested that biogenic opal-CT in the Chalk Sea was converted to alpha-quartz in the water column above the seabed as a result of a change of pH before being deposited on the sea floor. In this second model, a layer of flint is, therefore, directly sedimented on the sea floor.

More recently Jurkowska (2022), Jurkowska and Świerczewska-Gładysz (2020a, b, 2022) in their investigation of the Late Cretaceous marine European Basin have demonstrated that there are two mineralogical routes to Chalk silicifications and flints. One associated with the Chalk facies directly through alpha-quartz flints consisting of more than 99% SiO_2. The other is evident in the opoka facies that is rich in fossil siliceous sponges and their remains; here the opal-A/CT of the unaltered sponge material evolved to opal-CT with a SiO_2 content ranging from 79 to 85% and the charge deficiency balanced by Al_2O_3 (4.1 to 8.1%), CaO (0.7 to 5.3%), MgO (0.5 to 1.2%), K_2O (0.9 to 1.6%) and Fe_2O_3 (1.2 to 1.8%) (Jurkowska and Świerczewska-Gładysz 2020b; Table 2).

NOMENCLATURE OF DIAGENETIC SILICA NODULES

Flint and chert are the long established English terms used in this paper to describe the macroscopic silicifications we have studied. Chert refers to those from the sandy Lower Cretaceous strata of southern England and flint to those from the Chalk – thus differentiating between silicifications formed in sand-grade usually siliceous sediments (cherts) of Aptian and Albian age and those developed in silt-grade and clay-grade carbonate sediment (flint) of Upper Cretaceous age.

It is important to realise that the nomenclature and definition of these silica cemented diagenetic nodules varies regionally and nationally. Like sedimentary rocks they have long defied a universally accepted classification and nomenclature and it is best that the nuances of different national and regional schemes are understood and retained. In Poland, for example, where in recent years the most important research (Jurkowska and Świerczewska-Gładysz 2020a, b, 2022; Świerczewska-Gładysz 2022) has been undertaken on the silicifications in the Chalk

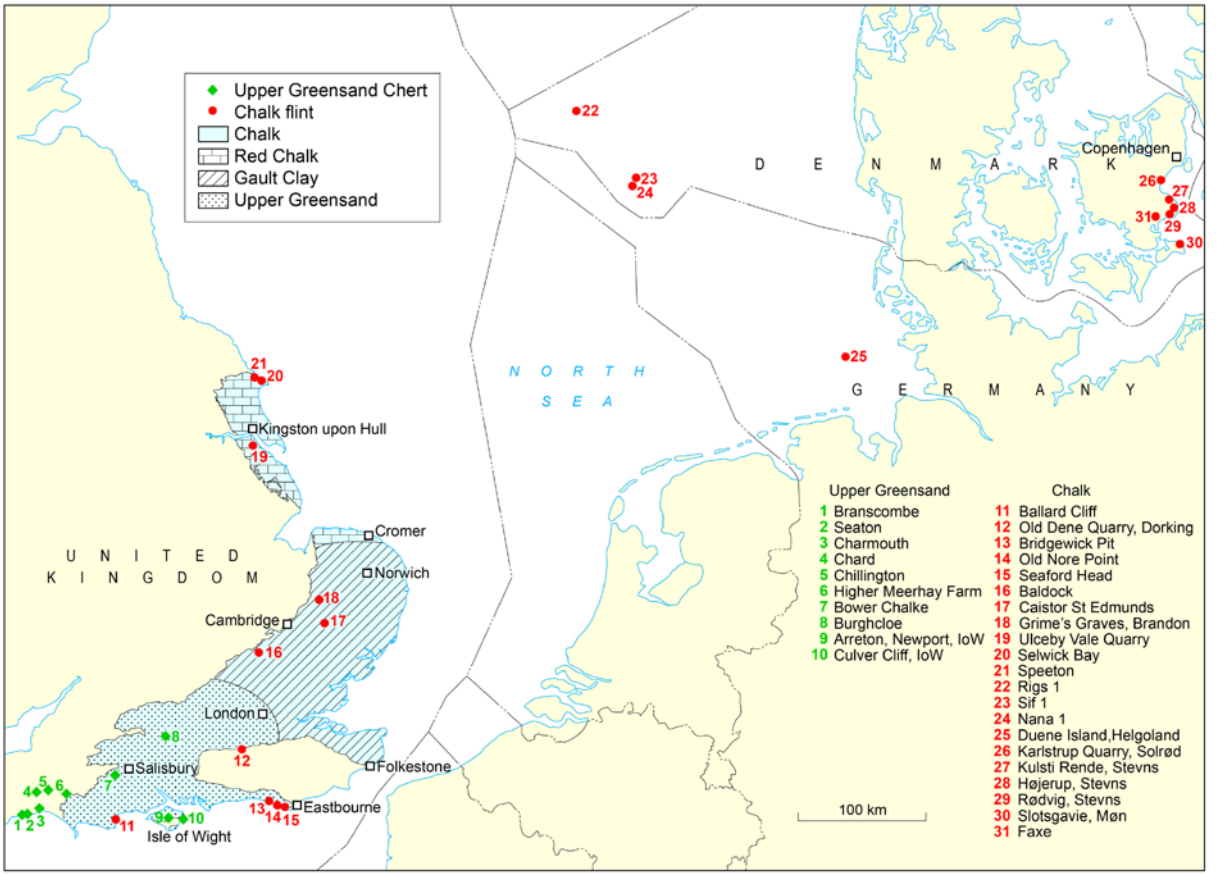

Text-fig. 2. Sample locations in England, the North Sea and Denmark. The surface and sub-surface distribution of Chalk, Red Chalk, Upper Greensand and Gault Clay for the United Kingdom

of the Late Upper Cretaceous Sea, a different use of these and related terms has evolved for the extensive opoka silicifcation lithofacies. This is defined by the dominance of opal-CT in its acid insoluble residue (15% HCl) and the presence of a distinctive texture comprising a framework of opal-CT lepispheres. Three types of siliceous nodules are distinguish in the opoka facies; (1) nodules containing 50–90% opal-CT that are referred to as *cherts* and these are usually grey and white in colour, (2) nodules containing 90–100% micro-quartz are referred to as *'flint'*, and (3) those with 90–100% nano-alpha quartz as 'chert ss', both the 'flint' and the 'chert ss' are usually black in colour. In the Cenomanian chalk of England the opoka silicification facies is only slightly developed but more extensively in northwest France (see later). We refer to its macroscopic silicifications as opal-CT flints so as to differentiate them within our nomenclature from alpha-quartz flints that may or may not contain moganite.

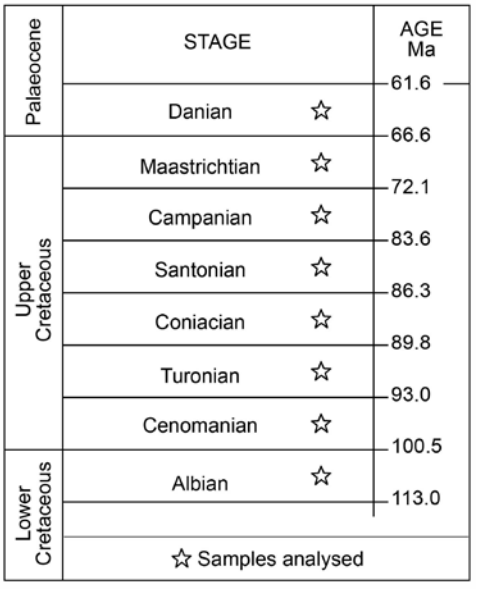

Text-fig. 3. Stratigraphical distribution of samples analysed.

FLINTS AND CHERTS: THEIR INVESTIGATION

The first part of our study was based around the analysis of the silica mineralogy and chemistry of 100 samples of flints and nano-quartz from the Upper Cretaceous Chalk of England, the North Sea and Denmark and 22 samples of Albian cherts from the Upper Greensand of southern England. The initial question posed is whether their silica mineralogies differ significantly as the latter have developed within a volcanogenic sedimentary setting, whereas the former, the Chalk flints, have formed within a non-volcanic setting (see later).

The second part of our study deals with different types of alpha-quartz flints recognized in the Chalk, and (b) establishing a model of flint development based on this new analytical data as well as established evidence on the field relations between flints and the host chalk in which they have developed.

Text-fig. 2 lists sample localities in England, the North Sea, and Denmark. Text-fig. 3 shows the stratigraphical range of samples investigated.

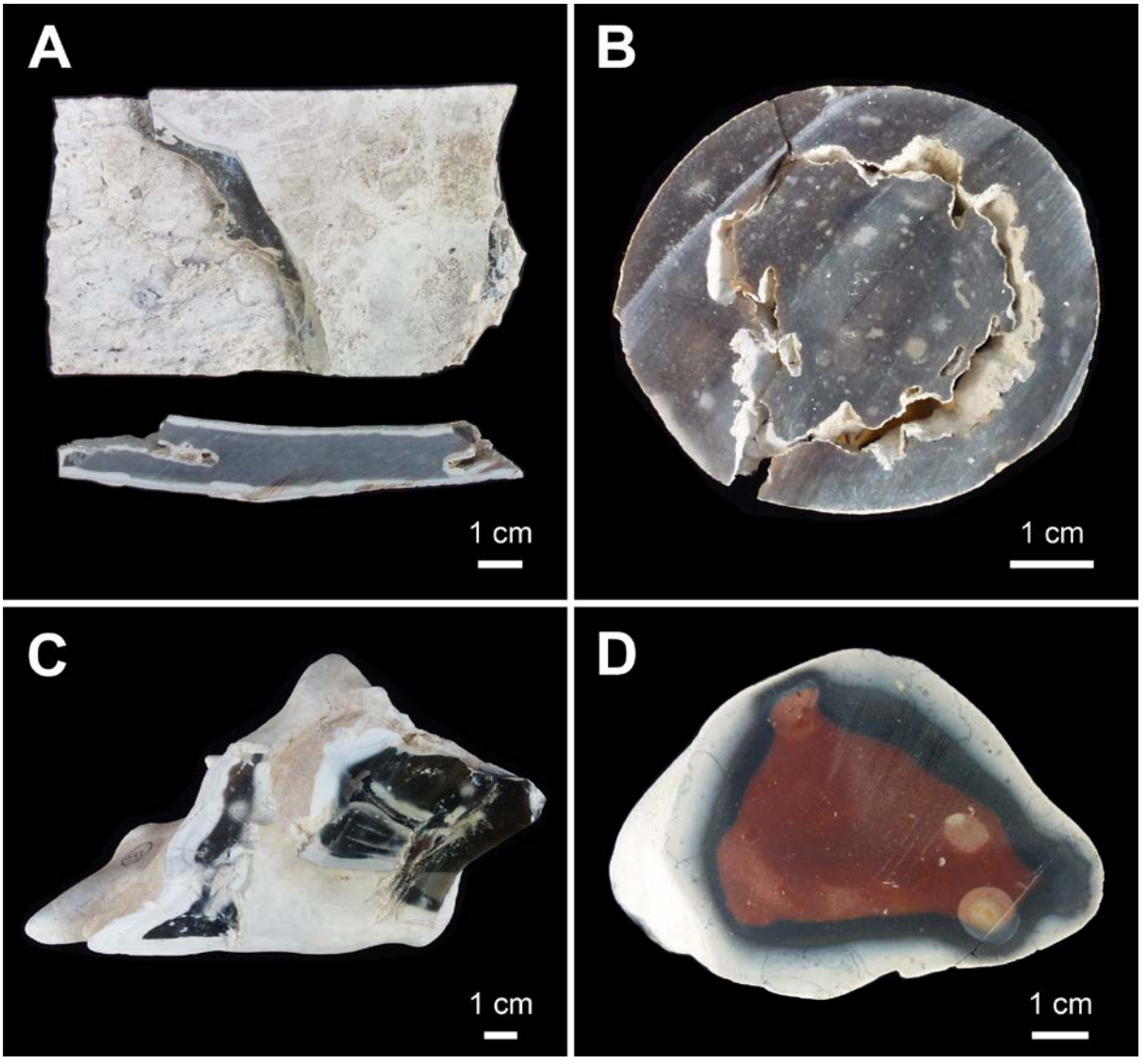

Text-fig. 4. General structure of flints. A – Surface of and a cross-section of a grey flint vein with a well-defined core and cortex. Newhaven Chalk Formation, Upper Santonian–Lower Campanian, Sussex, England. B – Cross-section of a vertical grey tubular flint with an internal mould of a fossil sponge. There is little or no cortex as this has been destroyed by differential compaction after lithification of the core (see later). Lewes Tubular Flint, *Micraster leskei* Zone, Upper Turonian, Shoreham cement Works, Sussex, England. C – *Zoophycos* nodule of the Black Flint Group with a well-developed white cortex. Turonian or higher. D – Flint of the Red Group (CVJRM19, Tables 1, 2–4) with an inner red and outer black zone in the core. The cortex consists of an inner pale grey zone and an outer white zone. Turonian, Helgoland.

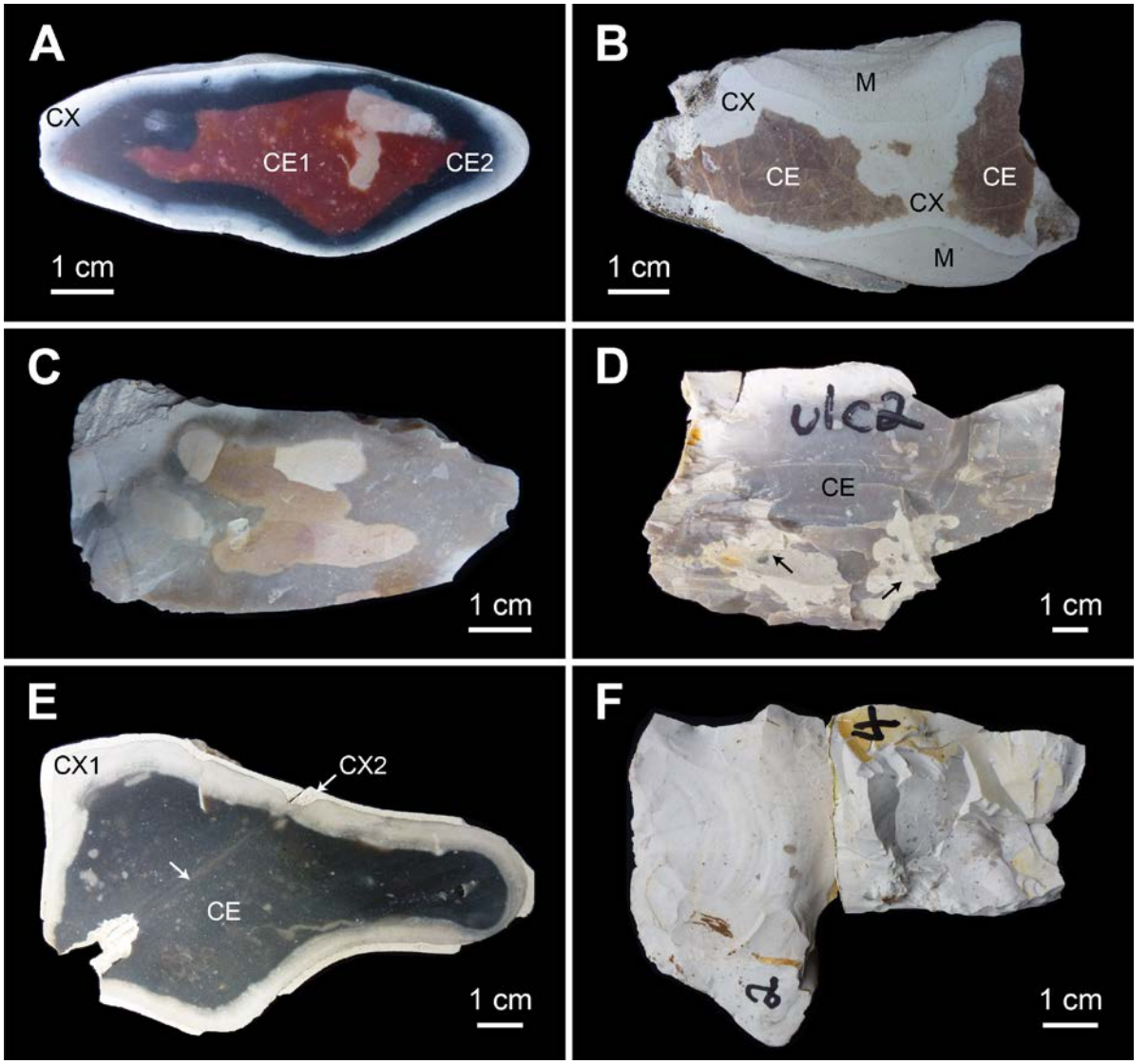

Text-fig. 5. Flint groups and varieties. A – Flint of the Red Group with a red inner (CE1) and a black outer (CE2) core with a grey to white cortex, Turonian. Duene Island, Helgoland, Germany. B – Brown Flint Band (BFB 1–3, Tables 1, 2–4) with core (CE), cortex (CX) and chalk matrix (M), Lower Cenomanian. Speeton, England. C – Ferruginous Flint Band (Tables 1, 2–4), Turonian. Melton Ross, Lincolnshire, England. D – Grey carious flint (Text-fig. 15, Ludborough Tabular Flint Band (Tables 6, 7), Turonian. Ulceby Vale Quarry, Lincolnshire, England. Core of grey carious flint with areas (arrows) of incompletely replaced chalk, Ludborough Tabular Flint Band (Text-fig. 15, Tables 6, 7), Turonian. Ulceby Vale Quarry, Lincolnshire, England. E – Core (CE) of a Grey flint cross-cut by a sealed flint fracture (arrow) with two generations of cortex development (CX1, CX2), prior to and after fracturing. Turonian. Baldock-Bypass, Cambridgeshire, England. F – White flint, base of the Flamborough Chalk Formation, Middle Santonian. Selwick Bay, Yorkshire, England.

TYPES OF ALPHA-QUARTZ FLINTS AND CHERTS

The general structure of flints (Chalk) and cherts (Upper Greensand) is similar. Both consist of a dense vitreous core – usually grey or black, rarely red or brown – often surrounded by a more porous cortex of paler colour ranging in texture from porcellaneous to gritty (Text-fig. 4). The outer part of the cortex may appear macroscopically transitional to, or sharply defined from, the surrounding strata. The 'model core' represents both the complete pore-filling of the original sediment and the replacement of its calcium carbonate components by silica. Other silicate components, if present, for example glauconite, quartz, feldspar grains, are usually preserved as

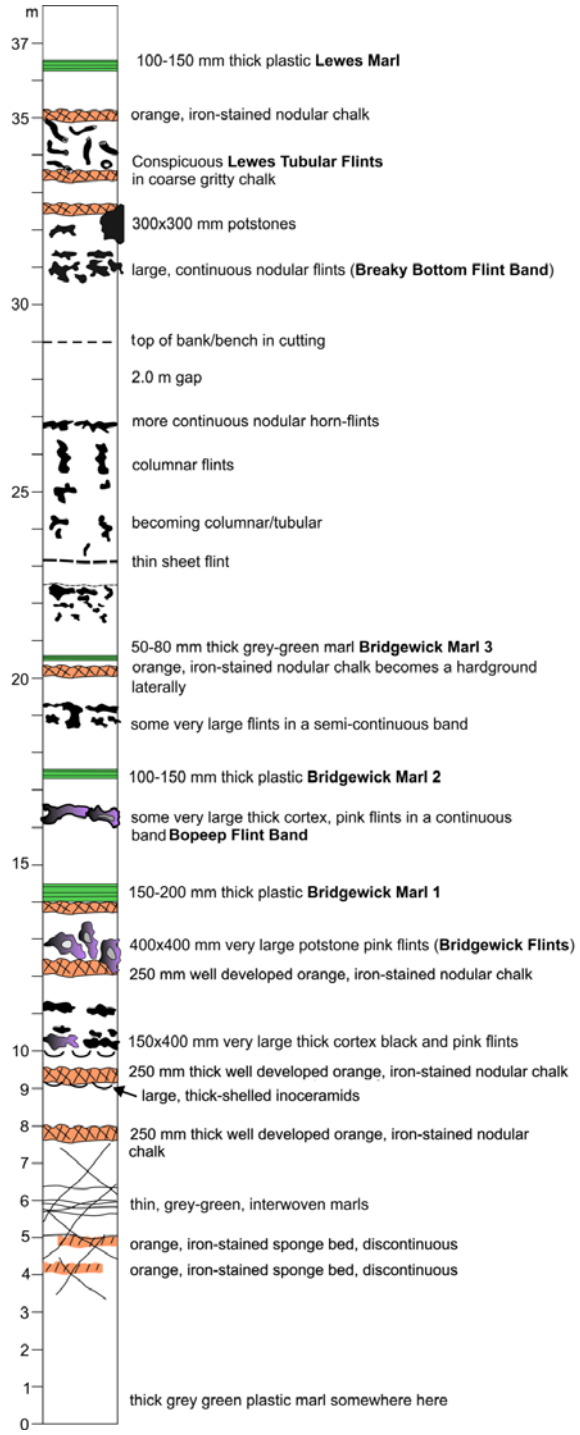

little-altered or pristine grains. The 'model cortex' represents the partially silicified host sediment with only part of its original pore space in filled with silica. The width of the cortex ranges from practically nothing to being wider than the core, and in some instances there is no core and the flint or chert consists only of cortex-like material (white flints and quasi or incipient cherts, see later). Macroscopic and microscopic evidence indicate that many flint nodules grew by extension from a central core region that encroached upon the surrounding sediment, with the cortex representing the original zone of active 'transformation.' The term cortex must be clearly differentiated from the "Patina," a term used by archaeologists (e.g. Shepherd 1972; Rottländer 2007) to describe the recent weathering discolouration and textures that develop particularly on the surfaces of broken or worked flints. Patina has, however, been used geologically by Gallois (2016, see later) for certain flint horizons in the Grimes Grave flint mining area (e.g. Pink Patina Flint Band, Chalky Patina Flint Band).

Eight groups of alpha-quartz flints are recognised in the Chalk based on colour, paramagnetic minerals, core/cortex definition, size, relationship to bedding, and location. Similar groupings of chert are present in the Upper Greensand but have not been considered in detail.

Red Flint Group: These are rare with limited distribution, best known from the Turonian chalk, particularly of Helgoland, an island in the North Sea (Text-fig. 2) and also from boreholes in the North Sea (Schmid 1986, p. 4). They are nodular in form, their cores have an inner red zone with an outer black one, surrounded by a white cortex (Text-figs 4D, 5A). Red flints have been interpreted as having started their development in the oxic zone of diagenesis at a time when the sediment contained considerable amounts of $Fe(OH)_3$, possibly of hydrothermal origin (Jeans *et al.* 2016). Other Turonian flints may display a reddish or pinkish tinge. Gallois (2016, p. 457) has recorded the Pink Patina Flint Band, at Grimes Grave. There are examples in the Bridgewick Beds, southern England and at Criel-Plage, Normandy, France (Text-fig. 6). The Turonian Ferruginous Flint Band of Lincolnshire has a pinkish tinge (Text-fig. 5C) and contains the

Text-fig. 6. Field section log for the Autoroute 16 cuttings near Dannes and Camier (Nord Pas De Calais and Somme) in the Upper Turonian Chalk (based on Mortimore 2019, fig. 14, p 39). The sequence can be matched precisely in the Lewes Nodular Chalk of southern England with the recognition of the Bridgewick Marls (1, 2 and 3) and the overlying Lewes Marl. Pink/purplish flints occur at three levels – at 10–10.5 m, 12.5–13.5 m (Bridgewick Flints), and at 16.0–16.5 m (Bopeep Flint Band). The purple or pink colour is present in the same flint bands in the coast sections between Criel Plage and St-Pierre-en-Port in Upper Normandy and at the Bridgewick Pit, Lewes, Sussex. However, when traced further afield these flint bands change their colour to black becoming the Floorstone (Bopeep Flint Band) and the Rough and Smooth flints (Bridgewick Flints) of Grimes Grave, Norfolk.

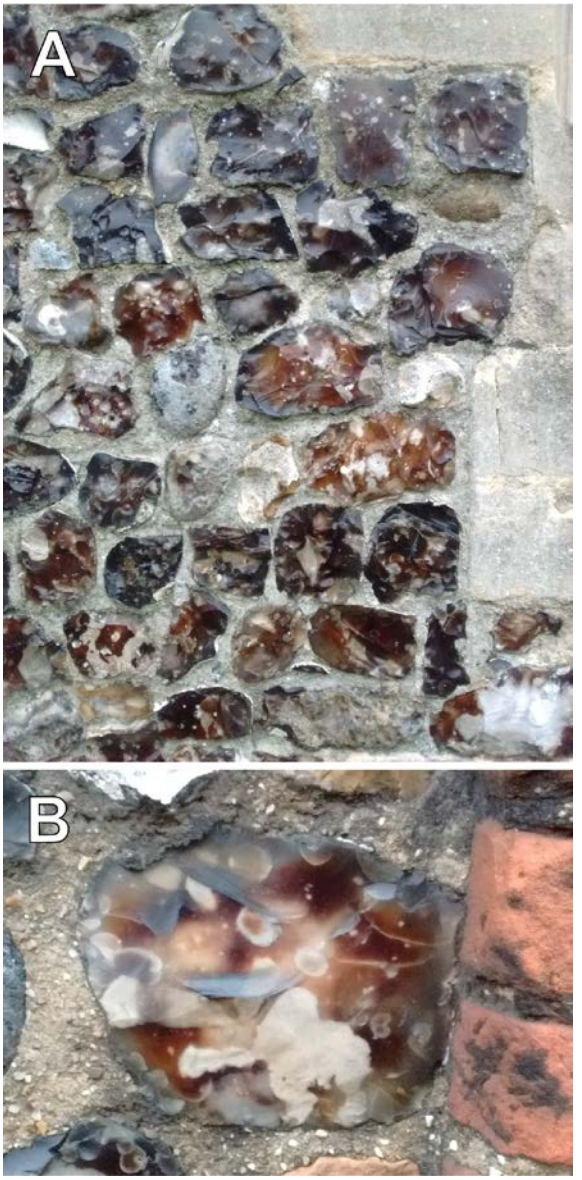

Text-fig. 7. Red knapped flints in the City of Norwich, England. A – Church of St Peters, Hungate. B – Norwich Cathedral, Close wall (photos: Tim Holt Wilson)

oxidized remains of small iron sulphide crystals. The "Craie à *Micraster normanniae*" at Etretat (Normandy, France) contains red brown flint bands in the Senonian Chalk (Kennedy and Juignet 1974, p. 5). Knapped flints with a distinct red glassy appearance have been recorded occasionally in mediaeval buildings in the City of Norwich (Text-fig. 7).

Brown Flint Group: Brown flints are rare in England**,** known only definitely from the Brown Flint Band in the Cenomanian chalk of Speeton, Yorkshire (Jeans *et al*. 2016, p. 236). The flints are nodular in overall form, the core is brown, often irregular in shape and is surrounded by a wide cortex (Text-fig. 5B). Lateral changes take place as this band is traced eastwards along strike at the base of the Speeton Cliffs. First seen at Red Cliff the colour of the core is brown (Text-fig. 5B), this is still recognizable at Pink Cliff but at White Cliff the core colour has changed to grey and pyrite crystals are present both in the flint and the chalk matrix (Jeans *et al*. 2016; Text-fig. 8 for locations). Further examples of this group could be the Chalky Patina Flint Band with their cores of "dark coffee brown translucent flints with few inclusions" and simple cortices that were recorded by Gallois (2016, p. 457) in boreholes sunk in the Turonian Chalk of Grimes Graves (Text-fig. 1). Brown and reddish-brown flints of Danian age are known from Faxe, Southern Zealand, Denmark where they may be associated with bryozoan debris (Text-figs 8, 9, 10).

Högberg and Olausson (2007) record brown flints in the Chalk from Vokslev, NE Jutland, Denmark. The nature of the brown colouring pigment is not known but could reflect the presence of fulvic and humic acids that are derived from the breakdown of chlorophyll and related plant pigments involved in photosynthesis. A similar situation occurs with the earliest calcite cements developed during diagenesis in organic-rich marine sediments, which are invariably of brown colour.

Black Flint Group: Black flints, with grey flints, appear to be the dominant flint variety in the Chalk of Denmark and England. They occur both as nodules, tabular flints and as veins and sheets cross-cutting or approximately parallel to the bedding (Text-fig. 11). The core is vitreous, black or very dark grey, sometimes with ghosts of bioturbation structures (Text-fig. 12A–C). A cortex may or may not be present. Black flints are best developed in soft chalks that have undergone minimal diagenetic modifications such as the Maastritchian to Danian chalks of Denmark and the Turonian chalk of eastern England, although they do also occur in the hardened chalk of Northern Ireland (Fletcher 1977: see later). Micheelsen's (1966) classic study of the physical and chemical composition and properties of flint was based on dark flints from Stevns, Denmark. His study provided data on density, grain size, thermal properties etc, but unfortunately neither the location of his samples nor the precise details of where they were collected are known. Consequently, for comparative purposes, a standard 50×50×50 mm cube of a near perfect black flint cut from the Floorstone, a particular tabular flint band of Turonian age mined at Grimes Graves,

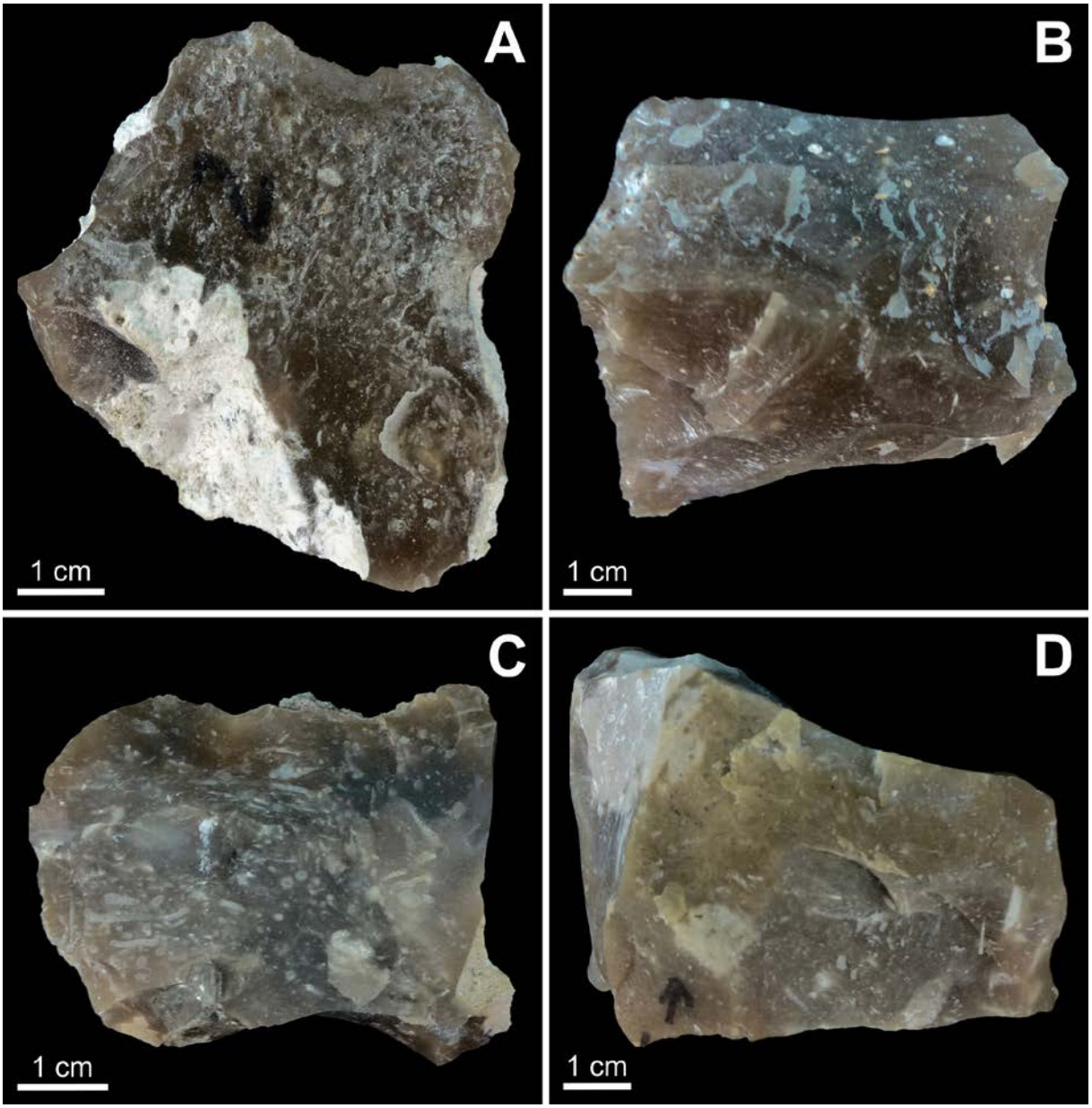

Text-fig. 8. Flints of the Brown Flint Group, Danian. Faxe, Denmark. A – Sample Faxe 4 (Tables 1, 2–4). B – Sample Faxe 6 (Tables 1, 2–4). C – Sample Faxe 3 (Tables 1, 2–4). D – Sample Faxe 5b with a sugary texture (Tables 1, 2–4).

Norfolk, has been used as a standard (Text-fig. 12A). The mineralogical composition of this flint cube determined by XRD (see Methods) was 20.1% moganite and 79.9% alpha-quartz. Assuming (1) it contained 1.27% free H_2O, the value used by Micheelsen (1966, p. 291) for his dark flint, and (2) the specific gravities of alpha-quartz and moganite are respectively 2.65 and 2.55, the 50 mm cube of Floorstone should by calculation have weighed 348.84 grams, whereas it weighed 346.98 grams.

Grey Flint group: Similar in form to black flints, grey flints occurring as nodules, tabular flints and as veins cross-cutting or parallel to the bedding. The core is somewhat less vitreous and there is more evidence of bioturbation structures. A cortex is usually present. Every gradation exists between black and grey flints. Grey and black flints are the commonest varieties of flint in southern England. Examples from the Cenomanian chalk of Dorset, the Turonian chalk of the Baldock Bypass (Text-fig. 5E), and

Text-fig. 9. Sample Faxe 8 (Tables 1, 2–4) of the Brown Flint Group with paler patches of coarser quartz, Danian. Faxe, Denmark.

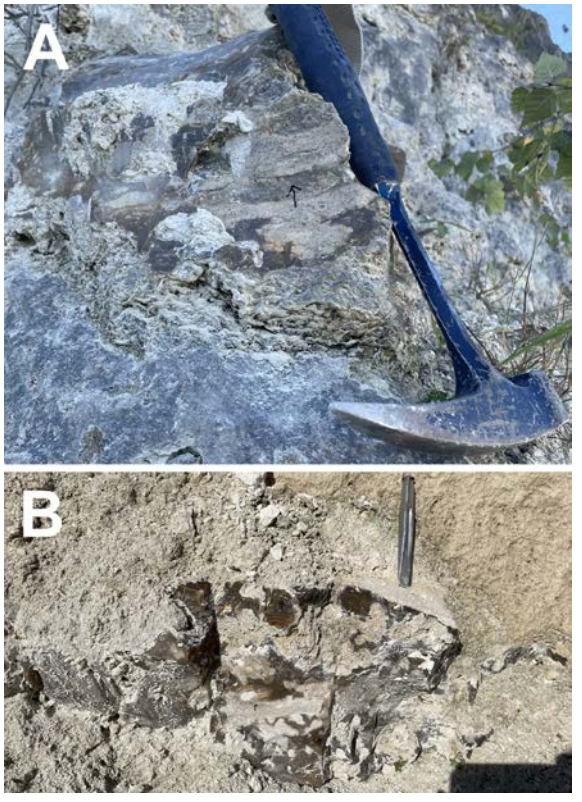

Text-fig. 10. Flints of the Brown Group. Danian. Faxe, Denmark. A – Brown flint-bryozoan reef complex with quartz-lined vug. B – Incompletely developed brown flint nodule.

the Campanian chalk of Newhaven, Sussex (Text-fig. 4A) have been investigated.

Grey Carious Flint Group: This group is characterized by poor differentiation between core and cortex. They are typically pale grey showing much evidence of bioturbation structures and incomplete replacement and pore-filling by silica of the original sediment (Text-fig. 5D). Grey carious flints display the same range of morphology as black and grey flints. They are abundant in the hardened chalks of northeast England where the bulk specific gravity of the chalk ranges from 2.11 to 2.24 (Jeans *et al*. 2014, table 3, values for Unit A, Louth Member). Grey carious flints occur also at certain horizons in the Chalk of southern England (Rory Mortimore, personal communication). All the samples analysed are from the disused Ulceby chalk pit in North Lincolnshire (Text-fig. 13) and are of similar Turonian age to the black flints of Grime's Graves in Norfolk.

White Flint Group: These show no core and their appearance is of flint made only of cortex displaying a porcellaneous texture on fracture surfaces (Text-fig. 5F). Their shape suggests they replicate bioturbation structures in the chalk sediment. We have investigated examples from near the base of the Santonian Flamborough Chalk Formation of Selwicks Bay, Yorkshire (Text-fig. 2). The relationship of these white flints to the porcellanites of the Danish Chalk is not clear, Madsen and Stemmerik (2010) refer to them as nodules although they are only known from boreholes where they are reported as tabular bodies. Superficially similar white flint is known from offshore Denmark and this is considered to occur in beds that are laterally continuous for 100's of metres and more (Jakobsen *et al*. 2000): they have been interpreted as primary deposits of silica spherules, precipitated in the lower part of the water column of the Chalk Sea admixed with coccolith debris (see later). The calcite contents of the Danish porcellanites are in the 18–21% range (Madsen and Stemmerik, 2010) in contrast to the lower values (5–9%) for the white flints we have investigated.

Sponge associated flint Group: Whole or fragmentary siliceous sponges may occur in flints. There is the long-standing assumption that siliceous sponges and their debris may have acted as seeds for the development of flints. Yeoman (2019) has suggested that some paramoudras are in fact silicified sponges – the evidence is weak. There is little doubt that the dissolution of siliceous sponge debris as well as radiolaria, diatoms, and other siliceous organisms of the Chalk Sea played a general role in providing the silica content of the sediment's pore

Text-fig. 11. Upper Maastrichtian Chalk in the sea cliffs at Rodvig Stevns, Denmark with black flints with narrow cortices occurring both as nodules and "nodular beds" arranged parallel to the overall bedding and also as high angle veins (arrows). Walking stick 80 cm. The insert shows a plexus of narrow black flint veins.

waters in which flints developed. A flint enclosing a near complete siliceous sclerosponge (Text-fig. 14) from the Campanian Newhaven Chalk Formation, Sussex has been examined for evidence of variation in its silica mineralogy and whether there is any evidence that the original biogenic silica of the sponge played a role in this variation. Samples of the separate spongiform body, when embedded in flint, and the cortex to the overall flint showed little variation ranging from a moganite content of 12–17% and alpha-quartz of 83–88%. This is in contrast to the silica mineralogy of the siliceous sponge remains in the opoka facies in Poland that are typically preserved as opal-A/CT (Jurkowska and Świerczewska-Gładysz 2020a, p. 15).

North Sea Flint Group: Six flint samples from the Danian Chalk of the Danish North Sea have been analyzed. They come from depths between 2056 and 2827 metres in wells Nana-1, Rigs-1, and Sif-1 (Text-fig. 2). Five of the samples were from porcellaneous flint bands such as reported by Lindgreen *et al.* (2010) in which there was no evidence of dark vitreous core material. One sample was from a dark vitreous flint, equivalent to black flint.

Clay-grade quartz: The quartz fraction (<1 μm) was extracted from five marl bands interbedded in the Lower and Middle Cenomanian Chalk of Speeton, Yorkshire. Grain morphology ranged from spherical to botryoidal with some possibly more angular grains (Text-fig. 15). Similarly shaped spheroidal siliceous silt size grains have been described from the acid insoluble residues (0.6–3.7%) of very pure chalks from Sussex that ranged in age from the Turonian to Campanian (Weir and Catt 1965). In these samples from the Santonian *Marsupites testudinarius* Zone over 60% of the total acetic acid insoluble residue consisted of fine silt size silica spherules (2–20 μm; Text-fig. 16A). The XRD pattern was close

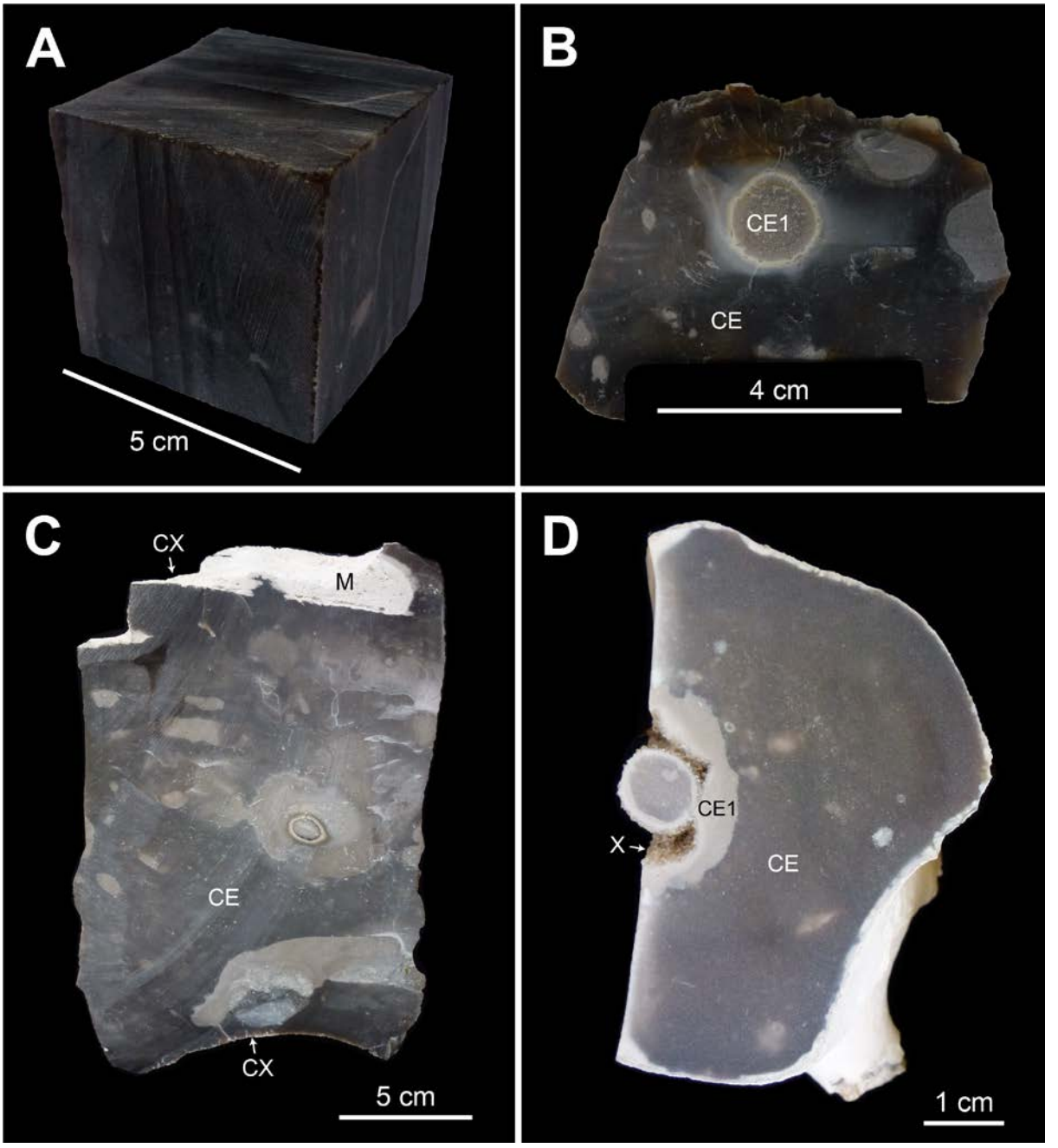

Text-fig. 12. Black and Grey Group Flints. A – 50×50×50 mm block of the black flint core from the Floorstone used as a standard in this study (Tables 2–5), Brandon Flint Series, Turonian, Grimes Graves, Norfolk, England, B – Fragment of a core (CE) of a black flint displaying remnant traces of bioturbations as paler grey patches of coarser grain including a circular patch (CE1) of coarse quartz, Beeston Chalk Formation, Upper Campanian, Caistor St Edmunds, Norfolk, England. C – Core of a "black" to grey flint displaying various burrow traces preserved in paler coarser grained flint. Note the very thin cortex (CX) and adhering chalk matrix (M). Beeston Chalk Formation, Upper Campanian, Caistor St Edmunds, Norfolk, England. D – Vug in the core (CE) of a grey flint lined with a very pale grey zone of coarser quartz (CE1) and then by a white zone of macroscopic quartz crystals (X) with crystal faces terminating into the vug. Seaford Chalk Formation. Coniacian, Seaford Head, Sussex, England.

to low-temperature tridymite, the presence of an alkali-soluble phase was linked to amorphous silica (Text-fig. 16B) but this was prior to the recognition of moganite by Flörke *et al.* (1976, 1984). Chemical analysis suggested they were extremely pure silica although some aluminium may be incorporated in the

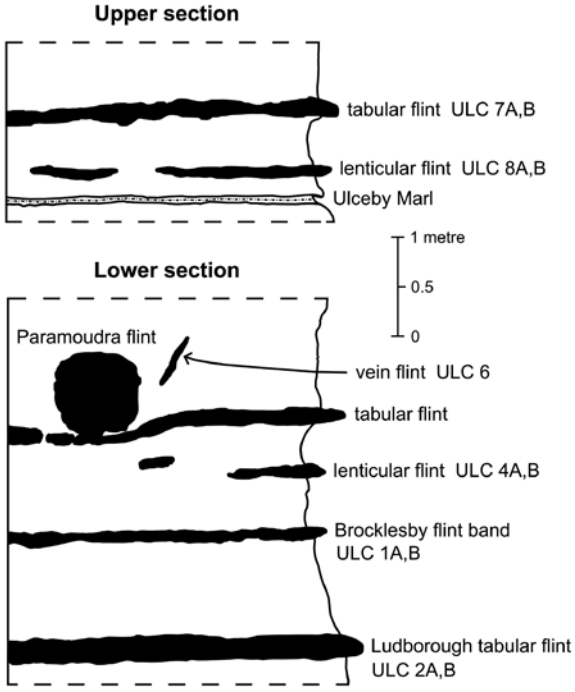

Text-fig. 13. Flint and sample horizons in the hard Turonian chalk of the Northern Chalk Province. Ulceby Vale Quarry, Lincolnshire, England.

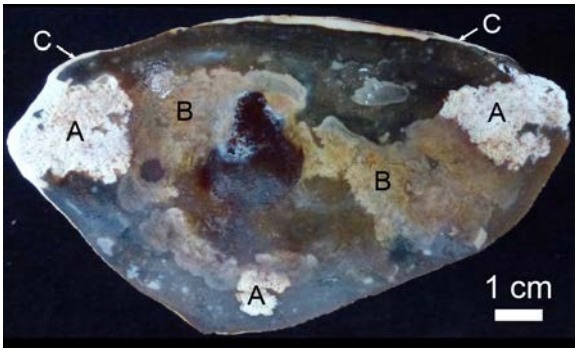

Text-fig. 14. Medial section through a flint nodule enclosing a sclerosponge with sampling locations; basal Campanian or uppermost Turonian Chalk. Bridgewick pit, Newhaven, East Sussex, England. A – RM5a, siliceous sponge. B – RM5b, siliceous sponge in flint matrix. C – RM5d, thin cortex to flint nodule.

tridymite. Snowflake-shaped euhedral αlpha-quartz crystals were present (Text-fig. 16C).

Cherts: Similar in form to flints displaying a similar range of macroscopic variation. They may occur either in nodular or bedded bodies generally arranged parallel to the bedding (Text-figs 17, 18), or as veins cross-cutting the stratigraphy. Some cherts do not contain a vitreous core; these are referred to as quasi or incipient cherts, they are equivalent to the White Group of flints. Cherts are present in the sandy lithofacies of the Lower Greensand and Upper Greensand of Aptian and Albian age (Hinde 1885; Hayward 1932; Richardson 1947; Humphries 1957; Padgham 1970; Hart 1973).

MINERALOGY, CHEMISTRY, PARAMAGNETIC PROPERTIES OF FLINTS AND CHERTS

All samples have been mineralogically and crystal size analysed by X-ray diffraction. Examples of the red, brown, black and grey flint groups have been analysed by wet chemical methods. Chemical composition of the nano silica particles have been determined by electron microprobe techniques. Bulk specific gravity measurement, calcium carbonate content and stable isotope analysis were carried out on examples of the carious grey and white flint groups and their chalk matrices. The results of all these analyses are tabulated in the Appendix 1. Examples of red, brown, black, grey, carious grey and white flints have been tested for the presence and type of paramagnetic minerals they may contain.

Analytical methods

Sampling: This was restricted to fresh unweathered flint and chert samples. Samples from nodules were either cut or drilled out using diamond impregnated saws or drilling tools. Flint flake samples were coarsely crushed. Sub-samples were finely ground (<125 μm) using an agate pestle and mortar, decalcified in 1. molar acetic acid, washed in deionized water and dried.

XRD mineralogical and crystal size analysis: Approximately one hundred samples of different varieties of flint and chert were characterized by X-ray diffraction (XRD).

The finely ground decalcified samples were mounted on glass slips for analysis. Powder diffraction data was collected on three instruments at the Department of Earth Sciences, University of Cambridge.

Instrument 1: D8-ADVANCE Bruker diffractometer operating in Bragg Brentano geometry at 40 KV × 40 mA, equipped with a primary Ge monochromator for Cu Kα_1 and a Sol-X solid state detector. Collections conditions: 17–23° in 2θ, 0.02° step size, divergence slits 0.2 mm, receiving slit 0.2 mm, 50 seconds per step; 66.5–70.5° in 2θ, 0.03° step size, divergence slits 0.2 mm, receiving slit 0.2 mm, 60 seconds per step.

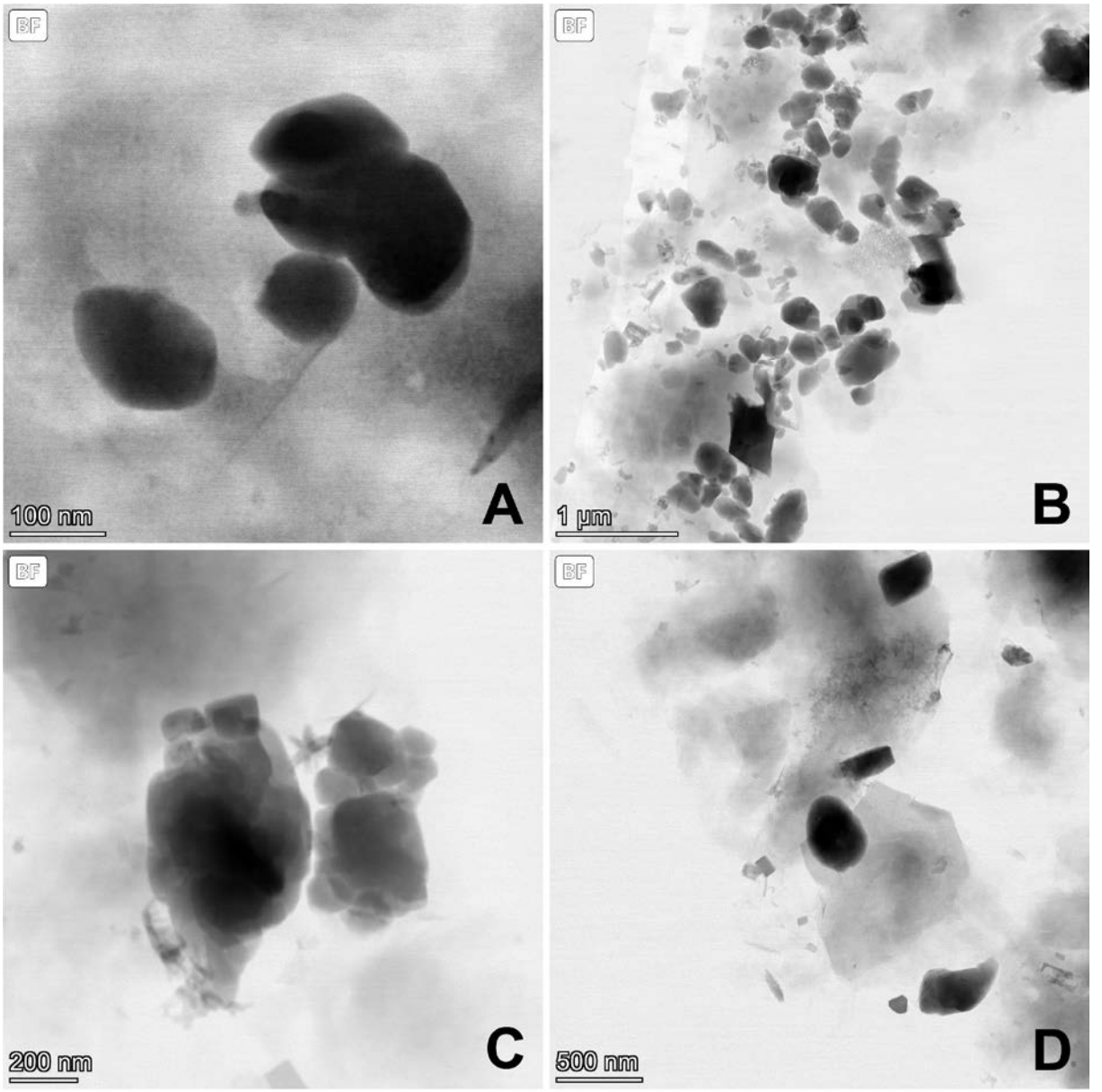

Text-fig. 15. Electron micrographs of silica nano-particles from Cenomanian chalks and marls. Speeton, Yorkshire, England. A – Single and aggregate subspherical nano-particles of silica, sample Ysa17. B – Subspherical nano-particles of silica and grains of other minerals, sample Ysa17. C – Aggregate grains of silica nano-particles, Ysa17. D – Sub spherical silica nano-particle and poorly defined clay minerals, sample Ysa55.

Instrument 2: D8-ADVANCE Bruker diffractometer operating in Bragg-Brentano geometry at 40 KV × 40 mA, equipped with a Vantec linear position sensitive detector set at a 3° aperture, using Cu Kα radiation. Collections conditions: 17–23° in 2θ, 0.02° step size, divergence slits 0.2 mm, 1.5 seconds per step; 66.5–70.5° in 2θ, 0.03° step size, divergence slits 0.2 mm, 2 seconds per step.

Instrument 3: D8-ADVANCE Bruker diffractometer operating in Bragg-Brentano geometry at 50 KV ×40 mA, equipped with a Lynxeye XE-T PSD detector, using Mo Kα radiation. Collection conditions: 5–40° in 2θ, 0.02° step size divergence slits 0.2 mm, 1.0 seconds per step. Quartz and moganite Rietveld refinements were performed with TOPAS Academic V6 software (Cohelo 2007). The instrumental parameters were refined on LaB6 NIST standard 660b for each instrument. Quartz and moganite crystal structures

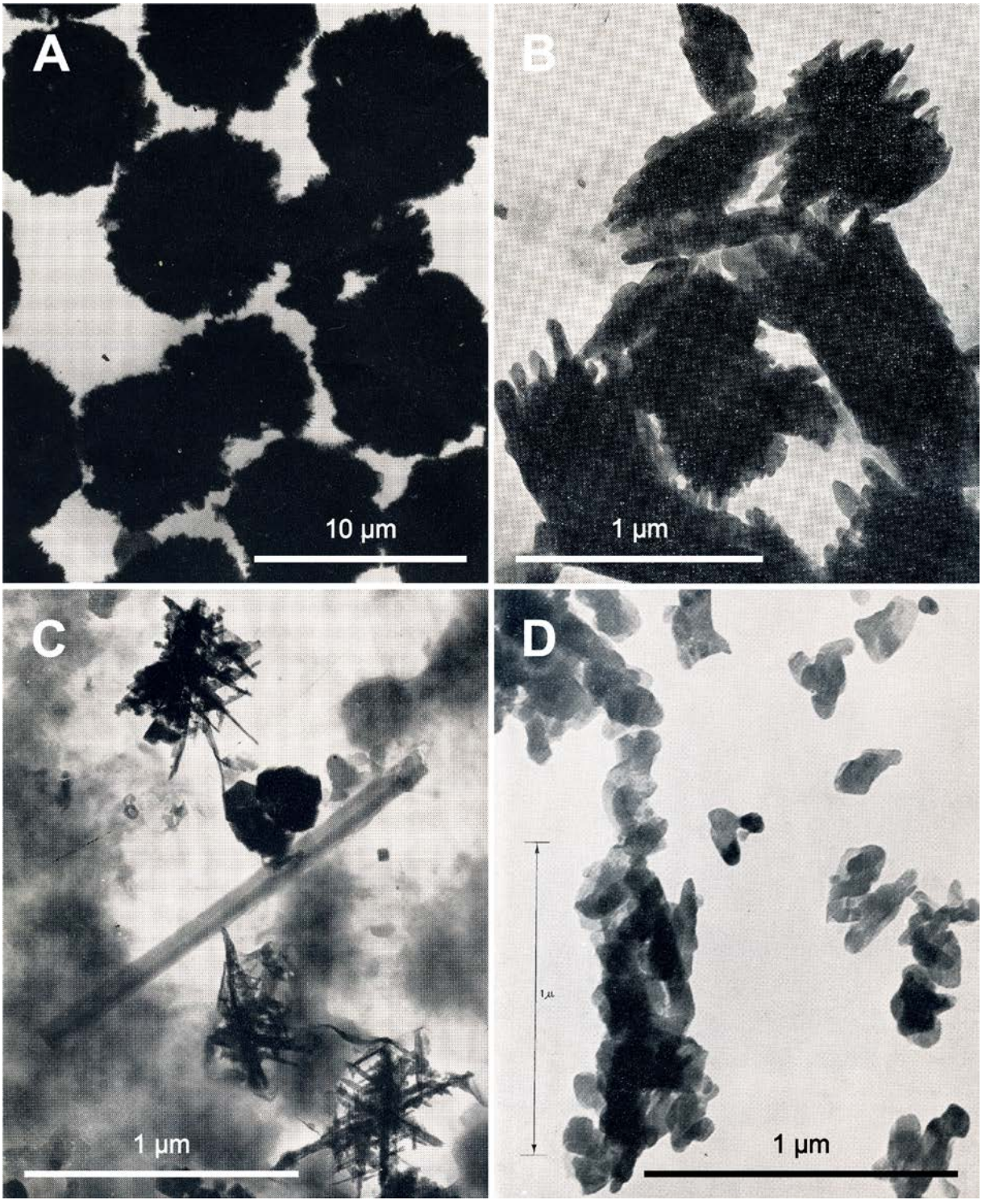

Text-fig. 16. Electron micrographs. A – Opaline silica/tridymite microspherules from the fine silt fraction, *Marsupities testudinarius* Zone, Santonian (Weir and Catt, 1965, p. 102). B – Quartz crystals with parallel elongated projections from the residue of the bisulphate fusion of the medium clay fraction, *Offaster pilula* Zone, Campanian (Weir and Catt, 1965, p. 102). C – Quartz crystals with open hexagonal structure, a lath-shaped mineral resembling palygorskite, apatite subhedra and a background of montmorillonite laths from the clay fraction, *Marsupities testudinarius* Zone, Santonian (Weir and Catt, 1965, p.102). D – Fine fraction of a decomposed flint, Lower Bracklesham Sands, Tertiary. Hampshire, England (Fairbairn and Robertson, 1972, p. 174).

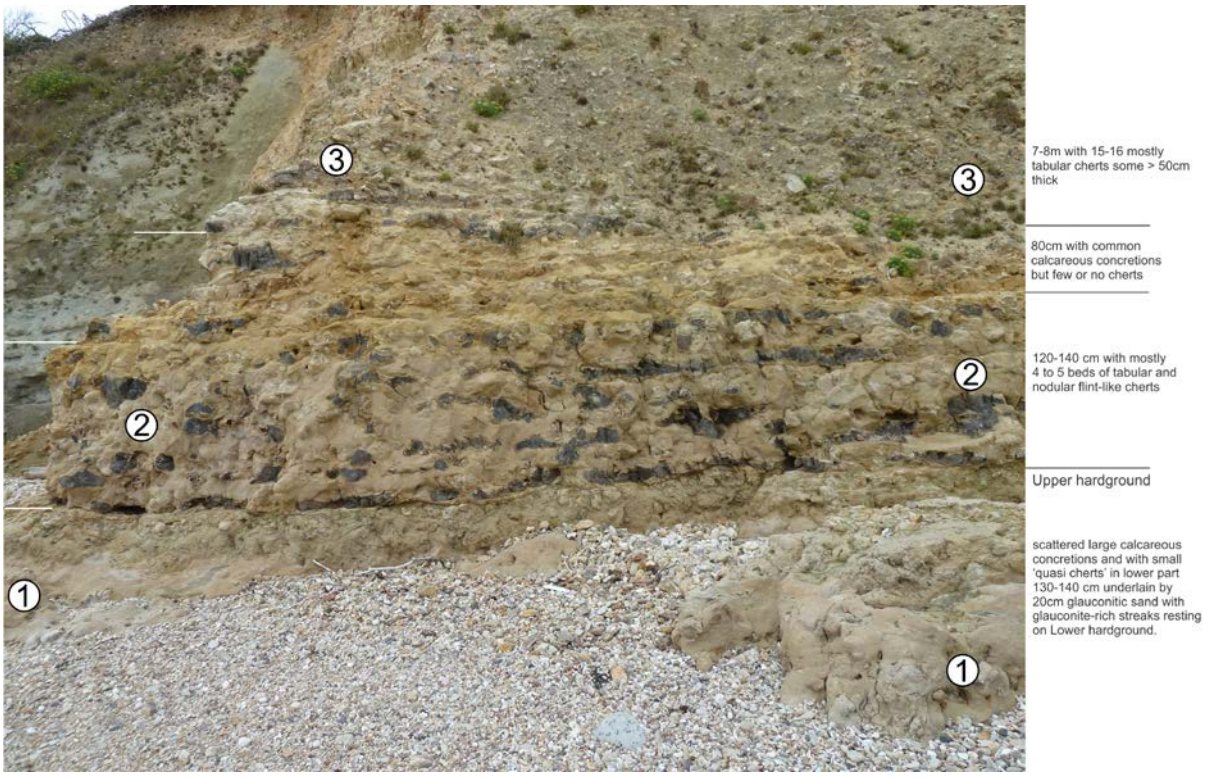

Text-fig. 17. Chert silicifications in the Upper Greensand Formation (Upper Albian) at Culverhole, Dorset. UK. (photo, lithologies: Ramues Gallois).

Text-fig. 18. Details of the Upper Greensand sequence at Culver Hole, Dorset**:** More detailed view of pale sandstone with Black chert nodules with narrow corticies in a pale sandstone. This is overlain by a bed containing incipient cherts, which lies beneath a pale sandstone with "bedded' grey chert with thick cortices. (photo: Ramues Gallois).

were obtained from the Inorganic Crystal Structure Database, ICSD, (Allmann and Hinek 2007) (reference codes: 90145 and 67669 respectively). The quantification analyses were performed on the 17–23° range for Cu Kα and 5–10.5° range for Mo Kα. No structural parameter was refined. The following parameters were refined: one Lorentzian peak shape function with a single parameter relative to crystal size (Cohelo 2007) convoluted with the Pseudo-Voigt function as refined on the LaB6 NIST standard for each crystal phase; scale factors; specimen displacement; one single parameter to account for background.

Text-fig. 19 illustrates the XRD pattern of a typical black flint in the 8.5–10.2° 2θ angular range for Mo Kα radiation. In some samples trace amounts of calcite, kaolinite and possibly tridymite (broad peak at 10.9° 2θ) are present.

Wet chemical analysis: Major, minor and REE element analysis was performed on thirty-two flint samples at the Department of Earth and Environmental Sciences, University of Greenwich.

Decalcified finely ground samples (0.5000 ±0.0005 g) were digested using the HF/$HClO_4$ methodology outlined in Jarvis and Jarvis (1988). This routine facilitates the removal of silicon, reducing matrix loading on the analytical instrumentation. Once digested, samples were analyzed for a suite of elements using a combination of a Thermo ICAP 6500 ICP-OES and a Thermo X2 ICP-MS. Calibration for all analyses was achieved using matrix matched standards prepared from ICP grade single element standards. The limits of determinations for all rare earth elements were found to be less than 0.1 mg/kg. A determination of expanded uncertainty (K = 2.95% confidence) derived from eleven measurements of duplicate preparations of a number of reference materials over five and a half days established uncertainty values of ±10–12% for the rare earth elements. The calculation of the cerium anomalies has been based on the following procedures:

$$\text{Ce anomaly} = \frac{\text{Ce s/n}}{(0.8 \times \text{La s/n}) + (0.2 \times \text{Sm s/n})}$$

Ce s/n, La s/n and Sm s/n refer respectively to the shale-normalised values of cerium (Ce), lanthanum (La) and samarium (Sm) for the particular sample relative to the Cody Shale (SCo-1) standard. Ce*(DCF) refer to the cerium anomalies associated with the decalcified flint material.

$$\text{Eu anomaly} = \frac{\text{Eu s/n}}{(5.40 \times \text{La s/n}) + (4.432 \times \text{Gd s/n})}$$

Eu s/n, Sm s/n and Gd s/n refers respectively to the shale-normalised values of europium (Eu), samarium (Sm) and gandolinium (Gd) for the particular sample relative to the Cody Shale (SCo-1) standard.

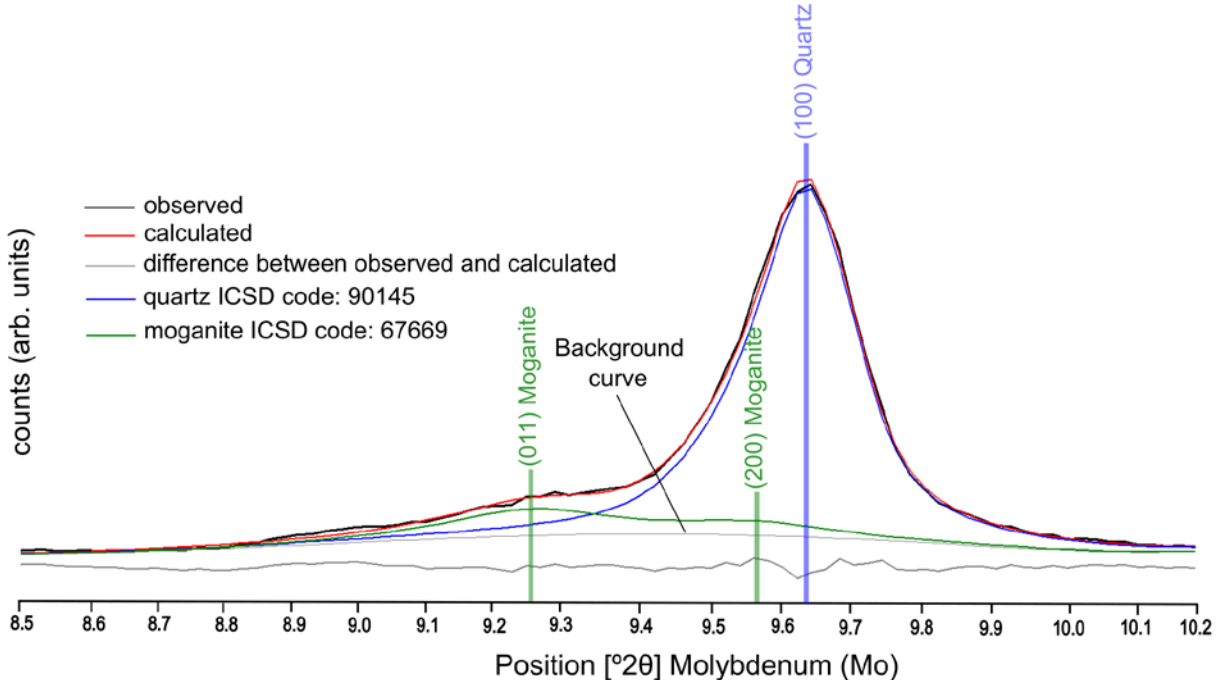

Text-fig. 19. Example of a XRD pattern of a flint in the 8.5–10.2° 2θ for Mo Kα. The vertical lines represent the expected peaks for quartz and moganite. The colored curves represent the result of the Rietveld refinement to fit the observed data in black.

Eu*(DCF) refers to the europium anomalies associated with the decalcified flint sample.

Bulk specific gravity measurement: This used the procedure described by Jeans (1980, p. 155; similar to B.S. 1377, 1975) with wax coated chalk or flint blocks (dried at 105ºC) weighed in air and then in water. Calcium carbonate content was carried out gravimetrically on the <125 μm ground sample using 1 molar acetic acid and collecting the insoluble residue on Whatman no. 42 filter paper, drying to constant weight at 105ºC.

Stable isotope analysis: This was carried out on both bulk samples of chalk and flint-containing chalk at the Godwin Laboratory for Palaeoclimate Research, Department of Earth Sciences, University of Cambridge. Samples were analysed for $^{18}O/^{16}O$ and $^{13}C/^{12}C$ using either a Micromass Multicarb Sample Preparation System attached to a VG SIRA Mass Spectrometer (prefix S) or a Thermo Electron Kiel Preparation Device attached to a MAT 253 Mass Spectrometer (prefix K). Each run of 30 samples was accompanied by ten reference carbonates and two control samples. The results (Table 5) are reported with reference to VPDB standard and the precision was better than ±0.6 per mil for $^{18}O/^{16}O$ and ±0.06 per mil for $^{13}C/^{12}C$.

Separation and chemical analysis of nano size silica particles from Chalk: This was carried out in the Departments of Chemical Engineering and Nanotechnology, and Earth Sciences, University of Cambridge. Results are shown in Table 10. Initial sample concentration made use of the different flocculation properties of fine-grained silica and the clay minerals in the <1 μm fraction of the acid-insoluble residues of the Chalk. Samples were decalcified with 1 molar acetic acid and then sequentially and centrifugally washed with deionized water until the point just prior to dispersion when a slight cloudiness/unclearness of the supernatant solution is present whilst the clay minerals are still flocculated. This cloudiness reflects the different flocculation/dispersion properties of fine silica and other mineral particles with much lower surfaces charges compared to those of the various clay mineral groups. This unclear supernatant liquid was siphoned off and its contents were concentrated and further purified by centrifugal washing and flocculation. A similar separation of fine silica can be achieved by using the reverse process during the flocculation of a dispersed mixture of clay minerals and silica particles. After the initial flocculation using a drop or two of concentrated calcium chloride solution, the supernatant solution will not be completely clear and will contain a concentration of fine-grained silica and other mineral particles with similar weak flocculation properties. Samples for analytical electron microscopy were prepared by diluting the silica particle concentrate until visibly clear, then sonicated for 30 mins, apply 3 μL of suspension to 300 mesh Cu grids with continuous carbon film, and dry fully. Energy dispersive spectroscopic analysis was carried out using a Thermo Scientific Talos F2000X G2 microscope. Samples for examination by a TESCAN MIRA3 FEG-scanning electron microscopy were prepared by diluting the silica particle concentrate until the suspension was visibly clear, then treated in an ultrasonic bath for 30 mins; 2 μL of this suspension was applied to a glass cover slip, dried, followed by two similar applications. The dried sample was coated with 10 nm Pt film using a Quorum Technologies Q150T ES coater.

Magnetic measurements: These were undertaken at the Department of Earth Sciences, University of Cambridge. The identification of magnetic particles in the flint samples was based on hysteresis loops, direct-current (DC) demagnetisation curves, and first-order reversal curves (FORCS) (Pike *et al.* 1999; Roberts *et al.* 2000) determined at room temperature using a Princeton Measurement Corporation MicroMag Accelerating Magnetometer (AGM). Samples were cut into 4 x 4 mm cubes and mounted on the probe. A total of 513 FORCs were acquired for samples that had a significant magnetic signal at 1 mT field step and an averaging time of 300 ms in discrete mode. FORCs were processed on FORCinel (Harrison and Feinberg 2008) using the VARIFORC algorithm (Egli 2013).

ANALYTICAL RESULTS

Red Flint Group

Mineralogy (Table 1): The Helgoland red flints investigated displayed little difference in the moganite content between the red inner core (15.7–16.7%) and the black outer part (13.1–16.6%). The pink-tinged Turonian Ferruginous Flint from Melton Ross, Lincolnshire has a moganite content of 9% within the range (4.3–11.4%) of other Turonian flints from the grey and carious flint group (see below) that are associated with the hardened chalks of Lincolnshire. Crystal size for moganite is 10–14 nm and for alpha-quartz 35–50 nm.

Chemistry (Tables 2–4): There are only four analyses, three are from the same flint. The silicon content in all samples is above 99%. Other major elements (Ti, Al, Fe, Mn, Mg, Ca, Na, K, P) make up

the remaining 1 percent. Compared to other groups of flints they display enhanced values of Al_2O_3, Fe_2O_3, and MnO_2. Minor and trace elements (Ba (2–5 ppm), Be, Cr, Cu, Ni, Sr, Co, V, Y, Zn, Zr and REEs) are all present. The cerium anomaly ranges from 1.0211 to 2.9749 and the europium anomaly from 0.0170 to 0.0508. The cerium anomaly is exceptionally high in comparison to any other flint samples analyzed and its significance is discussed later.

Paramagnetic properties: Analysis was restricted to a single red flint from Helgoland; there was a slight magnetic signal from its red core (Text-fig. 20A) that could reflect traces of greigite or magnetite. The presence of non-magnetic hematite as the

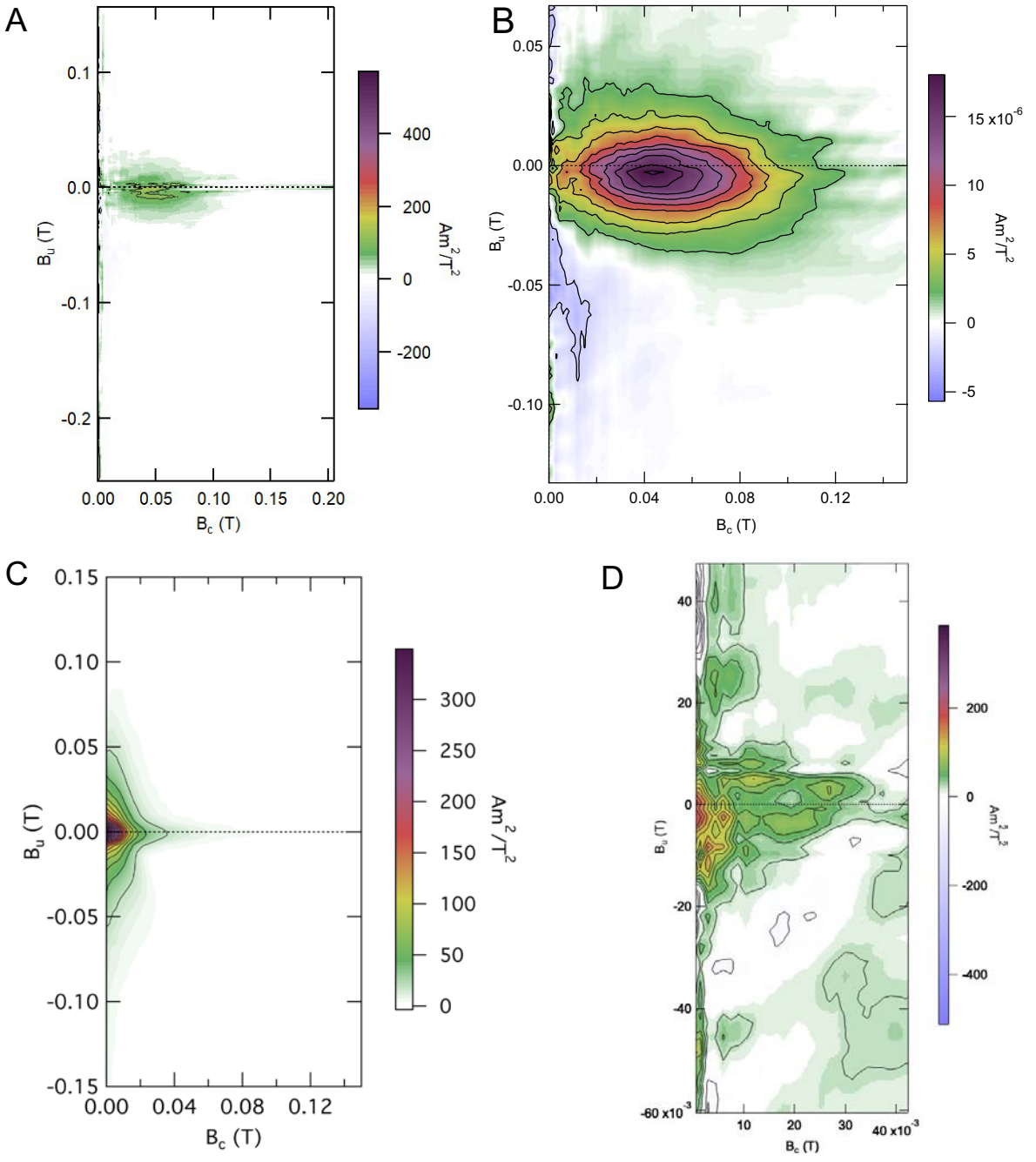

Text-fig. 20. Paramagnetic patterns from various flints of the oxic and suboxic zones of diagenesis. A – Red hematite core of Helgoland red flint CVJRM 19 containing traces of greigite and/or magnetite. B – Black outer core of Helgoland red flint CVJRM 19 containing greigite. C – Core of brown flint (Faxe 2) Faxe containing magnetite. D – Core of brown flint (YR3), Speeton complex pattern possibly resulting from magnetite and greigite.

red pigment is indicated by X-ray diffraction analysis. The outer black part of the core provided a strong paramagnetic signal of greigite (Text-fig. 20B).

Brown Flint Group

Mineralogy (Table 1): Two analyses of the brown core within a single flint from the Brown Flint Band show a wide range in moganite values (13.3, 38.1%). This suggests that an earlier phase of the core development (rich in moganite) may have been converted patchily to alpha-quartz during later diagenesis. A single cortex sample contained 7.4% moganite. Crystal size for moganite is 10.5–16.8 nm and 13.6–55.7 nm for alpha-quartz. The chalk associated with this flint band has a bulk SG of 2.24–2.33, averaging 2.30. The cores from seven brown flints of Danian age from Faxe, Denmark have a moganite range of 14 to 19% and a quartz range of 81 to 86%. Crystal size range for moganite is 20–38 nm and for quartz 20–45 nm.

Chemistry (Tables 2–4): The SiO_2 content in all samples is above 99%. Other major element oxides ($Ti0_2$, Al_2O_3, Fe_20_3, MnO, MgO, CaO, Na_2O, K_2O, P_2O_5) and trace elements (Ba (15–32 ppm), Be, Cr, Cu, Ni, Sr, Co, V, Y, Zn, Zr and REEs) make up less than 1%. Cerium anomaly ranges from 0.50 to 0.81 and the europium anomaly from 0.84 to 1.40.

Paramagnetic properties: Of the eight brown flints that have been investigated five contained paramagnetic signatures. The Brown Flint Band at Speeton had a complex pattern (Text-fig. 20D) which could result from both magnetite and greigite being present. Marked lateral reduction in the magnetic remanence in this band as it is traced laterally may be related to small iron sulfide nodules that developed during a late diagenetic phase of invasive sulfidisation as described by Jeans *et al.* (2016, pp. 246–247). Four of the seven brown flints from Faxe, Denmark, contained magnetite (Text-fig. 20C).

Black Flint Group

Mineralogy (Table 5): The standard 50 mm Floorstone cube consists of 20.1% moganite and 79.9% alpha-quartz. It is within the range of values displayed by both black flint nodules (13.6–21.1% moganite) and also the concordant and discordant black flint veins (15.4–24.0% moganite) that we investigated from the Danish Chalk. The vitreous cores of three black flint nodules from Denmark (Table 5, DNK 2a, 2b, and 3; DNK6 and 7; DNK 8, 9 and 10) were further investigated for cryptic variations in their moganite contents but showed insignificant differences. Paler patches of less vitreous flint (Text-fig. 12B, C) in the cores of black flints usually have a much lower moganite content than the surrounding black core – this is evident in flints from Denmark (Table 5, DKN 8–10; DKN 11, 12A, 12B, 13) and Caistor St Edmunds (Table 5, CSE 34a, 41, 42, 43, 44). The black flint SuR20 from the *Holaster planus* Zone chalk near Dorking investigated by Jeans (1978, p.117) displays the characteristic marked difference in moganite content between the core (20.8%) and the wide cortex (10.5%). Crystal size for the moganite is generally in the order of 10 nm, although a few samples have higher values (Table 5, RØD 4, DNK 9). The dimensions of alpha-quartz crystals are generally between 40 and 50 nm although in pale patches within cores the crystal size may be up to 100 nm or more.

Chemistry (Tables 2–4): The SiO_2 content in all 18 samples of nodules and veins is above 99%. The zoomorphic black flint from the Baldock Bypass has

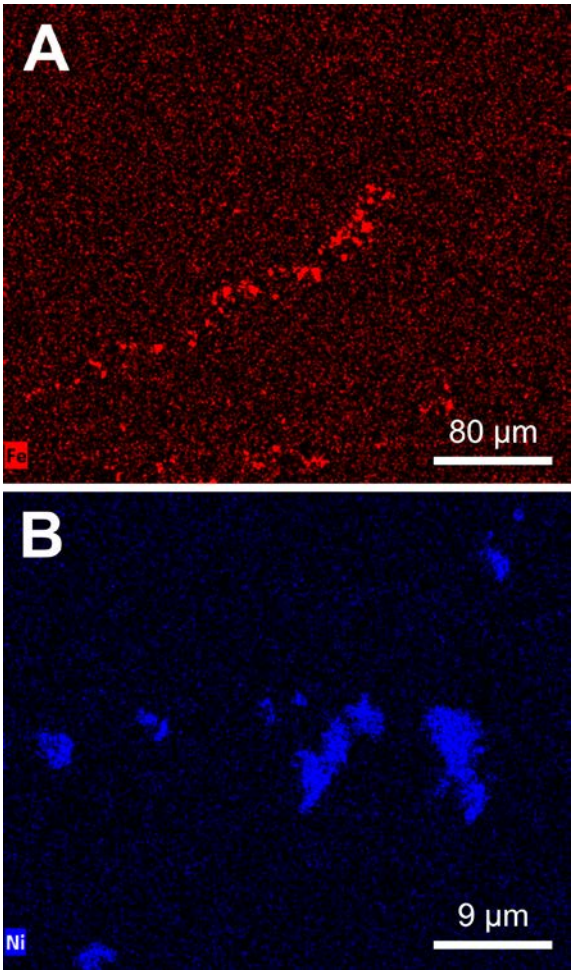

Text-fig. 21. Sulphide phases in the Turonian Floorstone (Black Flint Group), Grimes Grave, Norfolk, England. A – Fe sulfide traces. B – Ni sulfide traces.

enhanced Al_2O_3 values of 0.132 and 0.136%. Other major element oxides ($Ti0_2$, Al_2O_3, Fe_20_3, MnO, MgO, CaO, Na_2O, K_2O, P_2O_5) and trace elements (Ba (15–32 ppm), Be, Cr, Cu, Ni, Sr, Co, V, Y, Zn, Zr and REEs) make up less than 1%. Barium contents display two groups of values; sixteen samples have values between 2 and 7 ppm, whereas two samples (both veins) have much higher values (37,41 ppm). Cerium and europium anomalies range from 0.24 to 0.49 and from 0.24 to 0.49 respectively. No systematic chemical differences are apparent between black flint nodules and veins.

Paramagnetic properties: Nine black flint cores were investigated representing concordant and discordant flint sheets (RØD2, 5 and 8; SLO4), the nodule (HØJ1), the Floorstone, and two samples of paramoudras. No sample displayed any magnetic remanence. Traces of Fe and Ni sulfides are present (Text-fig. 21).

Grey Flint Group

Mineralogy (Table 6): Grey flints typically display the same pattern of moganite distribution as the black flints, with higher value in the core compared to those in cortex, although the general range of values is lower. Examples from the calcite-cemented Cenomanian chalk of Ballard Cliff (Text-fig. 2), with average bulk specific gravity of 2.17 (range 2.02–2.32), have moganite values ranging from 6.7 to 13.8% and alpha-quartz values ranging from 86.2 to 93.3%. Crystal size for moganite ranges from 10 to 13 nm and for alpha-quartz from 42.9 to 65 nm.

The flint nodule from the Turonian chalk of Baldock (Text-fig. 5E) has a grey to dark grey core and a white cortex with an inner (CX1) and outer zone (CX2). Cross-cutting the core is a sealed fracture (arrowed) that affected the form of both core and cortex, suggesting that its development and displacement was penecontemporaneous with the later stages of flint development when the core, cortex and the surrounding chalk were competent enough to preserve the fracture. The core of the Baldock flint nodule has a moganite content of 15.9–19.3% (alpha-quartz 80.7–84.1%), the inner cortex 18.4% (alpha-quartz 81.6%), and the outer cortex 23% (alpha-quartz 77%), with crystal sizes for moganite of 10–11 nm and for alpha-quartz of 25–41 nm.

Some grey flints contain mouldic cavities lined with macroscopic quartz crystals. These cavities may represent calcitic fossils, initially resistant to replacement by silica, that have subsequently been dissolved during diagenesis. In the example of grey flint from the Coniacian Chalk of Sussex (Text-fig. 12D) there is a zone of lighter grey flint (CE1), resembling the cortex, between the main core and the zone of quartz crystals. The moganite value of the main core CE is 14.7%, which decreases to 2.2% and then to 0.0% and 0.1% in the outer part of the transitional zone CE1 with macroscopic quartz lining the cavity (X).

A high-angle grey flint sheet vein from the Campanian chalk at Newhaven, Sussex (Text-fig. 4A) has a moganite value of 14.6% (alpha-quartz 85.4%) with a crystal size for moganite of 10 nm and 37 nm for alpha-quartz.

Paramagnetic properties: Three samples were egamined: RM13 from the Turonian chalk of the Baldock Bypass; RM16C (pale flint CE1) beneath the coarse quartz crystal zone in a vuggy flint nodule, Coniacian chalk, Newhaven, Sussex (Text-fig. 12D); and RM17, a *Zoophycos* flint (Text-fig. 4C) associated with a horizontal flint vein – none displayed any magnetic remanence.

Grey Carious Flint Group

Mineralogy (Table 6) **and isotope values** (Table 7): The moganite content of five flint samples range from 4.3 to 10.0% (alpha-quartz 90.0–95.7%). A discordant flint sheet/vein from the same location has a moganite content of 11.4%. The Ludborough Tabular Flint Band with a moganite value of 9.6% is considered to be the stratigraphical equivalent of the Floorstone in Norfolk, which has a value of 20.1%. The range of crystal sizes for moganite is 10–18.7 nm, and 49–75 nm for alpha-quartz. Measurements of the bulk density of these flints, their calcium carbonate content and their $\delta^{13}C$ and $\delta^{18}O$ values and those of the surrounding chalk matrix are shown in Table 7. The chalk matrix ranges in bulk density from 1.93 to 2.25 comparable to those (1.98 to 2.44) displayed by the cemented samples of Unit B of the Welton Formation of east England (Jeans *et al.* 2014, table 2), and are much higher than the average bulk density (1.64) of the uncemented but fully compacted Standard Louth Chalk at Dover (Jeans *et al.* 2014, table 1, p. 428). Comparison of the $\delta^{13}C$ (calcite) and $\delta^{18}O$ values of the chalk preserved within the carious flints with that of the surrounding chalk matrix demonstrates there are major differences in the $\delta^{18}O$ values whereas there is only a slight difference in the $\delta^{13}C$ values. In all examples the $\delta^{18}O$ values of the chalk matrix, ranging from -4.34 to -4.76‰ (average -4.52‰), are more negative than those of the chalk inside the flint nodules with its range from -2.21 to -4.33‰ (average -3.06‰). In contrast, the $\delta^{13}C$ values of the calcite within the flint nodules is only

slightly higher (1.91–2.35‰, average 2. ‰) than those of the chalk matrix (1.94–2.23, average 2.11‰). We suggest that the enhanced $\delta^{18}O$ values of the chalk matrix reflects the higher temperature of the pore fluids during cementation outside of the flint nodules, whereas these pore fluids did not penetrate or affect the chalk within the flints.

Paramagnetic properties: A single sample ULC2 from the Ludborough Tabular Flint (Text-fig.13) – the lateral equivalent band to the Floorstone of Grimes Grave – displayed very weak magnetic remanence that could not be resolved, possibly reflecting paramagnetic patterns from one or more phases.

White Flint Group

Mineralogy (Table 6) **and isotope values** (Table 7): The moganite values of four samples from Selwicks Bay, ranged from 0.0 to 0.9% (alpha-quartz 99.1 to 100%). Bulk specific gravity of the matrix chalk is high ranging from 2.375 to 2.486 (average 2.24). The flints contain an appreciable amount of calcite (5 to 9 wt %). The stable isotope values for the calcite within the nodules are different from those of the surrounding chalk matrix. The O^{18}/O^{16} values of the calcite within the flints ranges from -2.35‰ to -5.18‰ (averaging -3.87‰), not dissimilar to -3.40‰ to -4.06‰ (averaging -3.696‰) of the matrix calcite, whereas the C^{13}/C^{12} of the calcite in the flint is lighter (1.53 to 2.14‰, averaging 1.91‰) compared to that in the chalk matrix (2.21 to 2.46‰, averaging 2.365‰).

Paramagnetic properties: The only white flint examined (sample WF2) displayed no paramagnetic properties.

Sponge Associated Flint Group

Mineralogy (Table 8): Moganite contents range from 12 to 17% (alpha-quartz 83–88%) showing little difference between the silicified sponge (12.2%), the silicified sponge in the flint matrix (17%), and the cortex (12.2%). Crystal size for moganite is 10 nm and for alpha-quartz 40–52 nm. There is no chemical data for this flint.

North Sea Flint Group

The samples are from considerable burial depths ranging from 2057 to 2827 m.

Mineralogy (Table 8): Moganite values range from 0 to 3% (alpha-quartz 97–100%) displaying little difference between the white and black flints. The range of crystal size for moganite is 10–93 nm and for alpha-quartz 52–102 nm.

Clay-grade Quartz

Mineralogy (Table 8): Moganite values range from 2.2 to 29.9% (alpha-quartz 70.1–97.8%). The range of crystal size for moganite is 31.1–46.7 nm and 186.3–212.3 nm for alpha-quartz.

Chemistry (Table 9): This shows the elemental composition (expressed as atomic mass) of a series of individual nano quartz particles from marl samples from the Cenomanian Chalk of Speeton obtained by analytical transmission microscopy. The samples are dominated by oxygen (67–71%) and silicon (27–35%). Aluminium occurs as a minor element (0.4–2.1%). Sodium, magnesium, potassium, calcium, iron are consistent trace elements.

Upper Greensand Chert

Mineralogy (Table 10): Samples of the cores of eighteen cherts have moganite values ranging from 5.5 to 25.2% averaging 12.6%, and alpha-quartz values from 94.5 to 74.8% averaging 87.4%; they are within the compositional range shown by Chalk flints. Crystal size for moganite is in the 10 to 25 nm range averaging 12.5 nm, whereas alpha-quartz ranges from 27.0 to 74.9 nm averaging 40.7 nm. Samples of cortex from four cherts have moganite values ranging from 7.2 to 15.8% averaging 12.6%, and alpha-quartz values from 74.8 to 94.5% averaging 87.4%. The moganite crystal size ranges from 10 to 25 nm averaging 12.5 nm, and for alpha-quartz it ranges from 27 to 74.9 nm averaging 40.7 nm. No chemical analysis of these chert samples was carried out.

PATTERNS OF CHEMICAL VARIATION IN FLINTS

The limited number (31) of full chemical analyses of decalcified flint samples (Tables 2, 3, 4) suggests that the relationship between composition and our groupings of flint type is not straightforward. Samples have been arranged by their deduced diagenetic zones of development based largely upon their paramagnetic characteristics and also whether they developed as (a) nodules by the replacement of chalk and the infilling of its pore space, or as (b) veins reflecting voids or zones of enhanced porosity and pore size such as associated with fractures or cavities within the chalk. Thus arranged in Tables 2, 3 and 4 certain general

relationships become apparent in the pattern of major element oxides and the cerium anomalies.

The major elements in flints are dominated by silica (SiO_2) with its contents – calculated by difference – ranging from 99.329 to 99.889%. Other detected components occur in minor amounts. Al_2O_3 is the most abundant (0.043–0.375%), this is followed by Fe_2O_3 (0.011–0.152%), CaO (0.011–0.107%), Na_2O (0.021–0.081%) and K_2O (0.014–0.058%). TiO_2, MnO and MgO occur at even lower range of values (< 0.010%). Relatively high values of Al_2O_3 are restricted to the red flints and some of the brown flints, suggestive that under suitable circumstances, there is a link between the early development in the oxic or suboxic zones and the enhanced incorporation of Al into the developing flint.

When comparison is made between the bulk decalcified chemistry of flints and the composition of the nano-silica particles in clay assemblages of the Cenomanian Chalk (Table 9), the proportions are different. Silica is still the major component, but the other nine elements are appreciable minor components, particularly Al (up to 7%), Fe (up to 1.3%), Ca (up to 0.9%), K (up to 1.2%), and Mg (up to 1.7%). This suggests that Si^{4+} in these quartz/moganite nano particles has been partially replaced by Al^{3+} and Fe $^{3+}$, and the charge deficiency balanced by Ca^{2+} and Mg^{2+}.

Table 11 shows the calculated atomic ratios of one atom of each of the ten major elements to the number of silicon atoms in a sample of the Red Flint Group, the Floorstone, a vein flint from the Black Flint Group, and the average composition of nano silica particles derived from 18 individual analyses. For example, in the Red Flint Group the Al:Si, K:Si, and Mg:Si ratios are respectively 712, 2203 and 16991. The same values for the average nano-silica particle: silicon ratios are much lower being respectively 11, 102 and 54. For the vein flint SLO 1, the values are higher, being 1275 for Al, 2997 for K, and 33296 for Mg. We suggest that these variations reflect the restricted availability of cations in the pore solutions during the development of the flint and the competing demands of other mineral building processes taking place at the same time. In any particular diagenetic setting a consistent relationship might be expected between the geochemistry of the flint and its development, but this is not apparent with our limited data.

Minor elements (Table 3) – Ba, Be, Cr, Cu, Ni, Sr, Co, V, Y, Zn, Zr – display no systematic patterns of variations related either to the groupings of the flints or their further subdivision into nodular and vein types. The great majority of values are less than 5 ppm. There are occasional enhanced values of Sr (83 ppm), Cu (20 ppm) and Zn (20 ppm). Barium, supposedly an indicator of silica of sponge origin, displays its highest values of 37 and 40 ppm in samples from black flint veins. Otherwise, most veins and other black flints usually have barium values below 5 ppm.

The concentrations of REE in the flint samples is shown in Table 4 as well as the calculated cerium and europium anomaly for each sample. Cerium changes its valency from 4+ (insoluble) to 2+ (soluble) passing from oxic to anoxic conditions. The cerium anomaly (Ce*) is a measure of the degree to which this has occurred in diagenetic minerals at different stages of this transition. Under certain circumstances when there is very tight stratigraphical and mineralogical control the cerium anomaly has been used as a palaeo-redox indicator for sediments (e.g. Jeans *et al.* 2015, 2021) or when the development of a single nodule is considered.

Table 4 shows a general correlation between the varying values of Ce*(DCF) and the major groups of flint types. The Red Flint Group has the highest values ranging from ~1 to ~3; the Brown Flint Group ranges from 0.50 to 0.81; and the Black Flint Group from 0.24 to 0.48. There is no differentiation between flint nodules and associated flint veins of similar colour. Such variation in the Ce*(DCF) might suggest, for example – using the model for the Cenomanian–Turonian Anoxic Event (Jeans *et al.* 2021, Textfig. 15) – that the Red Flint Group was formed under anoxic condition, the Brown Flint Group under oxic to suboxic conditions, and the Black Flint Group under oxic to very oxic conditions. This contradicts the overriding evidence from the presence or absence of various paramagnetic and sulfide minerals (see later) that the reverse is the correct interpretation.

The pattern of cerium anomalies can be applied to the development of a single flint nodule, such as red flint CVJRM19. Its red core has a Ce*(DCF) of 1.02 and 1.16 (Table 4) , whereas the black outer core has an enhanced value of 2.97 suggesting development under more anoxic conditions. This interpretation is supported by the presence of hematite and the absence of paramagnetic minerals in the red core indicating oxic conditions, whereas the presence of paramagnetic greigite in the black outer core suggests suboxic conditions for its development.

The europium anomaly (Eu*) has been used to identify volcanic derived material in the Aptian Fullers earths in England (Jeans *et al.* 2000). Can the same approach be applied to the flints' Eu data as they are also associated with smectitic clays? The rare-earth element europium (Eu) has two valence

states (2^+, 3^+) in the crystallization of high temperature silicate magmas, where Eu^{2+} selectively replaces Ca^{2+} in the precipitation of calcium feldspars. This means that magma remaining after the precipitation of calcium feldspar will be deficient in europium relative to its neighbouring REEs, samarium and gandolinium. Evidence of this anomaly indicates that such a selective uptake has occurred in its past-history.

Table 4 shows that there is considerable variation in the Eu* from 0.37 to 2.02, suggesting that there was variation in the type and origin of volcanic dust finding its way into the Chalk Sea and, ultimately leaving its imprint on the trace element chemistry of flints. However, there is no evidence that there is any link between the Eu* anomaly and the groupings of flints we have described. Some of the variation in values could reflect varying hydrothermal contribution of silica-rich waters to the Chalk seas as suggested to explain the High Turonian Flint Maximum of Mortimore and Wood (1986). More recently Jurkowska (2022) have argued strongly that hydrothermal sources of silica played a dominant role in providing the silica used in flint formation.

GEOLOGICAL SETTINGS OF FLINT

Flints associated with trace fossils: The great majority of flints occur in bands of considerable lateral extent that reflect the general stratification of the Chalk but are not actually part of the primary depositional stratification. They have developed within the chalk sediment, infilling the pore space and also replacing the carbonate sediment within and surrounding bioturbations (Bromley *et al*. 1975; Bromley and Ekdale 1984; Bromley *et al*. 1986). Such flints are very varied in form and arrangement, ranging from single nodules to complex networks extending over large areas. Some of these varieties (zoomorphic flints) replicate accurately the feeding traces, shafts and tunnels of the thalassinids and other trace making organisms that are rarely, if ever fossilized. Included here are thalassinid hornflints named after thalassinid crustacean burrowers, Zoophycos flints named after *Zoophycos* a spiral trace fossil, and Chondrites flints named after *Chondrites* a branching trace fossil. The tube of a very lengthy trace fossil *Bathichnus paramoudrae* is frequently associated with large circular pipe-shaped flints that are often referred to as paramoudras. Many examples from this flint group cannot be related to a particular burrow type. They all appear to have developed not only as a replacement of the original fill of a single or a complex of overlapping burrows, but also to have extended into the surrounding chalk matrix.

The presence in these flints of partially silicified chalk, ghosts of the original structure and textures, unsilicified fossils such as belemnites, echinoids or inoceramid shell fragments, leaves no doubt that flint has replaced the original chalk sediment and infilled the original pore space. There can be little doubt that the development of such flints was related to localized microbial activity within the residual organic matter associated with infaunal burrowing activity as well as to the cyclical variation in the burial of organic matter. The original form of the burrow is usually preserved largely undistorted by the flint nodules that usually extends beyond the burrow having replaced the surrounding chalk sediment. This implies that the different burrow-types of flint started their development prior to the compaction of the surrounding sediment and the infill of the burrow.

The wide extent and the stratigraphical use of certain flint bands over 100s to 10,000s km^2, essentially parallel to the stratification of the Chalk, has been frequently remarked upon (e.g. Fletcher 1977; Wood and Smith 1978; Mortimore and Wood 1986; Felder 1986; Mortimore and Pomerol 1987; Mortimore *et al*. 2001; Mortimore 2011, 2014, 2019). These bands are of post-depositional diagenetic origin. It is uncertain whether they represent periods of enhanced availability of silica in the Chalk Sea or just widespread conditions in the sediment – such as the cyclic variation in the organic contents of the sediment that allowed these flint bands to develop.

A particularly important feature of flints – when they replace the infillings of burrow systems excavated by various organisms including those of callianaspid shrimps – is they leave little evidence that the burrow system had undergone appreciable compaction. This indicates that the host sediment was supported by both pore-fluid overpressure and cementation, preventing compaction during flint development. A flint band of wide extent may simply represent a zone within the chalk sediment where a plumbing system was maintained over a wide area, and this provided the developing flint nodules a consistent supply of silica or a period of enhanced organic material. Such systems may not necessarily be parallel to the actual bedding.

Flint veins and networks: Flint may also occur as simple veins or as vein networks that are either parallel to or crosscut the general stratigraphy of the Chalk (Text-fig. 11). Networks of fine flint veins may occur in individual flints (e.g. Bromley and Ekdale 1986, fig. 7.11; Text-fig. 5E), they are considered to represent stress fractures formed during the later stages of

flint development that have subsequently been sealed by silica precipitation. The development of flint veins is associated typically with localized stress and movement within the Chalk sediment. In these disturbed zones the original packing of the component grains will have been disturbed with the enhancement of the overall porosity and pore size. Experiments have demonstrated that very high super saturations are necessary for nucleation of cements in fine-grained sediments compared to nucleation in free solution. Prieto *et al*. (1990) and Putnis *et al*. (1994) demonstrated that the nucleation of barite ($BaSO_4$) in free solution requires a critical supersaturation of ~1000 times. Whereas in a fine-grained porous medium, such as silica gel, this increases to ~12000 times. The addition of trace amounts of an inhibitor – many are naturally occurring compounds – may increase the required critical super saturation to ~30,000 times. If such a disturbed zone developed locally in chalks where the super saturation of silica in the pore fluids was below that necessary for flint development, it could trigger localized flint development as veins when the silica concentration in the enlarged pores was in the range required for its precipitation and flint development.

Flints and aragonitic fossils: Organisms with part or total of their shells consisting of aragonite – ammonites and gastropods – were probably fairly common in the Chalk Sea judging from their abundance when they are preserved by early lithification of the enclosing sediment or, by the early diagenetic replacement of the shell by glauconite, apatite, iron sulphides, or calcite. The aragonite is never or very rarely preserved (we know of no examples), what is preserved is the impression of the exterior and interior form of the shell on the lithified chalk matrix. We are unaware of any flints in which there is evidence that aragonitic fossils are preserved, and this suggests that they had already been dissolved by the time the developing flint was firm enough to preserve the mould left by the dissolved aragonite shell. The shells of inoceramid bivalves consist of a thick prismatic layer of calcite with an inner layer of aragonite; large fragments of these bivalves may be common in flints, the prismatic layer is present, whereas the inner aragonitic layer is absent, neither is it represented by an empty mould, nor is there any evidence that a empty mould was present and has been infilled later by secondary minerals, including flint. The only association between flint development and the preservation of aragonitic shell material is in the lithified chalk associated with paramoudras where such fossils may occur (Bromley *et al.* 1975, fig. 9), but not in the flint itself.

STAGES OF FLINT DEVELOPMENT

The development of flints from the earliest stages as nano particles of alpha-quartz and moganite, either within the Chalk Sea or its sediment, can be followed through our interpretation of incompletely developed flints to the stage when they acted as coherent competent compact bodies. There is evidence from the presence of angular fragmented flints in intra-Chalk slides and slumping of Late Cretaceous age that indicate flints were already coherent bodies at the time (Mortimore 2018, pp. 27–65), although the first recycled Chalk flints occur as pebbles in the early Tertiary strata where they may still retain traces of their past history (see later).

The earliest stage we postulate produced very fine silica nano particles consisting of alpha-quartz and moganite associated with the smectite-mica clay assemblages typical of the Cenomanian Chalk of England (see later). The non-oxide chemistry of these particles (Table 9) is dominated by silicon (25–35%), and contain appreciable amounts of Al (0.4–7.3%) and trace amounts of Fe (<0.1–1.3%), Ca (<0.1–0.9%), Na (0.0–1.4%), Mg (0.0–1.7%), Ti (0–0.2%), and P (0.0–0.1%). Such compositions are markedly different from a variety of red, brown and black flints (Table 2). There appears to be little or no compositional overlap between them. The nano particles contain generally an order of magnitude higher proportions of Al, Fe, Ca, Na, Mg, Ti and P. It is only with some of the red and brown flints (Table 2) that the Al and Fe values are within the range exhibited by the nano-silica particles from Speeton. These flints have paramagnetic properties that indicate their development in the oxic and suboxic zones. Our interpretation of this pattern is that it represents the earliest diagenetic phase when reactive aluminium, derived perhaps from a background contribution of volcanic ash, soil-derived amorphous phases, hydrothermal sources or debris from Al-rich siliceous sponges, provides a source of reactive Al^{3+} and Fe^{3+} for mineral neoformation. This includes contributions to the early development of clay minerals, but also in substituting for Si^{4+} in the early formed silica minerals with the charge deficiency balanced by Mg^{2+}, Fe^{2+}, Ca^{2+}, K^{+}, and Ti $^{3+,4+}$ cations. These early formed silica nano particles are chemically different from the later diagenetically formed silica microspherules, such as reported by Weir and Catt (Text-fig. 16A–C), Fairbairn and Robertson (Text-fig. 16D), Jacobsen *et al*. (2000, 2004) and Lindgreen *et al*. (2010, 2011, 2012) (Text-fig. 22); these are similar to black flints in chemical composition with their depleted contents of Al, Fe, Ca, Na, Mg, Ti and P. This

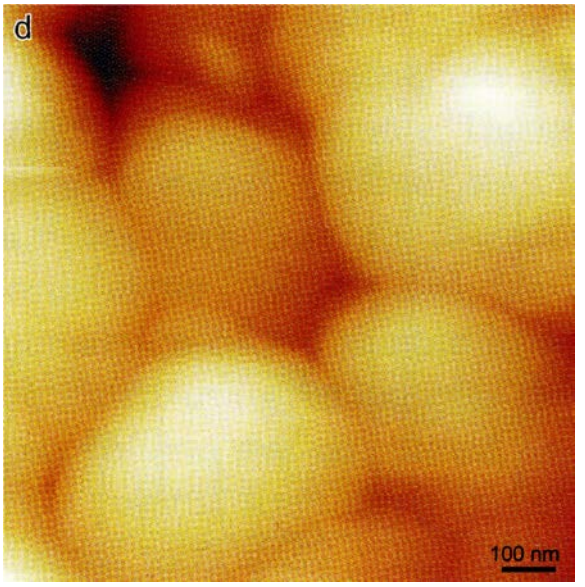

Text-fig. 22. Atomic force micrograph of the flint layer at the Cretaceous–Tertiary boundary shows the silica nanno-particles (a-quartz) in a porous botryoidal growth form. 2135.8 m depth, Nana-1 Well, Halfdan Field, North Sea (Holger *et al*. 2011, p. 530).

difference could represent either (1) a time-equivalent development to the very fine nano particles of silica as postulated for the Cenomanian samples from Speeton but in a setting depleted in reactive major elements, or (2) and perhaps more likely, a somewhat later diagenetic development when all the major elements other than Si had already been incorporated into authigenic clay minerals.

The next phase of flint development is specifically associated with nodule growth during diagenesis. It is linked to the conditions set up by microbial action in the infillings of sediment burrowers and the immediately surrounding chalk sediment. This could have been initiated in the oxic, suboxic or anoxic zones of diagenesis. Early stages of flint morphology resulting from this microbial activity have been preserved by the impregnation of the partially formed flint by hydrocarbons (Jakobsen *et al*. 2014) thereby inhibiting its further development. The silicification process started within the core of the future nodule replacing the calcitic components, followed by the infilling of the pore space by silica. Flint nodules often show evidence of outward growth from their primary development site (core) and encroachment into the surrounding sediment forming a cortex. Here the calcitic grains of the chalk have been only partly replaced by silica, leaving pore space unfilled. The fate of the dissolved calcite in this overall process is uncertain, and there is no evidence that it was precipitated in the proximity of the developing flint. Typically, the silica mineralogy of the core of such a flint contains a higher proportion of moganite than its cortex. There are some examples of incomplete flint development (White flint group) where there is no core and a considerable amount of unreplaced chalk.

Field relations indicate that flint nodules developed very slowly and were possibly incoherent for many millions of years. Their association with uncompacted burrows and the lack of pene-contemporaneous compaction suggests that during their development the nodules relied upon a sediment pore pressure regime that preserved the plumbing system within the surrounding sediment, and this allowed the Si^{4+} to migrate to sites of nodule formation. The importance of maintaining this system is demonstrated

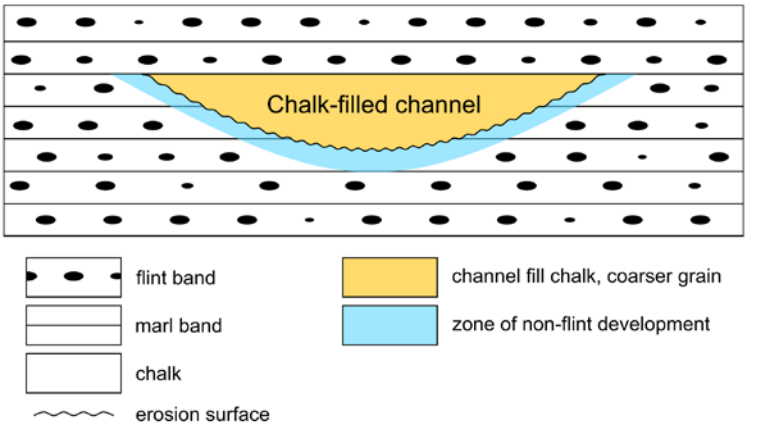

Text-fig. 23. Schematic cross-section through a pene-contemporaneous erosional channel filled with coarser grained chalk that has cut through a sequence of Turonian and Early Coniacian chalk containing flint horizons and marl seams. The flint horizons, although of regional occurrence, have not developed in the proximity of the channel whereas the marl bands are still present. Based on Gallois (2016, fig. 6) and Mortimore *et al.* (2017, p. 585).

where pene-contemporaneous sea floor channels have cut through a chalk sequence in which flints were developing. This would have drastically reduced the pore fluid pressure on either side of the channel causing sediment compaction and the collapse of the open plumbing system essential for the further development of silica nodules. Text-fig. 23, illustrating this feature, is based on Gallois (2016, fig. 6) and Mortimore *et al.* (2017, p. 585). Gallois mapped out an erosional channel in a Turonian chalk sequence containing flint and marl bands in a series of closely spaced boreholes near Grimes Grave in Norfolk (Text-fig. 1). Mortimore *et al*. (2017, p. 585) described phosphatic chalk-filled channels containing rolled chalk pebbles that are cut into Coniacian to Santonian chalks of the Stonehenge area containing regional marker marl bands and flint bands. The chalk filling the channels in both instances is coarser grained than the adjacent chalk and in neither instance are there rolled flint or proto-flint pebbles in the floor of the chalk-filled channel, but they do contain chalk pebbles. As present flint-bearing horizons are traced towards the channel, flints become less frequent and finally no longer occur before reaching the edge of the channel. This suggests that the development of flints on either side of the channel has been interrupted, most likely by the local release of pore-fluid pressure for some distance into the pile of chalk beds in which flints were developing. The loss of pore fluid pressure would have increased compaction, reduced porosity and permeability, thus cutting off the local sources of silica necessary for the further development of the proto-flint. The channel erosion would have released any proto-flints to form part of the active sediment in

Text-fig. 24. Red flint (CVJRM20, Tables 1, 2–4, 11) from the Turonian Chalk of Helgoland in vertical cross-section (A) and in plan view (B) containing an abundance of crushed echinoderms and their fragments. This flint may have originated as an accumulation of detrital silica nano-particles winnowed out of a flint-forming horizon by submarine erosion, then concentrated along with echinoderm debris, and subsequently developed during diagenesis into a flint layer.

the seafloor channel. They must have disintegrated into their components – silica grains and nano-particles. Once buried, accumulations of this detrital fine-grained silica, particularly if in association with fresh shell material, could have become preferred centres around which a new generation of flints could have developed. Such 'detrital' flints may be quite common in these circumstances, but perhaps their origin overlooked. Text-fig. 24 shows a red Turonian flint from Helgoland containing abundant broken echinoid fragments that could be such a flint.

Rory Mortimore (per. comm.) suggests that the unique sequence of flints filling the Mid-Turonian channel at Lewes, Sussex – floored by Strahan's Hardground – cut into the New Chalk Pit Formation might also be of such an origin (Mortimore *et al*. 2001, fig. 3.114). Evidence of the fracturing and partial flu-idification of a developing flint and its chalk matrix is not uncommon but it may occur without any sign of compaction; Text-fig. 5E shows a *Zoophycos* flint with a fractured and displaced cortex-core boundary followed by a second phase of cortex growth bridging the fractures. Evidence of differential compaction between flint and matrix only occurs when relatively uncemented chalk matrix loses its pore-fluid pressure. This is made apparent by the development of slickensides, both within and on the outer surface, of the cortex as a result of differential movement between the more competent flint core, and the less competent cortex and the even less competent chalk matrix (Text-fig. 25).

Earliest Flint and Chert Pebbles: The first derived flint and chert pebbles appear as detritus in the *Clay with Flints* strata of Upper Palaeogene

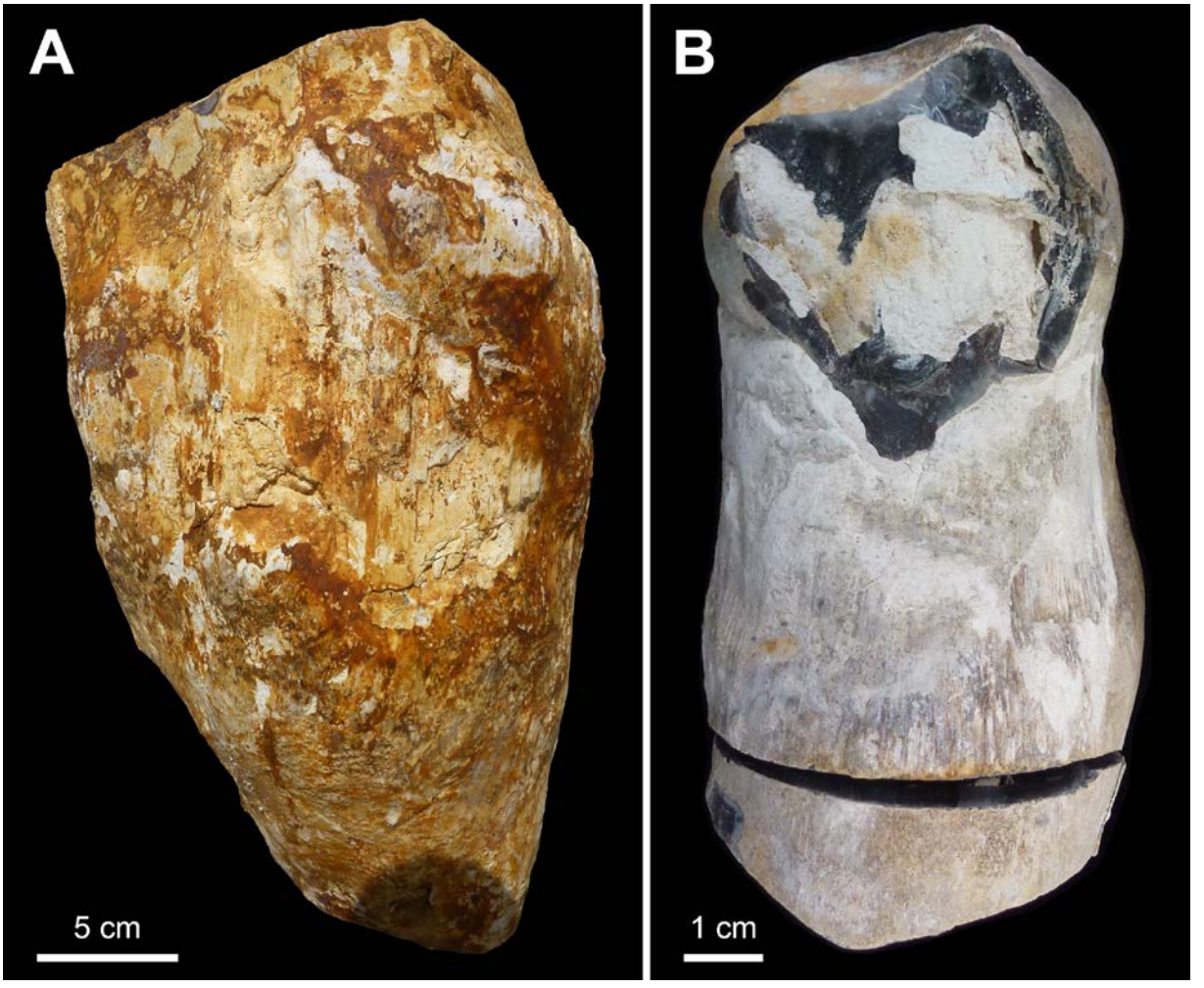

Text-fig. 25. Flint compaction features. A – Nose of a vertical torpedo-shaped Paramoudra with a slickensided surface caused by differential compaction between the competent flint and its chalk matrix, Beeston Chalk Formation, Upper Campanian, Caistor St Edmunds, Norfolk, England. B – Vertical Lewes Tubular Flint (Text-fig. 4B) showing a slickensided outer surface caused by differential compaction between the competent flint and the incompetent chalk matrix, *Micraster leskei* Zone, Upper Turonian, Shoreham cement Works, Sussex, England.

or younger age (<58 Ma) that blankets much of the Upper Greensand and Chalk in England. By this time some of them were "fully' formed, their cores hard and brittle enough to remain intact as rolled pebbles. Some of these rolled flints from the early Tertiary Blackheath Pebble Beds and the Lower Bracklesham sands show varying degrees of "desilicification" (Gardner 1881; Fairbairn and Robertson 1972) to a friable 'chalk – like siliceous' material consisting of elongate fragments 80–90 nm in diameter (Text-fig. 16D). Fairbairn and Robertson suggest that the decomposition process probably consisted of simple leaching of residual quartz crystals by alkaline solutions. An alternative interpretation could be the selective leaching of a cement of the more soluble moganite (not recognized at that time) to the elongated quartz crystals. This desilicification could reflect the incomplete development of the more robust flint pebbles that we know today. Three different aspects of the relationship between the morphology of flints and their relationship to the structure and diagenesis of the surrounding chalk sheds light on the timing and conditions controlling their development.

MODEL OF FLINT DEVELOPMENT IN DIFFERENT CHALK SETTINGS

Text-fig. 26 shows a hypothetical model based on our observations of the occurrence of different types of flint and their relationship with various chalk lithologies, clay mineral assemblages and cal-

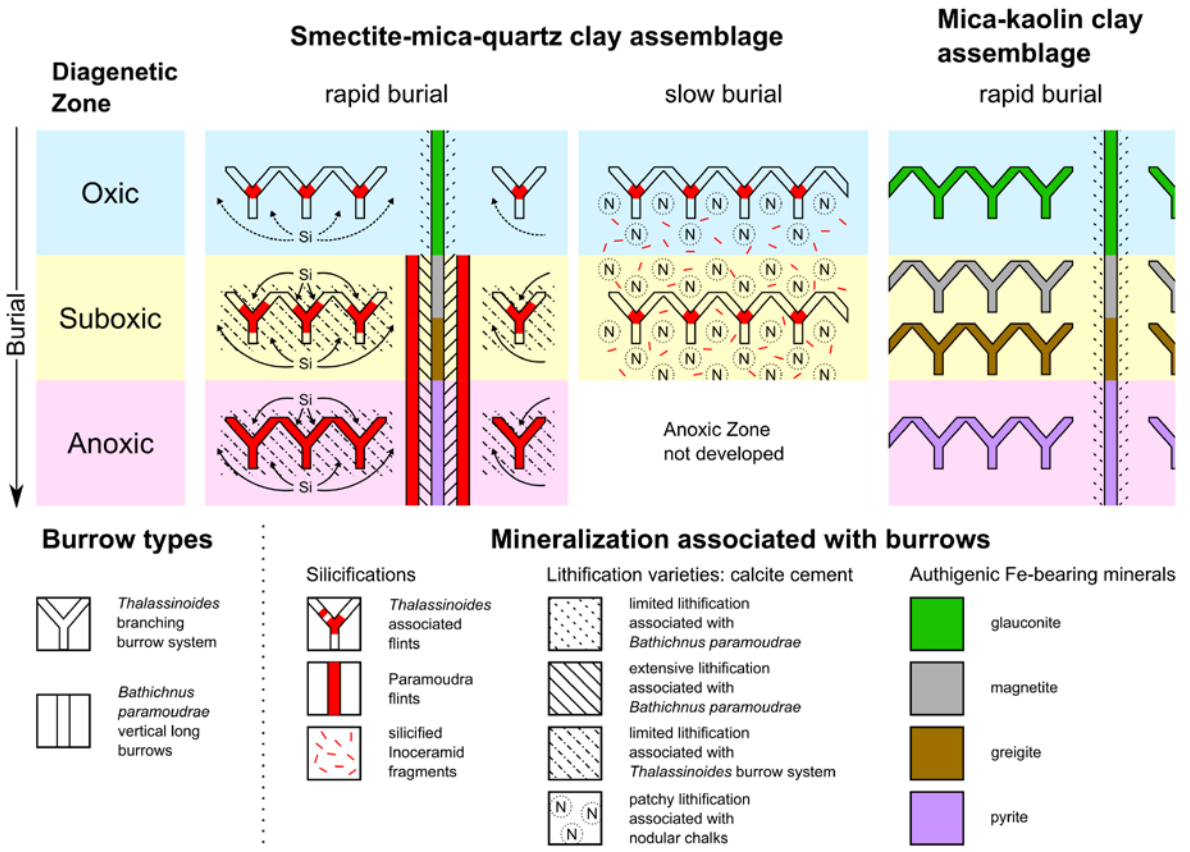

Text-fig. 26. Model linking flint development in the Chalk relative to clay mineralogy, cementation, permeability, depositional rates and the migration of Si in solution to sites of silicification. The initial subdivision is into chalks characterized by either (1) the detrital mica-kaolin clay mineral assemblage where silicifications are not evident, or (2) the smectite-mica-quartz clay assemblage where a-quartz/moganite silicifications may occur. This second group is further divided. First those chalks that were relatively rapidly deposited and included sufficient biodegradable organic matter to develop an anoxic zone of diagenesis where the main development of flints took place. Second, chalks characterized by slow deposition where all the bio-degradable organic matter was utilized in the oxic and suboxic zones of diagenesis and an anoxic zone did not develop – these chalk rarely contain flints and if they do they are usually incompletely developed and preserve traces of paramagnetic minerals, however silicified shell fragments (inoceramids in particular) are not uncommon. During early diagenesis the slowly deposited chalks were associated typically with the development of numerous local centres of calcite cementation resulting in the development of nodular chalks (Jeans 1980; Hu *et al*. 2014, p. 287, table 2) during the later phase of their suboxic diagenesis. The model indicates that these local centres of cementation restricted the diffusion of Si in solution to the sites where flint might have developed.

cite cementation histories. The model recognizes three contrasted situations from left to right. Two are associated with the smectite-mica clay assemblage with a high content of clay-grade quartz. In the third, associated with the kaolin-mica clay assemblage, clay-grade quartz is absent or only present in trace amounts. Early calcite cementation may occur in all three situations preserving the permeability essential for the development of flints, and providing a setting for callianaspid and *Bathichnus paramoudrae* burrows and feeding traces and their associated zones of calcite lithification. This early cementation developed either below the water-sediment interface on the Chalk seafloor or within burrows that allowed free circulation of seawater to lower levels in the sediment. In the first situation sufficient biodegradable organic matter was carried over into the later stages of intrinsic diagenesis with the development of anoxic conditions and the formation of black and grey flints associated with pyrite. The second situation is similar to the above but with the biodegradable organic matter being completely used up in the oxic and suboxic zones; an anoxic zone did not develop and here flints are rare and belong to the red or brown groups. The third situation is different, and is associated with Chalk containing a mica-kaolin clay assemblage and a low content of clay-grade quartz; biodegradable organic matter is abundant and this results in an anoxic zone with pyrite but without the development of flint.

SOURCE OF SILICA FOR FLINT AND CHERT DEVELOPMENT

Hexactinellid 'glass' sponges, alpha-quartz silicifications and clay-grade quartz are associated with the smectite-mica clay assemblage that appears first in southern England in the sandy marine Hythe and Sandgate Formations of Aptian age (Jeans 1978, Fig. 3). These forms of biotic and diagenetic silica gained much of their silica from the influence of volcanic activity and a plentiful supply of ash derived from the southern part of the North Sea. The ash was deposited on the London Platform then washed into the fringing Lower Cretaceous seas. Alpha-quartz cherts dominate in the sandy lithofacies (Hinde 1885; Hayward 1932; Richardson 1947; Humphries 1957; Padgham 1970; Hart 1973), whereas in the clay-rich fuller's earth beds there occur (a) very rare nodules cemented by opal-CT and clinoptilolite-heulandite zeolite that preserved the original volcanoclastic components of the ash, and (b) large barite nodules of diagenetic origin (Jeans *et al*. 1977, fig. 5, p. 25). In the younger sandy marine Upper Greensand of Upper Albian age both alpha-quartz/moganite and opal-CT silicifications are present and are associated with the smectite-mica clay assemblage. Their distribution is regionally distinct with the opal-CT variety being linked with the malmstone lithology rich in sponge spicules (Text-fig. 27). This volcanic association with cherts does not extend beyond very earliest Cenomanian times. The London Platform was submerged beneath the rising Chalk Sea. There are no records of volcanic ash bands in the Cenomanian chalk in spite of the presence of marl bands of considerable lateral extent (Jeans 2024). However, the smectite-mica clay assemblage with its abundant quartz is carried over and its extent expands and by Turonian times it dominates the Chalk until the end of the Cretaceous some ~28 Ma later. Alpha-quartz/moganite and opal-CT flints are infrequent and localized in the Cenomanian Chalk of England. Text-fig. 28 illustrates their distribution with the alpha-quartz/moganite variety being restricted largely to the southwest and northeast parts of its outcrop and is associated with clay assemblages containing 15% or more quartz, whereas the opal-CT variety occurs in chalk with clay assemblages containing less than 15% quartz.

Turonian and younger chalks of England, the North Sea and Denmark are characterized by a varying abundance of alpha-quartz flints with the smectite-mica-quartz clay assemblage (e.g. Weir and Catt 1965; Perrin 1971; Morgan-Jones 1977; Lindgreen *et al*. 2002, 2008; Drits *et al*. 2004; Wray and Jeans 2014). There is little evidence of any considerable contribution of volcanic ash to this post-Cenomanian Chalk Sea. A number of widespread bands of decomposed ash do occur (Wray 1995, 1999; Wray and Wood 1995, 1998, 2002; Wray *et al*. 1995, 1996; Wray and Jeans 2014) but they are the exception. In contrast to the Aptian and Albian phase of silicification that was under the influence of local volcanism, the source of the silica for the flints of the Upper Cretaceous must lie elsewhere. The clue to their origins is the relationship in the Cenomanian Chalk of southern England between the different clay mineral assemblages and the distribution of opal-CT and alpha-quartz flints (Text-fig. 28). Opal-CT flints are restricted to chalk characterized by smectite-mica clay assemblages with less than 15% quartz. This chalk is in juxtaposition to others containing the detrital mica-kaolinite clay assemblage representing the soil mineral weathering products of the adjacent lowing-lying landmasses. The colloidal products

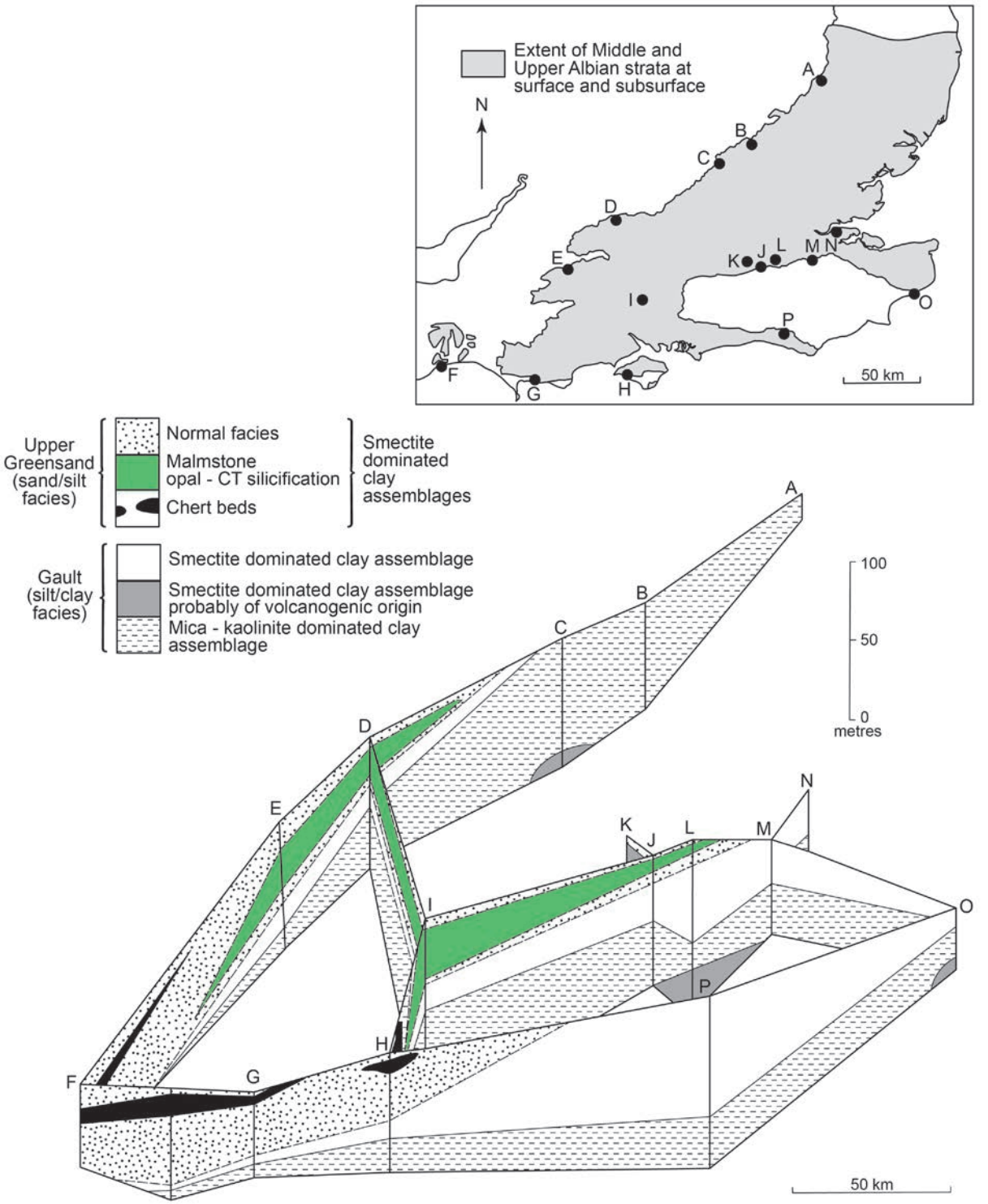

Text-fig. 27. Fence diagram (after Jeans 2006, fig. 34) showing the regional distribution of the quartz/moganite chert beds and the opal-CT malmstone of the Upper Greensand in relation to the main lithofacies and the distribution of the smectite-mica-quartz and the kaolin-mica clay assemblages in the Middle and Late Albian strata of southern England. Insert shows locations and the extent of the Middle and Upper Albian strata at outcrop and in the subsurface A: Hockwold cum Wilton, Norfolk; B: Arlesey, Bedfordshire; C: Leighton Buzzard, Bedfordshire; D: Kingston Lisle, Berkshire; E: Devizes, Wiltshire; F: Sidmouth, Devon; G: White Nothe, Dorset; H: Compton Bay, Isle of Wight; I: Winchester, Hampshire; J: Buckland, Surrey; K: Fetcham Mill, Surrey; L: Warlingham, Surrey; M: Trotiscliffe, Kent; N: East Tilbury/Higham, Essex/Kent; O: Folkestone, Kent; Glyndebourne, Sussex.

of this deep weathering formed an outer fringing zone to the detrital zone of clay deposition, and it is here where opal-CT flints and the low quartz smectite-mica clay assemblage developed. Alpha-quartz flints are restricted largely to the southwest part of the Cenomanian chalk with rare occurrences in the

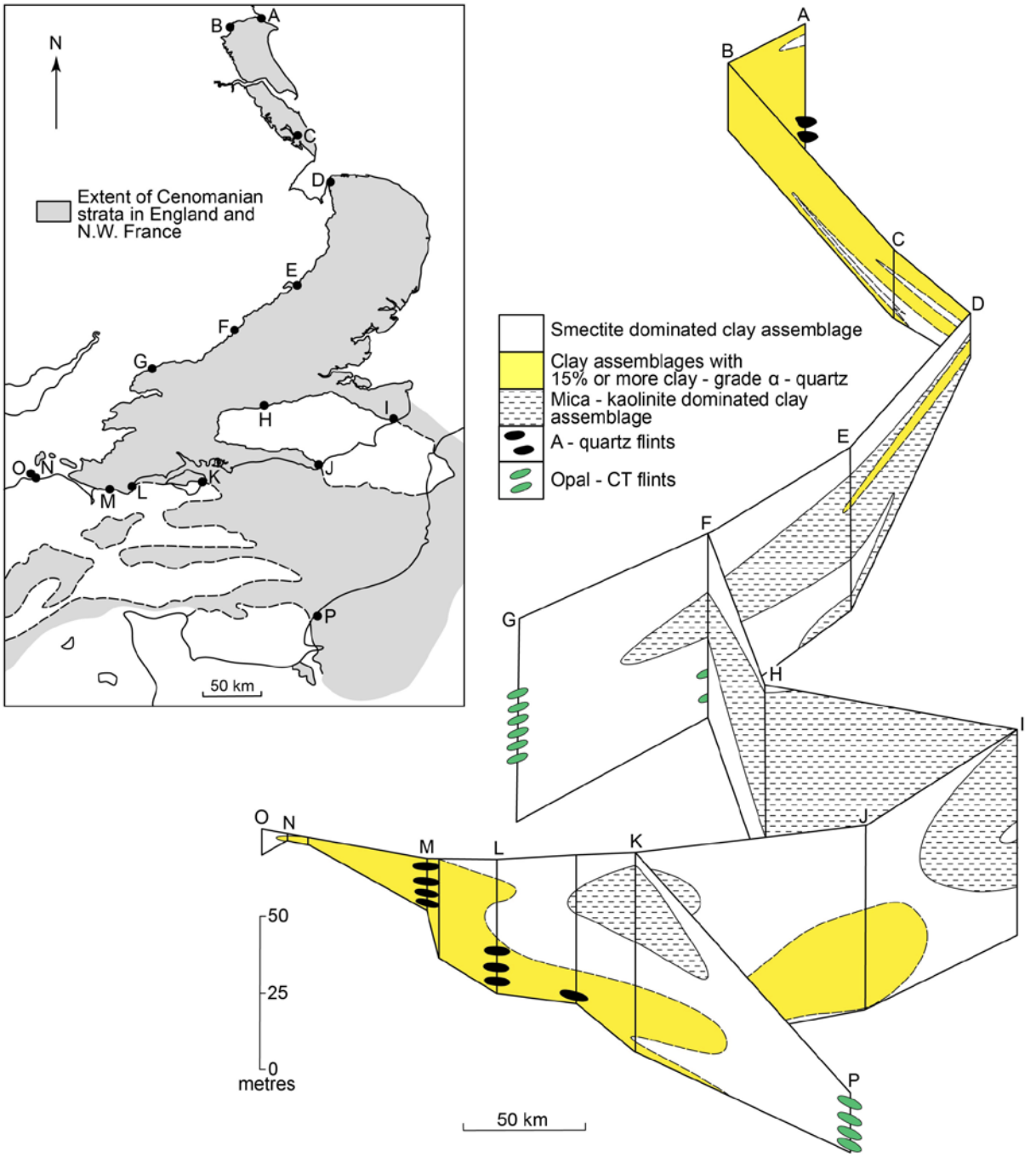

Text-fig. 28. Fence diagram (after Jeans 2006, Fig. 46) showing the regional distribution of alpha-quartz/moganite and opal-CT flints in relation to the distribution of the smectite-mica-quartz and the kaolinite-mica clay assemblages in the Cenomanian Chalk of England and Normandy, France; the smectite-mica-quartz assemblage is subdivided into a low quartz assemblage (<15%) and a high quartz assemblage (≥15%). Insert shows the locations and distributions of the Cenomanian Chalk and coeval strata at the surface and subsurface. A: Speeton/Flixton, Yorkshire; B: North Grimston, Yorkshire; C: South Lincolnshire: D: North Noufolk; E: Cambridgeshire; F: Bedfordshire-Buckinghamshire; G: Liddington, Wiltshire; H: Fetcham Mill, Surrey; I: Fo;kestone/Dover, Kent; J: Eastbourne, Sussex; K: Culver Cliff, Isle of Wight; L: Ballard Cliff, Dorset: M: White Cliff, Dorset; N South Devon; O: Wilmington, Devon; P: St Jouin, Normandy.

northeast at Speeton (Text-fig. 28), they are associated with smectite-mica clay assemblages containing 15% and more quartz. This suggests another source of silica, perhaps the incursion of silicon enriched oceanic waters from the proto-North Atlantic ocean such has been suggested by Jurkowska and Świerczewska-Gładysz (2020b) to explain the regional and stratigraphical patterns of alpha-quartz and opal-CT flints in the Campanian–Maastrichtian European Basin. Here the Mid-Polish Basin with its areas of opoka facies is characterized by opal-CT flints (cherts of Jurkowska and Świerczewska-Gładysz 2020) whereas those regions of the Chalk Sea, poor in silicon, such as the Anglo-Paris and the North German basins, are characterized by alpha-quartz flints having derived their silica either directly or indirectly, through the siliceous skeletons of planktonic organisms such as radiolaria and diatoms as well as sedentary sponges, from influxes of silicon-rich waters from the proto-Atlantic ocean. In the Anglo-Paris Basin those parts of the Cenomanian chalk with their opal-CT flints (Jukes-Browne and Hill 1889; Jeans 1978, fig. 5; Text-fig. 28) are here recognized as a weak development of the opoka facies.

BURIAL DIAGENESIS/METAMORPHISM OF MOGANITE

Our investigations have demonstrated the widespread presence of moganite in the Chalk flints and clays of England and Denmark, extending its distribution from the Campanian chalks of Poland, Belgium and France (Jurkowska and Świerczewska-Gładysz 2020). Moganite may form a major component of flints and nano-quartz. It is, however, a rare component in flints and cherts older than 100 Ma (Heaney and Post 1992) suggesting that it is geologically unstable, and inverts to alpha-quartz. Our study has not revealed the rate at which this change has taken place or the circumstances under which it occurs. However, its initial development is clearly part of other intrinsic diagenetic processes in the Chalk. Evidence of the effects of deep burial and enhanced temperature on the long-termed change of moganitic flints to purely alpha-quartz flints could be sought in the flinty chalks of Northern Ireland, where their burial and temperature history beneath the 1.5–2.0 km pile of Tertiary basalts has been studied by Maliva and Dickson (1997); here flints of the Black flint group are well represented and it is suggested that the hardening of the Chalk by cementation took place after the full development of the flints in contrast to those of the Carious Grey Flint Group of northeastern England (see earlier) where calcite cementation interfered with flint development. Chalk hydrocarbon fields where burial and temperature histories have been systematically studied may also provide critical evidence although flints are very rare in the North Sea Late Cretaceous Chalk Formations primary returning in the Late Maastrichtian and Danian in many hydrocarbon fields (R.N. Mortimore *pers. comm*.). The limited data (Table 4) we have on flint samples from the North Sea, recovered from present burial depths between 2000 and 2800 m, suggests that moganite does not survive such burial and enhanced temperatures.

CONCLUSIONS

Our investigation of Chalk flints has indicated that there is a general pattern of morphological, mineralogical, paramagnetic and isotopic characters, and geological setting that reflects their development and provides a working classification. A geological model for their development has been put forward to explain (1) their occurrence not only in the anoxic zone of diagenesis, but also in the oxic and various phases of the sub-oxic zone, and (2) how their development and mineralogy is related to the internal plumbing system and to the different clay mineral facies of the Chalk. The results of chemical analysis of the different flint groups has, at this stage of our investigation only pointed the direction in which future research should proceed. The next step would be to investigate the major and minor element and silicon isotope variations in a stratigraphically well defined regional packet of chalk displaying flint formation at different stages of diagenesis. The Turonian chalk of England and France with their variously colour flints, well-developed flint cycles, which includes the ‘Flint Maxima” (Mortimore and Wood 1986), might be a good starting point.

Acknowledgements

We wish to thank the following for very considerable help in this project. For providing or collecting flint and chert samples and for use of field photographs as illustrations – Steve Boreham, Ramues Gallois, Paul Hildreth, John Lord, Rory Mortimore, Peter Squirrel (Needham Chalk (HAM) Ltd), Christian Spaeth, Peter Toft, Christopher Wood and Mark Woods. Holger Lindgreen for hospitality during the first author’s two visits to Denmark and for passing on his flint project

to Cambridge. Ljiljana Fruk of the Department of Chemical Engineering and Biotechnology (University of Cambridge) for allowing collaboration with her research team and use of the Thermo Scientific Talos F2000X G2 microscope purchased with a grant from the Engineering and Physical Science Research Council (Underpinning Multi-User Equipment Call (EP/P030467/1)). Tim Holt-Wilson for the images of red flints in the walls of the City of Norwich. Anders Högberg (Linnaeus University) and Debra Olausson (Lund University), archeologists based in Sweden, for providing us with the chemical analyses of flint samples carried out by David Wray. Richard Harrison for suggesting that paramagnetic studies would be a useful tool in differentiating between magnetite, greigite and pyrite within flints. Rosa Danisi for advice and help with the XRD analysis. Sarah Humbert for help with library matters. Philip Stickler, Jessica White and Vivien Brown for their patience and skill in dealing with the text-figures and untidy texts. Dick Merriman, Ian Platten, Rory Mortimore and Ramues Gallois for their most helpful comments and suggestions.

REFERENCES

Allmann, R. and Hinek R. 2007. The introduction of structure types into the Inorganic Crystal Structure Database ICSD. *Acta Crystallographica* A, **63**, 412–417.

Bromley, R.G. and Ekdale, A.A. 1984. Trace fossil preservation in flints in the European Chalk. *Journal of Palaeontology*, **58**, 298–311.

Bromley, R.G., Schulz, M.-G. and Peake, N.B. 1975. Paramoudras: giant flints, long burrows and early diagenesis of chalks. *Det Kongeluge Danske Videnskabernes Seiskab, Biologiske Skifter*, **20**, 1–130.

Bromley, R.G. and Ekdale, A.A. 1986. Flint and fabric in the European Chalk. In: de Sieveking G. and G. Hart M.B. (Eds), The scientific study of flint and chert, 71–82. Cambridge University Press, Cambridge.

Byrne, J.M. and Amor, M. 2023. Biomagnetism: insights into magnetic minerals produced by microorganisms. *Elements*, **19**, 208–214.

Clayton C.J. 1986. The chemical environment of flint formation in Upper Cretaceous chalks. In: de Sieveking, G and Hart, M.B. (Eds), The scientific study of flint and chert, 43–54. Cambridge University Press, Cambridge.

Cohelo, A. 2007. TOPAS-Academic, Coelho Software, Brisbane, Australia. http://www.topas-academic.net/Technical_Reference.pdf

Curry, D. 1986. Foraminferids from decayed chalk flints and some examples of their use in geological interpretation. In: de Sieveking G. and G. Hart M.B. (Eds), The scientific study of flint and chert, 99–103. Cambridge University Press, Cambridge.

Drits, V.A., Lindgreen, H., Sakharov, B.A., Jacobsen, H.J. and Zviagina, B.B. 2004. The detailed structure and origin of clay minerals at the Cretaceous/Tertiary boundary, Stevns Klint (Denmark). *Clay Minerals*, **39**, 367–390.

Fairbairn, P.E. and Robertson, R.H.S. 1972. The decomposition of flint. *Scottish Journal of Science*, **1**, 165–174.

Fletcher, T.P. 1977. Lithostratigraphy of the Chalk (Ulster White Limestone Formation) in Northern Ireland. Report 77/24, 33 pp. Institute of Geological Sciences, Geological Survey of Northern Ireland.

Flörke, O.W., Jones, J.B. and Schmincke, H.-U. 1976. A new microcrystalline silica from Gran Canaria. *Zeitschrift für Kristallographie*, **143**, 156–165.

Flörke, O.W., Flörke, U. and Giese, U. 1984. Moganite, a new microcrystalline silica-mineral. *Neues Jahrbuch für Mineralogie, Abhandlungen*, **149**, 325–336.

Gallois, R.W. 2016. The stratigraphy of the Middle Chalk (Upper Cretaceous) succession at Mundford, Norfolk, UK. *Proceedings of the Geologists' Association*, **127**, 451–463.

Gardner, J. S. 1881. Excursion to the Hampshire Coast. *Proceedings of the Geologists' Association*, **6**, 316–320.

Gehlen, M., Beck, L., Calas, G., Flank, A.M., Van Bennekom, A.J. and Van Beusekom, J.E.E. 2002. Unravelling the atomic structure of biogenic silica: evidence of the structural association of Al and Si in diatom frustules. *Geochemica Cosmochemica Acta*, **66**, 1601–1609.

Gry, H. and Sondergaard, B. 1958. The occurring of flint and chert types in Denmark with special reference to the petrography with English Summary. *The Danish National Institute of Building Research and the Academy of Technical Sciences. Committee on alkaline reactions in concrete. Progress Report Series D-Nr.2*, 63 pp.

Gurova, M., Andreeva, P., Nikolov, A., Barbov, B. and Kostadinova-Avramova. M. 2020. Heat alterations of flint artefacts: archaeological evidence, experiments and analyses. *Bulgarian e-journal of Archaeology*, **10**, 111–141.

Hancock, J.M. 1975. The petrology of the Chalk. *Proceedings of the Geologists' Association*, **86**, 499–535.

Harrison, R. J. and Feinberg, J. M. 2008. FORCinel: An improved algorithm for calculating first-order reversal curve distributions using locally weighted regression smoothing. *Geochemistry, Geophysics, Geosystems*, **9**, Q05016.

Hart, M.B. 1973. Some observations on the Chert Beds (Upper Greensand) of south west England. *Proceedings of the Ussher Society*, **2**, 599–608.

Hayward, H A. 1932. The geology of the Lower Greensand in the Dorking-Leith Hill District, Surrey. *Proceedings of the Geologists' Association*, **43**, 1–31.

Heaney, P.J. and Post, J.E. 1992. The widespread distribution of a novel silica polymorph in microcrystalline quartz varieties. *Science*, **255**, 441–443.

Heath, G.R. and Moberley, R. 1971. Initial Reports of the Deep Sea Drilling Project, 7, 991. U.S. Government Printing Office, Washington, D.C.

Hildreth, P.N. 2013. The Vale House Flints Member, a flint rich unit of the Burnham Chalk Formation of the Northern Province in East Yorkshire and Lincolnshire. *Proceedings of the Yorkshire Geological Society*, **59**, 177–186.

Hildreth, P.N. 2019. The distribution and form of flint, with particular reference to the Chalk Group (Upper Cretaceous) of the Northern Province, UK. *Proceedings of the Yorkshire Geological Society*, **62**, 178–186.

Hinde, G.J. 1885. Beds of sponge remains in the Lower and Upper Greensand of southern England. *Philosophical Transactions of the Royal Society, London*, **176**, 403–453.

Högberg, A. and Olausson, D. 2007. Scandinavian Flint – an Archaeological Perspective. Aarhus University Press, 158 pp. Denmark.

Hu, X-F., Jeans, C.V. and Dickson, J.A.D. 2012. Geochemical and stable isotope patterns of calcite cementation in the Upper Cretaceous Chalk, UK: Direct evidence from calcite-filled vugs in brachiopods. *Acta Geologica Polonica*, **62**, 143–172.

Humphries, D.W. 1957. Chert: its age and origin in the Hythe Beds of the Western Weald. *Proceedings of the Geologists' Association*, **67**, 296 –313.

Jakobsen, F., Lindgreen, H. and Springer, N. 2000. Precipitation and floccolation of spherical nano-silica in the North Sea chalk. *Clay Minerals*, **35**, 175–184.

Jakobsen, F., Lindgreen, H. and Nytoft, H.P. 2014. Oil-impregnated flint in Danian chalk in the Tyra Field, North Sea Central Graben. *Journal of Petroleum Geology*, **37**, 43–54.

Jarvis, K.E. and Jarvis, I. 1988. Determination of the rare earth elements and yttrium in 37 international silicate reference materials by inductively coupled plasma-atomic emission spectrometry. *Geostandards Newsletter*, **12**, 1–12.

Jeans, C.V. 1968. The origin of the montmorillonite of the European Chalk with special reference to the Lower Chalk of England. *Clay Minerals*, **7**, 311–329.

Jeans, C.V. 1978. Silicifications and associated clay assemblages in the Cretaceous marine sediments of southern England. *Clay Minerals*, **13**, 101–126.

Jeans, C.V. 1980. Early submarine lithification in the Red Chalk and Lower Chalk of eastern England: a bacterial control model and its implications. *Proceedings of the Yorkshire Geological Society*, **43**, 81–157.

Jeans, C.V. 1986. Features of mineral diagenesis in hydrocarbon reservoirs: an introduction. *Clay Minerals*, **21**, 429–441.

Jeans, C.V. 2006. Clay Mineralogy of the British Cretaceous. *Clay Minerals*, **41**, 47–150.

Jeans, C.V., Merriman, R.J. and Mitchell, J.G. 1977. Origin of the Middle Jurassic and Lower Cretaceous Fuller's earths in England. *Clay Minerals*, **12**, 11–44.

Jeans, C.V., Merriman, R.J., Mitchell, J.G., and Bland, D.J. 1982. Volcanic clays in the Cretaceous of southern England and Northern Ireland. *Clay Minerals*, **17**, 105–156.

Jeans, C.V., Wray, D.S., Merriman, R.J. and Fisher, M.J. 2000. Jurassic and Cretaceous volcanogenic clays in Jurassic and Cretaceous strata of England and the North Sea basin. *Clay Minerals*, **35**, 25–55.

Jeans, C.V., Mitchell, J.G., Fisher, M.J., Wray, D.S. and Hall, I.R. 2001. Age, origin and climatic signal of English Mesozoic clays based on K/Ar signatures. *Clay Minerals*, **36**, 515–39.

Jeans, C.V., Long, D., Hu, X.-F. and Mortimore, R.N. 2014. Regional hardening of Upper Cretaceous Chalk in eastern England, UK: trace element and stable isotope patterns in the Upper Cenomanian and Turonian Chalk and their significance. *Acta Geologica Polonica*, **64**, 419–455.

Jeans, C.V., Wray, D.S. and Williams, C.T. 2015. Redox conditions in the Late Cretaceous Chalk Sea: the possible use of cerium anomalies as palaeoredox indicators in the Cenomanian and Turonian Chalk of England. *Acta Geologica Polonica*, **65**, 345–366.

Jeans, C.V., Turchyn, A.V. and Hu, X.-F. 2016. Sulfur isotope patterns of iron sulphide and barite nodules in the Upper Cretaceous Chalk of England and their regional significance in the origin of coloured chalks. *Acta Geologica Polonica*, **66**, 227–256.

Jeans, C.V., Wray, D. S., Williams, T.C., Bland, D.J. and Wood, C.J. 2021. Redox conditions, glacio-eustasy, and the status of the Cenomanian–Turonian Anoxic Event: new evidence from the Upper Cretaceous Chalk of England. *Acta Geologica Polonica*, **71**, 103–152.

Jukes-Browne, A.J. and Hill, W. 1889. Occurrence of colloidal silica in the Lower Chalk of Berkshire and Wiltshire. *Quarterly Journal of the Geological Society*, **45**, 403–421.

Jurkowska, A. and Świerczewska-Gładysz, E. 2020a. Evolution of Late Cretaceous Si cycling reflected in the formation of siliceous nodules (flints and cherts). *Global and Planetary Change*, **195**, 1–26, 103334.

Jurkowska, A. and Świerczewska-Gładysz, E. 2020b. New model of Si balance in the Late Cretaceous epicontinental European Basin. *Global and Planetary Change*, **186**, 1–17, 103108.

Jurkowska, A. and Świerczewska-Gładysz, E. 2022. Opoka – a mysterious carbonate-siliceous rock: an overview of general concepts. *Geology, Geophysics & Environment*, **48**, 257–278.

Jurkowska, A. 2022. The biotic-abiotic control of Si burial in marine carbonate systems of the pre-Eocene Si cycle. *Global Biogeochemical Cycles*, **36**, e2021GB007079.

Kennedy, W.J. and Juignet, P. 1974. Carbonate bank and slump beds in the Upper Cretaceous (Upper Turonian–Santonian) of Haute Normandie, France. *Sedimentology*, **21**, 1–42.

Lancelot, Y. 1973. Initial Reports of the Deep Sea Drilling Project 17**,** 377. U.S. Government Printing Office, Washington, D.C.

Lindgreen, H., Drits, V.A., Sakharov, B.A., Jakobsen, H.J., Salyn, A.L., Dainyak, L.G. and Krøyer, H. 2002. The structure and diagenetic transformation of illite-smectite and

chlorite-smectite from the North Sea Cretaceous–Tertiary chalk. *Clay Minerals*, **37**, 429–450.

Lindgreen, H., Jakobsen, F. and Springer, N. 2010. Nano-size quartz accumulation in reservoir chalk, Ekofisk Formation, South Arne Field, North Sea. *Clay Minerals* **45**, 171–183.

Lindgreen, H., Dritz, V.A., Salyn, A.L., Jakobsen, F. and Springer, N. 2011. Formation of flint horizons in North Sea chalk through marine sedimentation of nano-quartz. *Clay Minerals*, **46**, 525–537.

Lindgreen, H. and Jakobsen, F. 2012. Marine sedimentation of nano-Quartz forming flints in North Sea Danian chalk. *Marine and Petroleum Geology*, **38** (1), 73–82.

Madsen, H.B., Stemmerik, L. and Surlyk, F. 2010. Diagenesis of silica-rich mound-bedded chalk, the Coniacian Arnager Limestone, Denmark. *Sedimentary Geology*, **223**, 51–60.

Madsen, H.B. and Stemmerik, L. 2010. Diagenesis of Flint and Porcellanite in the Maastrichtian Chalk of Stevns Klint, Denmark. *Journal of Sedimentary Research*, **80**, 578–588.

Maliva, R.G. and Dickson, J.A.D. 1997. Ulster White Limestone Formation (Upper Cretaceous) of Northern Ireland: effects of basalt loading on chalk diagenesis. *Sedimentology*, **44**, 105–112.

Micheelsen, H.I. 1966. The structure of dark flint from Stevns, Denmark. *Meddelser fra Dansk Geologisk Forening*, **16**, 286–368.

Morgan-Jones, M. 1977. Mineralogy of the non-carbonate material from the Chalk of Berkshire and Oxfordshire, England. *Clay Minerals*, **12**, 331–344.

Mortimore, R.N. 2011. A chalk revolution: what have we done to the Chalk of England? *Proceedings of the Geologists' Association*, **122**, 232–297.

Mortimore, R.N. 2014. *Logging the Chalk*, 357 pp. Whittles Publishing, Caithness.

Mortimore, R.N. 2019. Flints in the Late Cretaceous Chalk of NW Europe. *Deposits Magazine*, **58**, 36–45.

Mortimore, R.N. and Wood, C.J. 1986. The distribution of flint in the English Chalk, with particular reference to the 'Brandon Flint Series' and the high Turonian flint maximum. In: de Sieveking, G and Hart, M.B. (Eds), The scientific study of flint and chert, 7–19. Cambridge University Press, Cambridge.

Mortimore, R.N. and Pomerol, B. 1987. Correlation of Upper Cretaceous White Chalk (Turonian to Campanian) in the Anglo-Paris Basin. *Proceedings of the Geologists' Association*, **98**, 97–143.

Mortimore, R. N., Wood, C.J. and Gallois, R.W. 2001. British Upper Cretaceous Stratigraphy. *Geological Conservation Review Series* **23**, 558 pp. Joint Nature Conservation Committee; Peterborough, U.K.

Mortimore, R.N., Gallagher, L.T., Gelder, J.T., Moore, I.R., Brooks, R. and Farrant, A.R. 2017. Stonehenge: a unique Late Cretaceous phosphatic Chalk geology: implications for sea-level, climate and tectonics and impact on engineering and archaeology. *Proceedings of the Geologists' Association*, **128**, 564–598.

Padgham, R.C. 1970. A study, mainly petrological and petrochemical in the Folkestone Beds of the Weald. Thesis. University of London (unpublished).

Perrin, R.M.S. 1971. *The Clay Mineralogy of British Sediments*. Mineralogical Society (Clay Minerals Group) London, 247 pp.

Pike, C., Roberts, A. and Verosub, K.1999. Characterizing interactions in fine magnetic particle systems using first order reversal curves. *Journal of Applied Physics*, **85** (9), 6660–6667.

Prieto, M., Putnis, A. and Fernandez-Diaz, L. 1990. Factors controlling the kinetics of crystallization: supersaturation evolution in a porous medium: Application to barite crystallization. *Geological Magazine*, **127**, 485–495.

Putnis, A., Prieto, M. and Fernandez-Diaz, L. 1995. Fluid supersaturation and crystallization in porous media. *Geological Magazine*, **132**, 1–13.

Richardson, J. A. 1947. Chert formation in the Bargate Beds nr Churt, Surrey. *Proceedings of the Geologists' Association,* **58**, 161–177.

Roberts, A., Pike, C. and Verosub, K. 2000. First-order reversal curve diagrams: A new tool for characterizing the magnetic properties of natural samples. *Journal of Geophysical Research*, **105** (B12), 28461–28475.

Rottländer, R. 2007. The formation of patina on flint. *Archeometry,* **17**, 106–110.

Schmid, F. 1986. Flint stratigraphy and its relationship to archaeology. In: de Sieveking, G and Hart, M.B. (Eds), The scientific study of flint and chert, 1–5. Cambridge University Press, Cambridge.

Schmid, F. and Spaeth, Ch. 1991. Der braunrot Feuerstein aus dem Turon von Helgoland. *Geologisches Jahrbuch*, Reihe A, Heft **120**, 97–104.

Schmid, F and Spaeth, Ch. 1978. Zur Alterstellung des braunroten Kreide-Feuersteins von Helgoland. *Neues Jahrbuch fur Geologie und Paläontologie Monatshefte*, Heft 7, 427–429.

Shepherd, W. 1972. Flints. Its Origin, Properties and Uses, Faber and Faber, London, 255 pp.

Skertchly, S.B.J. 1879. On the manufacture of gunflint: the Methods of Excavating for Flint, the Age of Palaeolithic Man and the Connection between Neolithic Art and the Gun-flint Trade, 80 pp. Geological Survey of Great Britain, HMSO, London.

Slotznick, S.P., Egli, R. and Lascu, I. 2023. Magnetofossils: Relicts and Records of Deep Time and Space. *Elements*, **19**, 215–221.

Tresise, G.R. 1961. The nature and origin of chert in the Upper Greensand of Wessex. *Proceedings of the Geologists' Association*, **72**, 333–356.

Weir, A.H. and Catt, J.A. 1965. The mineralogy of some Upper

Chalk samples from the Arundel area, Sussex. *Clay Minerals*, **6**, 97–110.

Whitham, F. 1993. The stratigraphy of the Upper Cretaceous Flamborough Chalk Formation north of the Humber, north-east England. *Proceedings of the Yorkshire Geological Society*, **49**, 235–258.

Williams, C.L. 1986. The cherts of the Upper Greensand (Cretaceous) of south-east Devon. In: de Sieveking, G and Hart, M.B. (Eds), The scientific study of flint and chert, 63–70. Cambridge University Press, Cambridge.

Wolfe, M.J. 1968. Lithification of a carbonate mud: Senonian chalk in Northern Ireland. *Sedimentary Geology*, **2**, 263–290.

Wood, C.J. and Smith, E.G. 1978. Lithostratigraphical classification of the Chalk in North Yorkshire, Humberside and Lincolnshire. *Proceedings of the Yorkshire Geological Society*, **42**, 263–287.

Wood, C.J. and Schmid, F. 1991. Upper Cretaceous of Helgoland (NW Germany): Lithology, Palaeontology and Biostratigraphy. *Geologische Jahrbuch*, **A120**, 37–61.

Wray, D.S. 1995. Origin of clay-rich beds in Turonian chalks from Lower Saxony, Germany – a rare earth element study. *Chemical Geology*, **119**, 161–173.

Wray, D.S. 1999. Identification and long-range correlation of bentonites in Turonian–Coniacian (Upper Cretaceous) chalks of northwest Europe. *Geological Magazine*, **136**, 361–371.

Wray, D.S. and Wood, C.J. 1995. Geochemical identification and correlation of tuff layers in Lower Saxony, Germany. *Berliner Geowissenschaftliche Abhandlungen*, **E16.1**, 215–226.

Wray, D.S. and Wood, C.J. 1998. Distinction between detrital and volcanogenic clay-rich beds in Turonian–Coniacian Chalks of eastern England. *Proceedings of the Yorkshire Geological Society*, **52**, 95–105.

Wray, D.S. and Wood, C.J. 2002. Identification of a new bentonite in sediments of mid-Turonian age from Lower Saxony, Germany and its correlation within NW Europe. *Austrian Academy of Science Series: Schriftenreihe der Erdwissenschaftlichen Kommissionen*, **15**, 47–58.

Wray, D.S., Kaplan, U. and Wood, C.J. 1995. Tuff vorkommen und ihre bio- und eventstratigraphie im Turon des Teutoberger Waldes, Der Egge und Des Haarstrangs. *Geologie und Paläontologie in Westfalen*, **37**, 1–53.

Wray, D.S., Wood, C.J., Ernst, G. and Kaplan, U. 1996. Geochemical subdivision and correlation of clay-rich beds in Turonian sediments of northern Germany. *Terra Nova*, **8**, 603–610.

Wray, D.S. and Gale, A.S. 2006. The palaeoenvironment and stratigraphy of Late Cretaceous Chalks. *Proceedings of the Geologists' Association*, **117**, 145–162.

Wray, D.S. and Jeans, C.V. 2014. Chemostratigraphy and provenance of clays and other non-carbonate minerals in chalks of Campanian age (Upper Cretaceous) from Sussex, southern England. *Clay Minerals*, **49**, 327–340.

Yeomans, R. 2018. Paramoudra: observations on large flint structures from the Chalk (Upper Cretaceous) and flint formation. *Proceedings of the Yorkshire Geological Society*, **62**, 210–216.

Manuscript submitted: 17th March 2025
Revised version accepted: 2nd September 2025

APPENDIX 1

Mineralogy, crystal size and chemistry of Cretaceous flints, cherts and nano-quartz from western Europe.

Sample	Location: Flint form	Sample type	Age	Moganite		Quartz	
				Content %	Crystal size nm	Content %	Crystal size nm
STANDARDS							
Crushed quartz				1.4[±0.9]	26.1[±17.1]	98.6[±0.9]	611.7±59.8]
<2um crushed quartz				1.1[±2.8]	18.1[±46.7]	98.9[±2.8]	58.7[±5.5]
RED FLINT GROUP							
	Duene Island, Helgoland						
CVJRM19 red(1)	nodular flint	inner red core	Turonian	15.1[±1.4]	10.6[±1.2]	84.9[±1.4]	44.0[±1.8]
CVJRM19 red(2)	nodular flint	inner red core	Turonian	16.5[±1.3]	10.4[±1.0]	83.5[±1.3]	37.3[±1.4]
CVJRM20 red(3)	nodular flint	inner red core	Turonian	16.7[±2.1]	10.0[±1.8]	83.3[±2.1]	49.8[±3.0]
CVJRM19 black(1)	nodular flint	outer black core	Turonian	16.6[±1.3]	14.2[±1.4]	83.4[±1.3]	38.0[±1.8]
CVJRM19 black(2)	nodular flint	outer black core	Turonian	13.1[±2.7]	12.1[±3.0]	86.9[±2.7]	35.1[±3.3]
Grey pink pyritic type							
Ferruginous Flint Band	Melton Ross, Lincs	core	Turonian	9.0[±1.4]	10.0[±2.1]	91.0[±1.4]	57.3[±2.0]
BROWN FLINT GROUP							
	Brown Flint Band, Speeton						
BFB 1	nodular flint	core	Cenomanian	38.1[±1.9]	10.5[±0.4]	61.9[±1.9]	13.6[±1.0]
BFB 2	nodular flint	core	Cenomanian	13.3[±1.5]	10.0[±1.7]	86.7[±1.5]	55.7[±2.4]
BFB 3	nodular flint	cortex	Cenomanian	7.4[±1.6]	16.8[±4.0]	92.6[±1.6]	51.9[±3.2]
	Faxe Quarry, Denmark						
Faxe 2	nodular flint	core	Danian	15.8[±0.9]	20.0[±0.6]	84.2[±0.9]	35.0[±1.1]
Faxe 3	nodular flint	core	Danian	14.9[±0.6]	20.0[±0.6]	85.1[±0.6]	30.0[±0.8]
Faxe 4	nodular flint	core	Danian	16.1[±0.8]	20.0[±0.6]	83.9[±0.8]	28.0[±0.8]
Faxe 5	nodular flint	core	Danian	17.4[[±0.9]	20.0[±0.6]	82.6[±0.9]	31.0[±0.8]
Faxe 6	nodular flint	core	Danian	18.9[±0.9]	20.0[±0.6]	81.1[±0.9]	32.0[±1.0]
Faxe 7	nodular flint	core	Danian	16.4[±0.9]	20.0[±0.6]	83.6[±0.9]	20.0[±0.6]
Faxe 8	nodular flint	core	Danian	14.0[±0.9]	38.0[±1.1]	86.0[±0.9]	45.0[±1.4]

Table 1. Quantitative silica mineralogy and crystal size of standard quartz and decalcified examples of flints of the Red flint and the Brown flint groups. Sample location, type and age are listed.

	SiO_2 %	TiO_2 %	Al_2O_3 %	Fe_2O_3 %	MnO %	MgO %	CaO %	Na_2O %	K_2O %	P_2O_5 %	Total non-SiO_2 %
RED FLINT GROUP											
CVJRM19 red inner core	99.687	0.005	0.101	0.113	0.0010	0.003	0.015	0.040	0.032	0.003	0.313
CVJRM19 black outer core	99.767	0.003	0.077	0.073	0.0011	0.003	0.011	0.036	0.027	0.002	0.233
CVJRM20 red inner core	99.577	0.005	0.118	0.126	0.0016	0.004	0.042	0.045	0.036	0.011	0.423
Grey pink pyritic type											
Ferruginous Flint Band	99.633	0.005	0.138	0.058	0.0005	0.003	0.089	0.034	0.025	0.014	0.367
BROWN FLINT GROUP											
Brown Flint Band, Speeton 1	99.329	0.012	0.375	0.079	0.0005	0.008	0.049	0.079	0.058	0.010	0.671
Brown Flint Band, Speeton 2	99.399	0.012	0.309	0.077	0.0004	0.008	0.042	0.081	0.058	0.007	0.601
Faxe 2	99.786	0.000	0.089	0.024	0.000	0.002	0.033	0.030	0.023	0.013	0.214
Faxe 3	99.666	0.006	0.134	0.039	0.000	0.013	0.067	0.034	0.032	0.009	0.334
Faxe 4	99.775	0.004	0.063	0.022	0.000	0.010	0.069	0.025	0.018	0.013	0.225
Faxe 5	99.799	0.004	0.063	0.026	0.001	0.004	0.043	0.026	0.019	0.015	0.201
Faxe 6	99.809	0.004	0.066	0.035	0.001	0.007	0.035	0.024	0.017	0.002	0.191
Faxe 7	99.884	0.002	0.043	0.011	0.000	0.001	0.022	0.021	0.014	0.002	0.116
Faxe 8	99.821	0.003	0.070	0.026	0.000	0.001	0.029	0.025	0.019	0.006	0.179
BLACK FLINT GROUP											
Floorstone	99.59	0.005	0.094	0.152	0.0016	0.002	0.064	0.042	0.032	0.017	0.410
Zoomorphic type											
CVJRM17(1) Baldock Bypass,Turonian	99.687	0.005	0.136	0.022	0.0004	0.006	0.059	0.039	0.040	0.007	0.313
CVJRM17 (2) Baldock-Bypass, Turonian	99.695	0.005	0.132	0.021	0.0003	0.005	0.059	0.038	0.040	0.007	0.305
Nodular type											
FRU1 large paramoudra	99.769	0.004	0.078	0.015	0.0003	0.003	0.045	0.038	0.030	0.018	0.231
HOJ 1	99.727	0.005	0.097	0.023	0.0004	0.003	0.050	0.043	0.037	0.015	0.273
Vein type											
KUL 1	99.626	0.005	0.111	0.037	0.0006	0.003	0.093	0.049	0.035	0.040	0.374
RM 3	99.808	0.005	0.060	0.022	0.0002	0.004	0.045	0.033	0.025	0.005	0.198
SLO 1	99.813	0.003	0.066	0.024	0.0003	0.002	0.025	0.033	0.026	0.008	0.187
SLO 2	99.802	0.003	0.064	0.028	0.0004	0.003	0.032	0.033	0.027	0.008	0.198
SLO 3	99.773	0.004	0.084	0.019	0.0003	0.003	0.036	0.038	0.032	0.011	0.227
SLO 4(1)	99.794	0.003	0.069	0.025	0.0005	0.002	0.030	0.035	0.029	0.012	0.206
SLO 4(2)	99.794	0.003	0.069	0.026	0.0004	0.003	0.030	0.034	0.029	0.012	0.206
RØD 1	99.765	0.003	0.069	0.019	0.0003	0.002	0.046	0.041	0.031	0.023	0.235
RØD 2	99.782	0.003	0.063	0.018	0.0002	0.002	0.041	0.041	0.029	0.021	0.218
RØD 3	99.713	0.005	0.097	0.019	0.0002	0.003	0.050	0.046	0.036	0.027	0.287
RØD 4	99.637	0.004	0.081	0.022	0.0002	0.003	0.107	0.044	0.034	0.068	0.363
RØD 5	99.746	0.003	0.062	0.013	0.0001	0.002	0.038	0.040	0.029	0.017	0.254
RØD 6	99.751	0.003	0.078	0.016	0.0003	0.003	0.052	0.042	0.033	0.022	0.249
RØD 8	99.795	0.003	0.070	0.011	0.0001	0.002	0.034	0.040	0.032	0.013	0.205

Table 2. Major elemental composition of flints. Sample location and ages are listed in Tables 1 and 5.

	Ba ppm	Be ppm	Cr ppm	Cu ppm	Ni ppm	Sr ppm	Co ppm	V ppm	Y ppm	Zn ppm	Zr ppm
RED FLINT GROUP											
CVJRM19 red inner core	2.25	0.24	0.79	1.05	2.21	1.43	0.23	1.47	0.30	5.77	0.94
CVJRM19 black outer core	1.82	0.31	0.46	2.66	0.71	0.96	0.19	1.57	0.17	6.34	1.24
CVJRM20 red inner core	5.38	0.27	1.01	2.06	1.78	2.29	0.25	1.25	0.74	6.21	1.20
Grey pink pyritic type											
Ferruginous Flint Band	5.23	0.14	0.02	9.93	1.39	4.81	0.24	1.15	0.97	2.30	2.96
BROWN FLINT GROUP											
Brown Flint Band, Speeton 1	31.93	0.31	0.45	20.02	<0.6	7.88	0.63	2.36	0.69	0.95	2.39
Brown Flint Band, Speeton 2	14.94	0.33	1.02	1.12	1.33	7.74	0.60	2.45	0.58	0.92	1.49
Faxe 2	2.07	0.05	1.40	<0.2	<0.6	4.73	0.21	1.22	1.50	2.47	1.34
Faxe 3	2.55	0.07	1.91	0.51	<0.6	5.13	0.82	1.36	1.76	5.08	1.89
Faxe 4	2.37	0.06	1.67	0.33	<0.6	8.62	0.17	0.94	2.09	3.41	0.96
Faxe 5	1.83	0.07	1.95	<0.2	<0.6	4.29	0.09	0.92	1.72	1.25	1.07
Faxe 6	1.39	0.12	2.04	<0.2	<0.6	2.53	0.78	0.94	0.42	2.63	1.54
Faxe 7	1.02	0.08	1.16	<0.2	<0.6	2.13	0.02	0.72	0.40	1.01	3.22
Faxe 8	1.12	0.07	1.17	<0.2	<0.6	3.32	0.27	0.91	0.82	3.79	1.34
BLACK FLINT GROUP											
Floorstone	2.27	0.90	1.38	2.49	<0.6	3.60	0.23	1.39	0.96	1.72	1.38
Zoomorphic type											
CVJRM17(1) Baldock Bypass, Turonian	2.80	0.14	2.18	1.73	0.84	2.96	0.24	2.18	0.80	0.61	1.38
CVJRM17(2) Baldock Bypass, Turonian	2.09	0.14	1.55	1.65	<0.6	2.91	0.23	2.10	0.83	0.85	1.37
Nodular type											
FRU 1 large paramoudra	2.48	0.15	2.18	5.09	0.60	6.23	0.28	1.33	1.97	4.99	1.14
HØJ 1	1.41	0.16	1.12	3.58	1.44	8.48	0.30	1.62	1.66	13.09	1.76
Vein type											
KUL 1	6.34	0.15	2.50	4.43	2.96	10.39	0.61	1.90	2.77	6.30	4.09
RM3	37.02	0.09	0.46	1.18	0.74	3.35	0.11	1.36	0.57	17.25	0.71
SLO 1	1.67	0.15	0.78	1.54	0.85	5.46	0.18	1.06	0.52	7.83	1.45
SLO 2	7.79	0.15	0.83	1.27	1.00	4.36	0.21	1.69	0.65	6.86	1.26
SLO 3	40.53	0.16	0.07	2.61	2.65	83.40	0.22	2.39	0.86	8.97	1.45
SLO 4 (1)	1.96	0.17	1.35	1.36	1.68	5.15	0.17	1.79	0.72	7.98	1.26
SLO 4 (2)	2.28	0.17	1.39	1.44	2.27	5.12	0.16	1.91	0.74	7.98	1.28
RØD 1	4.95	0.17	0.87	0.91	<0.6	6.10	0.26	1.40	1.86	3.47	1.73
RØD 2	2.75	0.18	0.71	2.36	<0.6	5.58	0.23	1.03	1.61	7.64	1.38
RØD 3	7.03	0.21	2.73	1.57	<0.6	6.80	0.30	1.27	2.45	20.88	2.03
RØD 4	4.11	0.17	0.86	1.19	<0.6	10.71	0.31	1.32	4.62	3.19	0.95
RØD 5	2.82	0.17	<0.2	2.28	2.82	4.90	0.25	0.83	1.53	3.26	0.94
RØD 6	3.89	0.17	0.77	2.05	0.75	6.31	0.28	1.54	1.93	6.72	1.79
RØD 8	7.19	0.16	0.29	0.58	<0.6	5.23	0.27	0.79	1.33	5.13	1.20

Table 3. Minor elemental composition of flints. Sample location and age are listed in Tables 1 and 5.

	P_2O_5 %	La ppm	Ce ppm	Pr ppm	Nd ppm	Sm ppm	Eu ppm	Gd ppm	Tb ppm	Dy ppm	Ho ppm	Er ppm	Tm ppm	Yb ppm	Lu ppm	Ce* [Flint]	Eu* [Flint]
RED FLINT GROUP																	
CVJRM19 red inner core	0.003	0.31	0.86	0.07	0.31	0.06	0.01	0.06	0.01	0.05	0.01	0.03	0.00	0.03	0.00	1.02	0.67
CVJRM19 black outer core	0.002	0.15	0.64	0.03	0.13	0.02	0.01	0.02	0.00	0.02	0.00	0.01	0.00	0.01	0.00	2.97	2.02
CVJRMS 20 red inner core	0.011	0.68	1.65	0.19	0.78	0.16	0.03	0.15	0.02	0.12	0.02	0.06	0.01	0.04	0.01	1.16	0.78
Grey pink pyritic type																	
Ferruginous Flint Band	0.014	1.24	1.39	0.30	1.26	0.25	0.05	0.22	0.03	0.16	0.03	0.07	0.01	0.05	0.01	0.56	0.86
BROWN FLINT GROUP																	
BFB 1	0.010	0.79	1.35	0.23	1.00	0.21	0.05	0.18	0.03	0.14	0.03	0.06	0.01	0.05	0.01	0.79	1.04
BFB 2	0.007	0.66	1.12	0.19	0.78	0.16	0.04	0.14	0.02	0.11	0.02	0.05	0.01	0.04	0.01	0.81	1.08
Faxe 2	0.013	1.57	1.80	0.43	1.73	0.35	0.08	0.33	0.04	0.25	0.04	0.11	0.01	0.08	0.01	0.56	1.40
Faxe 3	0.009	1.77	2.32	0.49	1.99	0.41	0.09	0.38	0.05	0.30	0.05	0.14	0.02	0.10	0.01	0.63	0.92
Faxe 4	0.013	1.81	1.86	0.48	1.95	0.42	0.10	0.41	0.05	0.32	0.06	0.16	0.02	0.11	0.01	0.50	0.97
Faxe 5	0.015	1.64	1.90	0.40	1.62	0.33	0.08	0.33	0.04	0.27	0.05	0.13	0.02	0.09	0.01	0.58	0.99
Faxe 6	0.002	0.39	0.52	0.12	0.47	0.09	0.02	0.10	0.01	0.08	0.01	0.03	0.01	0.03	0.01	0.65	0.84
Faxe 7	0.002	0.38	0.43	0.10	0.43	0.09	0.02	0.10	0.01	0.07	0.01	0.03	0.00	0.03	0.00	0.55	0.84
Faxe 8	0.006	0.87	1.01	0.24	0.96	0.19	0.04	0.20	0.02	0.15	0.02	0.07	0.01	0.05	0.01	0.59	1.07
BLACK FLINT GROUP																	
Floorstone	0.017	0.86	0.85	0.21	0.90	0.18	0.04	0.17	0.02	0.13	0.03	0.07	0.01	0.06	0.01	0.48	0.92
Zoomorphic type																	
CVJRM17(1) Baldock Bypass, Turonian	0.007	1.06	0.81	0.19	0.77	0.14	0.03	0.13	0.02	0.11	0.02	0.06	0.01	0.05	0.01	0.24	0.90
CVJRM17(2) Baldock Bypass, Turonian	0.007	1.07	0.77	0.19	0.79	0.14	0.03	0.13	0.02	0.12	0.02	0.06	0.01	0.06	0.01	0.39	0.90
Nodular type																	
FRU 1	0.018	1.56	1.14	0.34	1.46	0.28	0.06	0.29	0.04	0.25	0.05	0.14	0.02	0.10	0.01	0.37	0.85
HOJ 1	0.015	1.37	1.10	0.31	1.32	0.25	0.06	0.26	0.04	0.23	0.04	0.12	0.01	0.08	0.01	0.41	0.94
Vein type																	
Kul 1	0.040	2.45	1.95	0.51	2.09	0.40	0.10	0.40	0.06	0.39	0.08	0.22	0.03	0.17	0.02	0.49	1.00
RM 3	0.005	0.55	0.38	0.09	0.39	0.07	0.02	0.07	0.01	0.06	0.01	0.04	0.01	0.04	0.01	0.27	1.15
SLO 1	0.008	0.44	0.41	0.11	0.48	0.09	0.02	0.09	0.01	0.07	0.01	0.04	0.00	0.03	0.00	0.46	0.89
SLO 2	0.008	0.59	0.50	0.13	0.54	0.10	0.02	0.10	0.02	0.10	0.02	0.05	0.01	0.05	0.01	0.44	0.80
SLO 3	0.011	0.82	0.62	0.15	0.64	0.13	0.03	0.13	0.02	0.11	0.02	0.06	0.01	0.05	0.01	0.40	0.93
SLO 4(1)	0.012	0.57	0.50	0.13	0.56	0.10	0.02	0.11	0.02	0.10	0.02	0.05	0.01	0.04	0.01	0.45	0.37
SLO 4(2)	0.012	0.58	0.51	0.13	0.56	0.11	0.03	0.11	0.02	0.10	0.02	0.05	0.01	0.04	0.01	0.44	1.10
ROD 1	0.023	1.44	1.03	0.30	1.28	0.25	0.06	0.25	0.04	0.25	0.05	0.13	0.02	0.10	0.01	0.37	0.97
ROD 2	0.021	1.22	0.85	0.25	1.06	0.20	0.05	0.21	0.03	0.20	0.04	0.11	0.01	0.08	0.01	0.35	0.87
ROD 3	0.027	1.86	1.53	0.44	1.89	0.38	0.09	0.36	0.06	0.34	0.07	0.17	0.02	0.12	0.02	0.41	0.98
ROD 4	0.068	3.22	2.22	0.65	2.77	0.54	0.13	0.57	0.09	0.57	0.12	0.33	0.04	0.24	0.03	0.36	0.94
ROD 5	0.017	1.20	0.92	0.26	1.10	0.22	0.05	0.22	0.03	0.20	0.04	0.11	0.01	0.08	0.01	0.39	0.91
ROD 6	0.022	1.50	1.08	0.30	1.31	0.26	0.06	0.26	0.04	0.26	0.05	0.14	0.02	0.10	0.01	0.37	0.93
ROD 8	0.013	1.07	0.86	0.24	1.03	0.20	0.05	0.20	0.03	0.19	0.04	0.10	0.01	0.08	0.01	0.41	1.01

Table 4. Rare earth element composition of flints and calculated Ce*(DCF) and Eu*(DCF) values. Sample location and age are listed in Tables 1 and 5.

Sample	Location: Flint form	Sample type	Age	Moganite		Quartz	
				Content %	Crystal size nm	Content %	Crystal size nm
BLACK FLINT GROUP							
	Hojerup, Stevns, Denmark						
KUL1	nodule	core	uppermost Maastrichtian	14.2[±1.8]	11.2[±1.8]	85.8[±1.8]	51.8[±2.6]
ROD1	discordant vein	core	Upper Maastrichtian	18.6[±1.5]	10.0[±1.2]	81.4[±1.5]	44.3[±1.7]
ROD2	discordant vein	core	Upper Maastrichtian	19.1[±1.5]	10.0[±1.2]	80.9[±1.5]	44.5[±1.8]
ROD3	discordant vein	core	Upper Maastrichtian	17.7[±2.0]	10,0[±1.7]	82.3[±2.0]	45.9[±2.2]
ROD4	concordant vein	core	Upper Maastrichtian	20.9[±1.4]	10.1[±1.0]	79.1[±1.4]	45.8[±1.8]
ROD5	concordant vein	core	Upper Maastrichtian	18.2[±2.1]	11.0[±1.6]	81.8[±2.1]	32.4[±2.0]
ROD6	concordant vein	core	Upper Maastrichtian	17.7[±2.1]	10.0[±1.8]	82.3[±2.1]	47.8[±2.8]
ROD8	discordant vein	core	Upper Maastrichtian	19.6[±2.0]	10.0[±1.5]	80.4[±2.0]	41.0[±2.3]
SLO2	concordant vein	core	Lower Maastrichtian	15.4[±1.5]	10.0[±1.4]	84.6[±1.5]	51.3[±2.2]
SLO3	discordant vein	core	Lower Maastrichtian	16.1[±1.3]	11.1[±1.1]	83.9[±1.3]	48.9[±1.8]
SLO4	discordant vein	core	Lower Maastrichtian	24.0[±1.5]	10.0[±0]	76.0[±1.5]	27.2[±1.2]
FRU1	paramoudra	core	Lower Maastrichtian	14.4[±2.3]	10.0[±2.2]	85.5[±2.3]	44.6[±2.7]
HOF1	nodule	core	Upper Maarstritchtian	13.6[±1.2]	13.3[±1.4]	86.4[±1.2]	39.0[±1.6]
HOF2	nodule	core	Upper Maastritchtian	0.0[±2.4]	–	100.0[±2.4]	202.1[±26.6]
	Karlstrup, Stevns, Denmark						
DNK1	nodule	pale patch, dark core	Danian	3.1[±1.1]	10.1[±5.1]	96.9[±1.1]	64.4[±2.1]
	Sigersley Quarry						
DNK2a	nodule	centre, dark core	Upper Maastrichtian	18.5[±0.9]	10.1[±0.8]	81.5[±0.9]	43.8[±1.3]
DNK2b	nodule	rim, dark core	Upper Maastrichtian	19.2[±1.2]	10.0[±1.0]	80.8[±1.2]	43.4[±1.5]
DNK3	nodule	rim, dark core	Upper Maastrichtian	20.2[±1.2]	10.0[±0.9]	79.8[±1.2]	37.0[±1.4]
	Fahse Quarry						
	nodule	rim, dark core	Middle Danian	16.8[±1.2]	10.0[±1.0]	83.2[±1.2]	39.4[±1.4]
DNK5	nodule/?white flint	cortex of DNK4	Middle Danian	–	–	100.0[±1.2]	68.5[±2.4]
	Hojerup, Stevns, Denmark						
DNK6 [HOP, OP]	nodule	dark core, rim	Top Maastrichtian	16.3[±1.3]	10.0[±1.1]	83.7[±1.3]	32.6[±1.3]
DNK7 [HOF, 3P]		dark core, centre	Top Maastrichtian	16.1[±1.2]	10.0[±1.1]	83.9[±1.2]	46.9[±1.7]
DNK8 [-HOF, 1]	nodule	dark core, pale patch nr rim	Upper Maastrichtian	14.7[±1.1]	10.0[±1.1]	85.3[±1.1]	51.0[±1.7]
DNK9 [-1HOF, 2]		dark core, pale patch nr centre	Upper Maastrichtian	0.5[±0.4]	27.0[±22.6]	99.5[±0.4]	117.0[±2.9]
DNK10 [-HOF, 3]		dark core, pale patch	Upper Maastrichtian	5.9[±1.0]	10.2[±2.3]	94.1[±1.0]	61.7[±1.9]
DNK11 [-2HOF]	nodule	dark core, rim	Upper Maastrichtian	17.2[±1.2]	10.2[±1.1]	82.8[±1.2]	35.5[±1.3
DNK12a [-2HOF]		dark core	Upper Maastrichtian	3.1[±1.1]	10.1[±5.1]	96.9[±1.1]	64.4[±2.1]
DNK12b [-2HOF]		dark core, pale patch	Upper Maastrichtian	0.3[±0.3]	22.4[±20.7]	99.7[±0.3]	209.6[±5.1]
DNK13 [-2HOF]		dark core, pale sponge trace	Upper Maastrichtian	3.0[±1.0]	18.3[±6.2]	97.0[±1.0]	95.1[±4.1]
FLOORSTONE							
	Grimes Grave, Norfolk, England						
	concordant flint band	core	Turonian	20.1[±1.1]	10.0[±0.8]	79.9[±1.1]	42.7[±1.5]
	Old Dene Quarry, Surrey						
SuR20 OD1	nodule	core	Turonian	20.8[±0.8]	10.0[±0.6]	79.2[±0.8]	34.1[±0.9]
SuR20 OD2	nodule	cortex	Turonian	10.5[±1.0]	10.2[±1.2]	89.5[±1.0]	34.5[±0.9]

	Caistor St Edmunds, Norwich						
CSE33	paramoudra	dark core, pale patch	Campanian	8.5[±1.1]	18.0[±2.5]	91.5[±1.1]	51.2[±2.1]
CSE34a	paramoudra	dark core	Campanian	15.4[±1.8]	10.0[±1.6]	84.6[±1.8]	35.8[±1.8]
CSE34b	paramoudra	dark core	Campanian	16.0[±2.4]	13.1[±2.4]	84.0[±2.4]	36.8[±3.0]
CSE 41	paramoudra	dark core, pale patch	Campanien	1.7[±0.5]	10.0[±4.3]	98.3[±0.5]	404.7[±14.4
CSE 42	paramoudra	dark core	Campanian	20.2[±1.5]	10.1[±1.2]	79.8[±1.5]	40.3[±1.7]
CSE 43	paramoudra	dark core	Campanian	23.1[±1.5]	10.0[±1.1]	76.9[±1.5]	45.8[±1.9]
CSE 44	paramoudra	dark core, pale patch	Campanian	3.6[±0.7]	12.8[±3.0]	96.4[±0.7]	99.5[±2.7]

Table 5. Quantitative silica mineralogy and crystal size of decalcified examples of Black group flints. Sample location, type and age are listed.

Sample no.	Location: Flint form	Age	Moganite		Quartz	
			Content %	Crystal size nm	Content %	Crystal size nm
GREY FLINT GROUP						
	Ballard Cliff, Dorset					
1A1	nodular flint	Cenomanian	6.9[±0.6]	12.9[±1.5]	93.1[±0.6]	48.9[±1.0]
1A3	nodular flint	Cenomanian	6.7[±1.2]	10.6[±2.5]	93.3[±1.2]	43.7[±1.3]
1B2	nodular flint	Cenomanian	10.8[±1.1]	10.1[±1.5]	89.2[±1.1]	65.0[±1.9]
3A1	nodular flint	Cenomanian	8.6[±0.7]	10.1[±1.2]	91.4[±0.7]	48.6[±0.99]
3A2	nodular flint	Cenomanian	13.8[±0.8]	10.6[±0.8]	86.2[±0.8]	42.9[±1.0]
4A1	nodular flint	Cenomanian	7.2[±0.6]	13.0[±1.5]	92.8[±0.6]	56.0[±1.2]
4A2	nodular flint	Cenomanian	6.9[±0.8]	10.1[±1.6]	93.1[±0.8]	48.9[±1.0]
	Newhaven, Sussex					
Grey flint vein RM2 (Text-fig. 4A)	discordant vein	Campanian	14.6[±1.8]	10.0[±1.7]	85.4[±1.8]	37.0[±1.6]
Quartz vug grey flint RM16 (Text-fig 12D)	nodular flint					
RM16a	core CE	Coniacian	14.7[±1.6]	10.0[±1.6]	85.3[±1.6]	45.8[±1.9]
RM16b	CE/CE1 transition	Coniacian	2.2[±1.4]	10.0[±7.6]	97.8[±1.4]	106.0[±3.7]
RM16c	inner CE1	Coniacian	–	–	100[±0.7]	89.2[±3.9]
RM16d	Outer CE1	Coniacian	–	–	99.9[±1.0]	87.0[±3.2]
Grey flint nodule (Text-fig. 5E)	Baldock bypass, Hertfordshire					
RM13a	core CE	Turonian	19.3[±2.4]	10.0[±1.7]	80.7[±2.4]	25.1[±1.7]
RM13b	inner cortex CX1	Turonian	18.4[±1.5]	10.0[±1.2]	81.6[±1.5]	38.8[±1.6]
RM13c	outer cortex CX2	Turonian	23.0[±1.4]	10.0[±0.9]	77.0[±1.4]	28.0[±1.2]
RM13d	core sealed fracture, arrow	Turonian	15.9[±1.7]	11.1[±1.6]	84.1[±1.7]	41.2[±2.0]
GREY CARIOUS FLINT GROUP						
	Ulceby, Lincolnshire					
Ludborough Tabular Flint Band: Text-figs 5D, 13	UCL 2A	Upper Turonian	9.6[±1.0]	10.0[±1.5]	90.4[±1.0]	54.9[±1.6]
Brocklesby Flint Band: Text-figs 5D, 13	ULC 1A	Upper Turonian	7.7[±0.9]	10.0[±1.6]	92.3[±0.9]	75.5[±2.1]
lenticular nodular flint	ULC 4A	Upper Turonian	4.3[±0.8]	18.7[±3.5]	95.7[±0.8]	53.2[±1.5]
vein flint	ULC 6A	Upper Turonian	11.4[±1.1]	10.0[±1.1]	88.6[±1.1]	49.1[±1.4]
tabular flint	ULC 7A	Upper Turonian	10.0[±1.0]	10.0[±1.3]	90.0[±1.0]	55.8[±1.5]
WHITE FLINT GROUP						
Text-fig. 5F	Selwick Bay, Yorkshire					
Wf1	nodular flint	Santonian	0.8[±1.3]	10.0[±15.7]	99.2[±1.3]	58.7[±1.4]
Wf2	nodular flint	Santonian	–	–	100.0[±0.5]	63.6[±1.32]
Wf3	nodular flint	Santonian	–	–	100.0[±0.8]	64.6[±1.3]
Wf4	nodular flint	Santonian	0.9[±0.8]	14.7[±15.3]	99.1[±0.8]	52.6[±1.1]

Table 6. Quantitative silica mineralogy and crystal size of decalcified examples of the Grey, Grey Carious and White flint groups. Sample location, type and age are listed.

Sample no.	Flint			Calcite in flint		Chalk matrix	
	SiO_2 %	$CaCO_3$ %	bulk SG	$\delta^{13}C$ ‰	$\delta^{18}O$ ‰	$\delta^{13}C$ ‰	$\delta^{18}O$ ‰
GREY CARIOUS FLINT GROUP							
Ulceby Chalk Pit, Lincolnshire							
ULC1A, B	94.8	5.2	2.565	1.91	-2.46	2.1	-4.76
ULC2A, B	96.3	3.7	2.538	2.26	-2.33	2.06	-4.57
ULC4A, B	88.9	11.1	2.421	2.03	-3.98	2.2	-4.5
ULC6A	~ 97	~3	nd	2.27	-4.33	1.94	-4.43
ULC7A, B	~97	~3.0	2.544	2.35	-2.21	1.94	-4.43
ULC8A, B	nd	nd	2.598	nd	nd	2.23	-4.34
WHITE FLINT GROUP							
Selwick Bay, Yorkshire							
wf.1	95.14%	4.86%	2.409	1.53	-5.18	2.46	-3.56
wf.2	94.11	5.89	2.486	1.89	-2.35	2.45	-3.401
wf.3	91.09	8.91	2.375	2.09	-3.57	2.34	-3.77
wf.4	95.35	4.65	2.453	2.14	-4.38	2.21	-4.06

Table 7. Mineralogical, chemical and isotopic analysis of grey carious and white flints. nd – not determined.

Sample	Location; Flint form; Depth	Sample type	Age	Moganite		Quartz	
				Content %	Crystal size nm	Content %	Crystal size nm
SPONGE ASSOCIATED FLINT GROUP							
	Newhaven, East Sussex						
sponge [RM5a]	spongiform shaped flint RM5		base Campanian/ Upper Turonian	12.2[±1.8]	10.0[±2.0]	87.8[±1.8]	46.6[±2.2]
sponge [RM5c]	Text-fig .14		base Campanian/ Upper Turonian	12.9[±1.7]	10.0[±1.9]	87.1[±1.7]	49.2[±2.3]
sponge in flint matrix [RM5b]				17.0[±1.7]	10.0[±1.4]	83.0[±1.7]	52.4[±2.7]
cortex [RM5d]				12.2[±1.9]	10.0±2.1]	87.8[±1.9]	40.2[±1.9]
NORTH SEA FLINT GROUP							
NANA 1A	2125.93 m	cortex	Danian	0	0	100[±3.8]	61.9[±6.3]
NANA 1B	2135.8 m	cortex	Danian	1.1[±2.6]	23.8[±60.8]	98.9[±2.6]	51.8[±5.8]
RIGS 1A	2794.3 m	cortex	Danian	1.3[±1.4]	10.0[±13.7]	98.7[±1.4]	101.6[±4.3]
RIGS 1B	2826.84 m	core	Danian	2.8[±2.7]	27.2[±29.4]	97.2[±2.7]	79.1[±79.1]
SIF 1A	2057.53 m	cortex	Danian	2.9[±1.8]	93.0[±280.3]	97.1[±1.8]	65.2[±6.6]
SIF 1B	2079.34 m	cortex	Danian	–	–	100.0[±4.1]	73.2[±7.9]
CLAY-GRADE QUARTZ GROUP							
	Speeton, Yorkshire						
Ysa17	marl seam	nano-quartz	Cenomanian	6.0[±2.8]	40.6[±31.8]	94.0[±2.8]	186.3[±14.7]
Ysa25	marl seam	nano-quartz	Cenomanian	9.8[±5.9]	46.7[±58.6]	90.2[±5.9]	206.7[±37.9]
Ysa55	marl seam	nano-quartz	Cenomanian	5.6[±4.2]	–	94.4[±4.2]	199.0[±28.1]
Ysa77	marl seam	nano-quartz	Cenomanian	2.2[±3.0]	–	97.8[±3.0]	178.6[±26.8]
Ysa81	marl seam	nano-quartz	Cenomanian	29.9[±3.6]	31.1[±6.2]	70.1[±3.6]	212.3[±34.4]

Table 8. Quantitative silica mineralogy and crystal size of decalcified examples of (1) Sponge-associated and North Sea flint groups and (2) Clay-grade quartz. Sample location, depth, type and age are listed.

Sample	Analysis	O %	Si %	Al %	K %	Ca %	Fe %	Mn %	Ti %	P %
Ysa17	1	71.5	19.0	5.7	0.2	0.6	1.2	0.0	0.0	0.0
Ysa17	2	71.0	26.6	1.6	0.1	0.2	0.4	0.0	0.0	0.0
Ysa17	3	70.4	27.6	1.3	0.1	0.2	0.4	0.0	0.0	0.0
Ysa17	11	71.0	27.5	1.1	0.1	0.2	0.2	0.0	0.0	0.0
Ysa17	12	69.9	21.4	4.9	0.4	0.7	1.01	0.0	0.0	0.1
Ysa17	13	71.0	28.5	0.4	<0.1	<0.1	<0.1	0.0	0.0	0.0
Ysa55	4	64.1	35.0	0.6	0.1	0.1	1.1	0.0	0.0	<0.1
Ysa55	5	66.3	32.0	1.0	0.2	0.3	0.3	0.0	0.0	<0.1
Ysa55	6	66.1	25.6	4.7	1.0	0.9	0.9	0.0	0.0	0.1
Ysa55	7	69.8	15.7	7.3	0.7	0.8	1.3	0.0	0.0	0.0
Ysa55	8	67.2	27.9	2.1	0.1	0.2	0.7	0.0	0.0	0.0
Ysa55	9	68.9	27.4	1.8	0.2	0.2	0.2	0.0	0.0	0.0
Ysa55	10	70.4	28.9	0.4	<0.1	<0.1	<0.1	0.0	0.0	0.0
Ysa55	14	70.0	18.3	6.8	0.7	0.6	1.1	0.0	0.0	0.0
Ysa55	15	70.4	27.6	1.3	0.1	0.2	0.4	0.0	0.0	0.0
Ysa55	16	70.4	28.9	0.4	0.1	0.0	0.1	0.0	0.0	0.0
Ysa55	17	66.5	31.9	0.8	0.2	0.2	0.3	0.0	0.0	0.1
Ysa55	18	65.4	31.9	1.2	0.3	0.3	0.4	0.0	0.0	0.0

Table 9. Microprobe chemical analyses, expressed as atomic fraction percentage, of selected nano-quartz particles from the Cenomanian marls and chalk. Speeton, Yorkshire, England.

Location	Sample	Flint group	Sample type	Horizon	Moganite		Quartz	
					Content %	Crystal size nm	Content %	Crystal size nm
Culham	5C	chert	core	Upper Albian	14.1 [±0.6]	10[±0.6]	85.9[±0.6]	74.9[±1.63]
Chard	MR 4026	chert	core	Upper Albian	14.9[±3.3]	10.5[±3.3]	85.1[±3.3]	39.3[±3.3]
Burghcloe, Berkshire	MR 4054	chert	core	Upper Albian	6.4[±0.7]	10[±1.48]	93.6[±0.7]	29.3[±0.61]
Culver Clff, Isle of Wight	MR 4060	chert	core	Upper Albian	6.7[±0.6]	10[±1.2]	93.3[±0.6]	70.1[±1.3]
Arreton, Isle of Wight	MR 4061	chert	core	Upper Albian	9.3[±3.0]	10[[±4.7]	90.7[±3.0]	46.8[±3.5]
Arreton, Isle of Wight	MR 4061	chert	cortex	Upper Albian	15.8[±2.1]	10[±1.9]	84.2[±2.1]	29.7[±1.5]
Arreton, Isle of Wight	MR 6616	chert	core	Upper Albian	14.1[±4.1]	10.3[±4.0]	85.9[±4.1]	38.1[±3.7]
Arreton, Isle of Wight	MR 6166	chert	cortex	Upper Albian	13.7[±1.4]	10[±1,6]	86.3[±1.4]	44.2[±1.7]
Branscombe	MR 6621	chert	cortex	Upper Albian	25.2[±2.1]	10[±1.4]	74.8[±2.1]	29.1[±1.8]
Bindon Landslip	MR 6623	chert	core	Upper Albian	5.5 [±0.8]	10.0[±2.0]	94.5[±0.8]	49.06 [±1.04]
Chillington	MR 6834	chert	core	Upper Albian	15.7[±3.0]	10.1[±2.8]	84.3[±3.0]	34.3[±2.9]
Chillinghton	MR 6837	chert	core	Upper Albian	15.8[±2.7]	10.2[±2.5]	84.2[±2.7]	34.0[±2.6]
Bowers Chalke	MR 6839	chert	core	Upper Albian	11.8[±3.2]	10[±4.0]	88.2[±3.2]	39.7[±3.1]
Bowers Chalke	MR 6839	chert	cortex	Upper Albian	13.6[±1.0]	10.0[±1.1]	86.4[±1.0]	44.5[±1.2]
Higher Meerhay Farm	MR 14875	chert	core	Upper Albian	8.6[±0.6]	10.3[±0.9]	91.4[±0.6]	55.5[±1.1]
Charnmouth	MR 17273	chert	white core	Upper Albian	12.6[±2.5]	14.6[±3.5]	87.4[±2.5]	27.7[±2.1]
Charnmouth	MR 17273	chert	core	Upper Albian	15.3[±3.4]	10.3[±3.1]	84.7[±3.4]	33.8[±2.9]
Charnmouth	MR 17274	chert	core	Upper Albian	9.6[±0.5]	10.0[±0.8]	90.4[±0.5]	48.4[±0.8]
Culver Hole, Dorset	UG007	chert	cortex	Upper Albian	7.2[±0.7]	22.0[±0.7]	92.8[±0.7]	29.0[±0.9]
Culver Hole, Dorset	UG008	chert	core	Upper Albian	10.5[±0.9]	24.0[±0.7]	89.5[±0.9]	27.0[±0.8]
Culver Hole, Dorset	UG009	chert	core	Upper Albian	9.4[±0.8]	25.0[±0.8]	90.6[±0.8]	28.0[±0.8]
Culver Hole, Dorset	UG010	chert	core	Upper Albian	19.2[±0.8]	20.0[±0.6]	80.8[±0.8]	27.0[±0.8]

Table 10. Quantitative silica mineralogy and crystal size of decalcified examples of chert from the Upper Greensand (Upper Albian) of southwest England. Sample locations and age are listed. Samples MR 4026–MR 17274 are from the petrological collection of the Institute of Geological Sciences (London) – now the British Geological Survey – and were used in Jeans (1971, p.125).

Element	Nano-quartz Speeton silicon atoms	Red Flint Group CVJRM20 red inner core silicon atoms	Black Flint Group Floorstone silicon atoms	Black Flint Group Vein flint SLO 1 silicon atoms
Al	11	712	900	1275
Fe	52	1053	867	5708
Mg	54	16991	29923	33296
Ca	78	2203	176	4133
K	102	2203	217	2997
Na	110	1144	1221	1577
P	1267	9911	588	13621
Ti	~	26430	19948	12617
Mn	~	59468	59845	399553

Table 11. Element ratios expressed as atomic fractions between silicon and major elements in nano-quartz grains and examples from the red flint and the black flint groups.